Published for SISSA by Springer

Received: *July 11, 2017*
Revised: *September 8, 2017*
Accepted: *October 6, 2017*
Published: *October 26, 2017*

Search for new high-mass phenomena in the dilepton final state using 36 fb^{-1} of proton-proton collision data at $\sqrt{s} = 13$ TeV with the ATLAS detector

JHEP10(2017)182

The ATLAS collaboration

E-mail: atlas.publications@cern.ch

Abstract: A search is conducted for new resonant and non-resonant high-mass phenomena in dielectron and dimuon final states. The search uses 36.1 fb^{-1} of proton-proton collision data, collected at $\sqrt{s} = 13$ TeV by the ATLAS experiment at the LHC in 2015 and 2016. No significant deviation from the Standard Model prediction is observed. Upper limits at 95% credibility level are set on the cross-section times branching ratio for resonances decaying into dileptons, which are converted to lower limits on the resonance mass, up to 4.1 TeV for the E_6-motivated Z'_χ. Lower limits on the $qq\ell\ell$ contact interaction scale are set between 2.4 TeV and 40 TeV, depending on the model.

Keywords: Beyond Standard Model, Hadron-Hadron scattering (experiments)

ArXiv ePrint: 1707.02424

https://doi.org/10.1007/JHEP10(2017)182

Contents

1 Introduction

This article presents a search for resonant and non-resonant new phenomena, based on the analysis of dilepton final states (ee and $\mu\mu$) in proton-proton (pp) collisions with the ATLAS detector at the Large Hadron Collider (LHC) operating at $\sqrt{s} = 13$ TeV. The data set was collected during 2015 and 2016, and corresponds to an integrated luminosity of 36.1 fb^{-1}. In the search for new physics carried out at hadron colliders, the study of

JHEP10(2017)182

dilepton final states provides excellent sensitivity to a large variety of phenomena. This experimental signature benefits from a fully reconstructed final state, high signal-selection efficiencies and relatively small, well-understood backgrounds, representing a powerful test for a wide range of theories beyond the Standard Model (SM).

Models with extended gauge groups often feature additional U(1) symmetries with corresponding heavy spin-1 bosons. These bosons, generally referred to as Z', would manifest as a narrow resonance through its decay, in the dilepton mass spectrum. Among these models are those inspired by Grand Unified Theories, which are motivated by gauge unification or a restoration of the left-right symmetry violated by the weak interaction. Examples considered in this article include the Z' bosons of the E_6-motivated [1, 2] theories as well as Minimal models [3]. The Sequential Standard Model (SSM) [2] is also considered due to its inherent simplicity and usefulness as a benchmark model. The SSM manifests a Z'_{SSM} boson with couplings to fermions equal to those of the SM Z boson.

The most sensitive previous searches for a Z' boson decaying into the dilepton final state were carried out by the ATLAS and CMS collaborations [4, 5]. Using 3.2 fb^{-1} of pp collision data at $\sqrt{s} = 13\,\text{TeV}$ collected in 2015, ATLAS set a lower exclusion limit at 95% credibility level (CL) on the Z'_{SSM} pole mass of 3.4 TeV for the combined ee and $\mu\mu$ channels. Similar limits were set by CMS using the 2015 data sample.

This search is also sensitive to a series of other models that predict the presence of narrow dilepton resonances. These models include the Randall-Sundrum (RS) model [6] with a warped extra dimension giving rise to spin-2 graviton excitations, the quantum black-hole model [7], the Z^* model [8], and the minimal walking technicolour model [9]. In order to facilitate interpretation of the results in the context of these or any other model predicting a new dilepton resonance, limits are set on the production of a generic Z'-like excess.

In addition to the search for narrow resonances, results for non-resonant phenomena are also reported. Such models of these phenomena include an effective four-fermion contact interaction (CI) between two initial-state quarks and two final-state leptons ($qq\ell\ell$). Unlike resonance models, which require sufficient energy to produce the new gauge boson, the presence of a new interaction in the non-resonant regime can be detected at a much lower energy.

The most stringent constraints from CI searches are also provided by the ATLAS and CMS collaborations [4, 10], for couplings between quarks and leptons. Using 3.2 fb^{-1} of pp collision data at $\sqrt{s} = 13\,\text{TeV}$ collected in 2015, ATLAS set lower limits on the $qq\ell\ell$ CI scale of $\Lambda = 25\,\text{TeV}$ and $\Lambda = 18\,\text{TeV}$ at 95% CL for constructive and destructive interference, respectively, in the case of left-left interactions and assuming a uniform positive prior probability in $1/\Lambda^2$. Similar limits were set by CMS using the 2015 data set. Both the resonant and non-resonant models considered as the benchmark for this search are further discussed in section 2.

The presented search utilises the invariant mass spectra of the observed dilepton final states as discriminating variables. The analysis and interpretation of these spectra rely primarily on simulated samples of signal and background processes. The interpretation is performed taking into account the expected shape of different signals in the dilepton mass distribution. The use of the shape of the full dilepton invariant mass distribution reduces the uncertainties in the background modelling, thereby increasing the sensitivity of this search at high masses. This article is structured as follows: section 2 covers the theoretical motivation of the models considered in this search, followed by a description of the ATLAS detector in section 3, and a summary in section 4 of the data and Monte Carlo (MC) samples used. The event selection is motivated and described in section 5, with details of the background estimation given in section 6, and an overview of the systematic uncertainty treatment given in section 7. The event yields and main kinematic distributions are presented in section 8, followed by a description of the statistical analysis in section 9, and the results in section 10.

2 Theoretical models

2.1 E_6-motivated Z' models

In the class of models based on the E_6 gauge group [1, 2], the unified symmetry group can break to the SM in a number of different ways. In many of them, E_6 is first broken to $SO(10) \times U(1)_\psi$, with SO(10) then breaking either to $SU(4) \times SU(2)_L \times SU(2)_R$ or $SU(5) \times U(1)_\chi$. In the first of these two possibilities, a Z'_{3R} coming from $SU(2)_R$, where 3R stands for the right-handed third component of weak isospin, or a Z'_{B-L} from the breaking of SU(4) into $SU(3)_C \times U(1)_{B-L}$ could exist at the TeV scale, where B (L) is the baryon (lepton) number and $(B-L)$ is the conserved quantum number. Both of these Z' bosons appear in the Minimal Z' models discussed in the next section. In the SU(5) case, the presence of $U(1)_\psi$ and $U(1)_\chi$ symmetries implies the existence of associated gauge bosons Z'_ψ and Z'_χ that can mix. When SU(5) is broken down to the SM, one of the U(1) can remain unbroken down to intermediate energy scales. Therefore, the precise model is governed by a mixing angle θ_{E_6}, with the new potentially observable Z' boson defined by $Z'(\theta_{E_6}) = Z'_\psi \cos\theta_{E_6} + Z'_\chi \sin\theta_{E_6}$. The value of θ_{E_6} specifies the Z' boson's coupling strength to SM fermions as well as its intrinsic width. In comparison to the benchmark Z'_{SSM}, which has a width of approximately 3% of its mass, the E_6 models predict narrower Z' signals. The Z'_ψ considered here has a width of 0.5% of its mass, and the Z'_χ has a width of 1.2% of its mass [11, 12]. All other Z' signals in this model, including Z'_S, Z'_I, Z'_η, and Z'_N, are defined by specific values of θ_{E_6} ranging from 0 to π, and have widths between those of the Z'_ψ and Z'_χ.

2.2 Minimal Z' models

In the Minimal Z' models [3], the phenomenology of Z' boson production and decay is characterised by three parameters: two effective coupling constants, g_{BL} and g_Y, and the Z' boson mass. This parameterisation encompasses Z' bosons from many models, including the Z'_χ belonging to the E_6-motivated model of the previous section, the Z'_{3R} in a left-right symmetric model [13, 14] and the Z'_{B-L} of the pure $(B-L)$ model [15]. The minimal models are therefore particularly interesting for their generality, and because couplings are being directly constrained by the search. The coupling parameter g_{BL} defines the coupling of a new Z' boson to the $(B-L)$ current, while the g_Y parameter represents the coupling

	$Z'_{\mathrm{B-L}}$	Z'_{χ}	Z'_{3R}
γ'	$\sqrt{\frac{5}{8}}\sin\theta_{\mathrm{W}}$	$\sqrt{\frac{41}{24}}\sin\theta_{\mathrm{W}}$	$\sqrt{\frac{5}{12}}\sin\theta_{W}$
$\cos\theta_{\mathrm{Min}}$	1	$\sqrt{\frac{25}{41}}$	$\frac{1}{\sqrt{5}}$
$\sin\theta_{\mathrm{Min}}$	0	$-\sqrt{\frac{16}{41}}$	$-\frac{2}{\sqrt{5}}$

Table 1. Values for γ' and θ_{Min} in the Minimal Z' models corresponding to three specific Z' bosons: $Z'_{\mathrm{B-L}}$, Z'_{χ} and Z'_{3R}. The SM weak mixing angle is denoted by θ_{W}.

to the weak hypercharge Y. It is convenient to refer to the ratios $\tilde{g}_{\mathrm{BL}} \equiv g_{\mathrm{BL}}/g_Z$ and $\tilde{g}_{\mathrm{Y}} \equiv g_{\mathrm{Y}}/g_Z$, where g_Z is related to the coupling of the SM Z boson to fermions defined by $g_Z = 2M_Z/v$. Here $v = 246\,\mathrm{GeV}$ is the SM Higgs vacuum expectation value. To simplify further, the additional parameters γ' and θ_{Min} are chosen as independent parameters with the following definitions: $\tilde{g}_{\mathrm{BL}} = \gamma'\cos\theta_{\mathrm{Min}}$, $\tilde{g}_{\mathrm{Y}} = \gamma'\sin\theta_{\mathrm{Min}}$. The γ' parameter measures the strength of the Z' boson coupling relative to that of the SM Z boson, while θ_{Min} determines the mixing between the generators of the (B − L) and weak hypercharge Y gauge groups. Specific values of γ' and θ_{Min} correspond to Z' bosons in various models, as is shown in table 1 for the three cases mentioned in this section.

For the Minimal Z' models, the width depends on γ' and θ_{Min}, and the Z' interferes with the SM Z/γ^* process. For example, taking the 3R and B − L models investigated in this search, the width varies from less than 1% up to 12.8% and 39.5% respectively, for the γ' range considered. The branching fraction to leptons is the same as for the other Z' models considered in this search. Couplings to hypothetical right-handed neutrinos, the Higgs boson, and to W boson pairs are not considered. Previous limits on the Z' mass versus γ' were set by the ATLAS experiment. For $\gamma' = 0.2$, the range of Z' mass limits at 95% CL corresponding to $\theta_{\mathrm{Min}} \in [0, \pi]$ is 1.11 TeV to 2.10 TeV [16].

2.3 Contact interactions

Some models of physics beyond the SM result in non-resonant deviations from the predicted SM dilepton mass spectrum. Compositeness models motivated by the repeated pattern of quark and lepton generations predict new interactions involving their constituents. These interactions may be represented as a contact interaction between initial-state quarks and final-state leptons [17, 18]. Other models producing non-resonant effects are models with large extra dimensions [19] motivated by the hierarchy problem. This search is sensitive to non-resonant new physics in these scenarios; however, constraints on these models are not evaluated in this article.

The following four-fermion CI Lagrangian [17, 18] is used to describe a new interaction in the process $q\bar{q} \to \ell^+\ell^-$:

$$\mathcal{L} = \frac{g^2}{\Lambda^2}\left[\eta_{\mathrm{LL}}\left(\bar{q}_{\mathrm{L}}\gamma_\mu q_{\mathrm{L}}\right)\left(\bar{\ell}_{\mathrm{L}}\gamma^\mu \ell_{\mathrm{L}}\right) + \eta_{\mathrm{RR}}\left(\bar{q}_{\mathrm{R}}\gamma_\mu q_{\mathrm{R}}\right)\left(\bar{\ell}_{\mathrm{R}}\gamma^\mu \ell_{\mathrm{R}}\right) \right.$$
$$\left. + \eta_{\mathrm{LR}}\left(\bar{q}_{\mathrm{L}}\gamma_\mu q_{\mathrm{L}}\right)\left(\bar{\ell}_{\mathrm{R}}\gamma^\mu \ell_{\mathrm{R}}\right) + \eta_{\mathrm{RL}}\left(\bar{q}_{\mathrm{R}}\gamma_\mu q_{\mathrm{R}}\right)\left(\bar{\ell}_{\mathrm{L}}\gamma^\mu \ell_{\mathrm{L}}\right)\right],$$

where g is a coupling constant set to be $\sqrt{4\pi}$ by convention, Λ is the CI scale, and $q_{\mathrm{L,R}}$ and $\ell_{\mathrm{L,R}}$ are left-handed and right-handed quark and lepton fields, respectively. The symbol γ_μ denotes the gamma matrices, and the parameters η_{ij}, where i and j are L or R (left or right), define the chiral structure of the new interaction. Different chiral structures are investigated here, with the left-right (right-left) model obtained by setting $\eta_{\mathrm{LR}} = \pm 1$ ($\eta_{\mathrm{RL}} = \pm 1$) and all other parameters to zero. Likewise, the left-left and right-right models are obtained by setting the corresponding parameters to ± 1, and the others to zero. The sign of η_{ij} determines whether the interference between the SM Drell-Yan (DY) $q\bar{q} \to Z/\gamma^* \to \ell^+\ell^-$ process and the CI process is constructive ($\eta_{ij} = -1$) or destructive ($\eta_{ij} = +1$).

3 ATLAS detector

The ATLAS experiment [20, 21] at the LHC is a multipurpose particle detector with a forward-backward symmetric cylindrical geometry and a near 4π coverage in solid angle.[1] It consists of an inner detector for tracking surrounded by a thin superconducting solenoid providing a 2 T axial magnetic field, electromagnetic and hadronic calorimeters, and a muon spectrometer. The inner detector (ID) covers the pseudorapidity range $|\eta| < 2.5$. It consists of silicon pixel, silicon microstrip, and transition-radiation tracking detectors. Lead/liquid-argon (LAr) sampling calorimeters provide electromagnetic (EM) energy measurements with high granularity. A hadronic (steel/scintillator-tile) calorimeter covers the central pseudorapidity range ($|\eta| < 1.7$). The endcap and forward regions are instrumented with LAr calorimeters for EM and hadronic energy measurements up to $|\eta| = 4.9$. The total thickness of the EM calorimeter is more than twenty radiation lengths. The muon spectrometer (MS) surrounds the calorimeters and is based on three large superconducting air-core toroids with eight coils each. The field integral of the toroids ranges between 2.0 and 6.0 T m for most of the detector. The MS includes a system of precision tracking chambers and fast detectors for triggering. A dedicated trigger system is used to select events. The first-level trigger is implemented in hardware and uses the calorimeter and muon detectors to reduce the accepted rate to below 100 kHz. This is followed by a software-based trigger that reduces the accepted event rate to 1 kHz on average [22].

4 Data and Monte Carlo samples

This analysis uses data collected at the LHC during 2015 and 2016 pp collisions at $\sqrt{s} = 13$ TeV. The total integrated luminosity corresponds to 36.1 fb^{-1}, considering the periods of data-taking with all sub-detectors functioning nominally. The event quality is also checked to remove events which contain noise bursts or coherent noise in the calorimeters.

Modelling of the various background sources primarily relies on MC simulation. The dominant background contribution arises from the DY process, which was simulated using

[1]ATLAS uses a right-handed coordinate system with its origin at the nominal interaction point (IP) in the centre of the detector and the z-axis along the beam pipe. The x-axis points from the IP to the centre of the LHC ring, and the y-axis points upwards. Cylindrical coordinates (r, ϕ) are used in the transverse plane, ϕ being the azimuthal angle around the z-axis. The pseudorapidity is defined in terms of the polar angle θ as $\eta = -\ln\tan(\theta/2)$. Angular distance is measured in units of $\Delta R \equiv \sqrt{(\Delta\eta)^2 + (\Delta\phi)^2}$.

JHEP10(2017)182

the next-to-leading-order (NLO) POWHEG BOX [23] event generator, implementing the CT10 [24] parton distribution function (PDF), in conjunction with PYTHIA 8.186 [25] for event showering, and the ATLAS AZNLO set of tuned parameters [26]. A more detailed description of this process is provided in ref. [27]. The DY event yields are corrected with a rescaling that depends on the dilepton invariant mass from NLO to next-to-next-to-leading order (NNLO) in the strong coupling constant, computed with VRAP 0.9 [28] and the CT14NNLO PDF set [29]. The NNLO quantum chromodynamic (QCD) corrections are a factor of ~ 0.98 at a dilepton invariant mass ($m_{\ell\ell}$) of 3 TeV. Mass-dependent electroweak (EW) corrections were computed at NLO with MCSANC 1.20 [30]. The NLO EW corrections are a factor of ~ 0.86 at $m_{\ell\ell} = 3$ TeV. Those include photon-induced contributions ($\gamma\gamma \to \ell\ell$ via t- and u-channel processes) computed with the MRST2004QED PDF set [31].

Other backgrounds originate from top-quark [32] and diboson (WW, WZ, ZZ) [33] production. The diboson processes were simulated using SHERPA 2.2.1 [34] with the CT10 PDF. The $t\bar{t}$ and single-top-quark MC samples were simulated using the POWHEG BOX generator with the CT10 PDF, and are normalised to a cross-section as calculated with the Top++ 2.0 program [35], which is accurate to NNLO in perturbative QCD, including resummation of next-to-next-to-leading logarithmic soft gluon terms. Background processes involving W and Z bosons decaying into τ lepton(s) were found to have a negligible contribution, and are not included. In the case of the dielectron channel, multi-jet and W+jets processes (which contribute due to the misidentification of jets as electrons) are estimated using a data-driven method, described in section 6.

Signal processes were produced at leading-order (LO) using PYTHIA 8.186 with the NNPDF23LO PDF set [36] and the ATLAS A14 set of tuned parameters [37] for event generation, parton showering and hadronisation. Interference effects (with DY production) are not included for the SSM and E_6 model Z' signal due to large model dependence, but are included for the CI signal and for the Minimal model approach. Higher-order QCD corrections for the signal were computed with the same methodology as for the DY background. EW corrections were not applied to the Z' signal samples also due to the large model dependence. However, the EW corrections are applied to the CI signal samples, because interference effects are included.

The detector response is simulated with GEANT 4 [38], and the events are processed with the same reconstruction software [39] as used for the data. Furthermore, the distribution of the number of additional simulated pp collisions in the same or neighbouring beam crossings (pile-up) is accounted for by overlaying minimum-bias events simulated with PYTHIA 8.186 using the ATLAS A2 set of tuned parameters [37] and the MSTW2008LO PDF set [40], reweighting the MC simulation to match the distribution observed in the data.

5 Event selection

Dilepton candidates are selected in the data and simulated events by requiring at least one pair of reconstructed same-flavour lepton candidates (electrons or muons) and at least one reconstructed pp interaction vertex, with the primary vertex defined as the one with the highest sum of track transverse momenta (p_{T}) squared.

Electron candidates are identified in the central region of the ATLAS detector ($|\eta| < 2.47$) by combining calorimetric and tracking information in a likelihood discriminant with four operating points: *Very Loose*, *Loose*, *Medium* and *Tight* each with progressively higher threshold for the discriminant, and stronger background rejection, as described in ref. [41]. The transition region between the central and forward regions of the calorimeters, in the range $1.37 \leq |\eta| \leq 1.52$, exhibits poorer energy resolution and is therefore excluded. Electron candidates are required to have transverse energy (E_{T}) greater than 30 GeV, and a track consistent with the primary vertex both along the beamline and in the transverse plane. The *Medium* working point of the likelihood discrimination is used to select electron candidates while the *Very Loose* and *Loose* working points are used in the data-driven background estimation described in section 6. In addition to the likelihood discriminant, selection criteria based on track quality are applied. The selection efficiency is approximately 96% for electrons with E_{T} between 30 GeV and 500 GeV, and decreases to approximately 95% for electrons with $E_{\mathrm{T}} = 1.5$ TeV. The selection efficiency is evaluated in the data using a tag-and-probe method [42] up to E_{T} of 500 GeV and the uncertainties due to the modelling of the shower shape variables are estimated for electrons with higher E_{T} using MC events, as described in section 7. The electron energy scale and resolution have been calibrated up to E_{T} of 1 TeV using data collected at $\sqrt{s} = 8$ TeV and $\sqrt{s} = 13$ TeV [43]. The energy resolution extrapolated for high-E_{T} electrons (greater than 1 TeV) is approximately 1%.

Muon candidate tracks are, at first, reconstructed independently in the ID and the MS [44]. The two tracks are then used as input to a combined fit (for p_{T} less than 300 GeV) or to a statistical combination (for p_{T} greater than 300 GeV). The combined fit takes into account the energy loss in the calorimeter and multiple-scattering effects. The statistical combination for high transverse momenta is performed to mitigate the effects of relative ID and MS misalignments.

In order to optimise momentum resolution, muon tracks are required to have at least three hits in each of three precision chambers in the MS and not to traverse regions of the MS which are poorly aligned. This requirement reduces the muon reconstruction efficiency by about 20% for muons with a p_{T} greater than 1.5 TeV. Furthermore, muon candidates in the overlap of the MS barrel and endcap region ($1.01 < |\eta| < 1.10$) are rejected due to the potential relative misalignment between barrel and endcap. Measurements of the ratio of charge to momentum (q/p) performed independently in the ID and MS must agree within seven standard deviations, calculated from the sum in quadrature of the ID and MS momentum uncertainties. Finally, in order to reject events that contain a muon with poor track resolution in the MS, due to a low magnetic field integral and other effects, an event veto based on the MS track momentum measurement uncertainty is also applied. Muons are required to have p_{T} greater than 30 GeV, $|\eta| < 2.5$, and to be consistent with the primary vertex both along the beamline and in the transverse plane.

To further suppress background from misidentified jets as well as from light-flavour and heavy-flavour hadron decays inside jets, lepton candidates are required to satisfy calorimeter-based (only for electrons) and track-based (for both electrons and muons) isolation criteria. The calorimeter-based isolation relies on the ratio of the E_{T} deposited in a cone of size $\Delta R = 0.2$, centered at the electron cluster barycentre, to the total E_{T} measured for the electron. The track-based isolation relies on the ratio of the summed scalar p_{T} of tracks within a variable-cone of size $\Delta R = 10\,\mathrm{GeV}/p_{\mathrm{T}}$ to the p_{T} of the track associated with the candidate lepton. This variable-cone has no minimum size, meaning that the track-based isolation requirement effectively vanishes at very high lepton p_{T}. The tracks are required to have $p_{\mathrm{T}} > 1\,\mathrm{GeV}$, $|\eta| < 2.5$, meet all track quality criteria, and originate from the primary vertex. In all cases the contribution to the E_{T} or p_{T} ascribed to the lepton candidate is removed from the isolation cone. The isolation criteria, applied to both leptons, have a fixed efficiency of 99% over the full range of lepton momenta.

Calibration corrections are applied to electron (muon) candidates to match energy (momentum) scale and resolution between data and simulation [44, 45].

Triggers were chosen to maximise the overall signal efficiency. In the dielectron channel, a two-electron trigger based on the *Loose* identification criteria with an E_{T} threshold of 17 GeV for each electron is used. Events in the dimuon channel are required to pass at least one of two single-muon triggers with p_{T} thresholds of 26 GeV and 50 GeV, with the former also requiring the muon to be isolated. These triggers select events from a simulated sample of Z'_{χ} bosons with a pole mass of 3 TeV with an efficiency of approximately 86% and 91% for the dielectron and dimuon channels, respectively.

Data-derived corrections are applied in the samples to match the trigger, reconstruction and isolation efficiencies between data and MC simulation. For each event with at least two same-flavour leptons, the dilepton candidate is built. If more than two electrons (muons) are found, the ones with the highest E_{T} (p_{T}) are chosen. In the muon channel, only opposite-charge candidates are retained. This requirement is not applied in the electron channel due to a higher chance of charge misidentification for high-E_{T} electrons. There is no explicit overlap removal between the dielectron and dimuon channel, but a negligible number of common events at low dilepton masses enter the combination.

Representative values of the total acceptance times efficiency for a Z'_{χ} boson with a pole mass of 3 TeV are 71% in the dielectron channel and 40% in the dimuon channel.

6 Background estimation

The backgrounds from processes including two real leptons in the final state (DY, $t\bar{t}$, single top quark, WW, WZ, and ZZ production) are modelled using the MC samples described in section 4. In the mass range $120\,\mathrm{GeV} < m_{\ell\ell} < 1\,\mathrm{TeV}$ the corrected DY background is smoothed to remove statistical fluctuations due to the limited MC sample size compared to the large integrated luminosity of the data, by fitting the spectrum and using the resulting fitted function to set the expected event yields in that mass region. The chosen fit function consists of a relativistic Breit-Wigner function with mean and width fixed to M_Z and Γ_Z respectively [46], multiplied by an analytic function taking into account detector resolution, selection efficiency, parton distribution function effects, and contributions from the photon-induced process and virtual photons. At higher dilepton invariant masses the statistical uncertainty of the MC simulation is much smaller than that of the data through the use of mass-binned MC samples.

An additional background arises from W+jets and multi-jet events from which at most one real lepton is produced. This background contributes to the selected samples due to having one or more jets satisfying the lepton selection criteria (so called "fakes"). In the dimuon channel, contributions from W+jets and multi-jet production are found to be negligible, and therefore are not included in the expected yield. In the dielectron channel the contributions from these processes are determined with a data-driven technique, the *matrix method*, in two steps. In the first step, the probabilities that a jet and a real electron satisfy the electron identification requirements are evaluated, for both the nominal and a loosened selection criteria. The loosened selection differs from the nominal one by the use of the *Loose* electron identification criteria and no isolation criterion. Then, in the second step these probabilities are used to estimate the level of contamination, due to fakes, in the selected sample of events.

A probability r that a real electron passing the loosened selection satisfies the nominal electron selection criteria is estimated from MC simulated DY samples in several regions of E_{T} and $|\eta|$. The probability f that a jet passing the loosened selection satisfies the nominal electron selection criteria is determined in regions of E_{T} and $|\eta|$ in data samples triggered on the presence of a *Very Loose* or a *Loose* electron candidate. Contributions to these samples from the production of W and Z bosons are suppressed by vetoing events with large missing transverse energy ($E_{\mathrm{T}}^{\mathrm{miss}} > 25\,\mathrm{GeV}$) or with two *Loose* electron candidates compatible with Z boson mass, or two candidates passing the *Medium* identification criteria. The $E_{\mathrm{T}}^{\mathrm{miss}}$ is reconstructed as the negative vectorial sum of the calibrated momenta of the electrons, muons, and jets, in the event. Residual contributions from processes with real electrons in the calculation of f are accounted for by using the MC simulated samples.

The selected events are grouped according to the identification criteria satisfied by the electrons. A system of equations between numbers of paired objects (N_{ab}, with $E_{\mathrm{T}}^{a} > E_{\mathrm{T}}^{b}$) is used to solve for the unknown contribution to the background in each of the kinematic regions from events with one or more fake electrons:

$$\begin{pmatrix} N_{\mathrm{TT}} \\ N_{\mathrm{TL}} \\ N_{\mathrm{LT}} \\ N_{\mathrm{LL}} \end{pmatrix} = \begin{pmatrix} r^2 & rf & fr & f^2 \\ r(1-r) & r(1-f) & f(1-r) & f(1-f) \\ (1-r)r & (1-r)f & (1-f)r & (1-f)f \\ (1-r)^2 & (1-r)(1-f) & (1-f)(1-r) & (1-f)^2 \end{pmatrix} \begin{pmatrix} N_{\mathrm{RR}} \\ N_{\mathrm{RF}} \\ N_{\mathrm{FR}} \\ N_{\mathrm{FF}} \end{pmatrix} . \tag{6.1}$$

Here the subscripts R and F refer to real electrons and fakes (jets), respectively. The subscript T refers to electrons that satisfy the nominal selection criteria. The subscript L corresponds to electrons that pass the loosened requirements described above but fail the nominal requirements.

The background is given as the part of N_{TT} that originates from a pair of objects with at least one fake electron:

$$N^{\text{Multi-jet \& W+jets}} = rf(N_{\mathrm{RF}} + N_{\mathrm{FR}}) + f^2 N_{\mathrm{FF}} . \tag{6.2}$$

The true paired objects on the right-hand side of eq. (6.2) can be expressed in terms of measureable quantities ($N_{\mathrm{TT}}, N_{\mathrm{TL}}, N_{\mathrm{LT}}, N_{\mathrm{LL}}$) by inverting the matrix in eq. (6.1).

The estimate is extrapolated to the full mass range considered by fitting an analytic function to the dielectron invariant mass (m_{ee}) distribution above ~ 125 GeV to mitigate effects of limited event counts in the high-mass region and of method instabilities due to a negligible contribution from fakes in the Z peak region. The fit is repeated by increasing progressively the lower edge of the fit range by ~ 10 GeV per step until ~ 195 GeV. The weighted mean of all fits is taken as the central value and the envelope as the uncertainty. Additional uncertainties in this background estimate are evaluated by considering differences between the estimates for events with same-charge and opposite-charge electrons as well as by varying the electron identification probabilities. The uncertainty on this background can, due to the extrapolation, become very large at high mass, but has only a negligible impact on the final results of this analysis.

7 Systematic uncertainties

Systematic uncertainties estimated to have a non-negligible impact on the expected cross-section limit are considered as nuisance parameters in the statistical interpretation and include both the theoretical and experimental effects on the total background and experimental effects on the signal.

Theoretical uncertainties in the background prediction are dominated by the DY background, throughout the entire dilepton invariant mass range. They arise from the eigenvector variations of the nominal PDF set, as well as variations of PDF scales, the strong coupling (α_{S} (M_Z)), EW corrections, and photon-induced (PI) corrections. The effect of choosing different PDF sets are also considered. The theoretical uncertainties are the same for both channels at generator level, but they result in different uncertainties at reconstruction level due to the differing resolutions between the dielectron and dimuon channels.

The PDF variation uncertainty is obtained using the 90% CL CT14NNLO PDF error set and by following the procedure described in refs. [16, 47, 48]. Rather than using a single nuisance parameter to describe the 28 eigenvectors of this PDF error set, which could lead to an underestimation of its effect, a re-diagonalised set of 7 PDF eigenvectors was used [29], which are treated as separate nuisance parameters. This represents the minimal set of PDF eigenvectors that maintains the necessary correlations, and the sum in quadrature of these eigenvectors matches the original CT14NNLO error envelope well. The uncertainties due to the variation of PDF scales and α_{S} are derived using VRAP with the former obtained by varying the renormalisation and factorisation scales of the nominal CT14NNLO PDF up and down simultaneously by a factor of two. The value of α_{S} used (0.118) is varied by ± 0.003. The EW correction uncertainty was assessed by comparing the nominal additive $(1{+}\delta_{\mathrm{EW}}{+}\delta_{\mathrm{QCD}})$ treatment with the multiplicative approximation $((1{+}\delta_{\mathrm{EW}})(1{+}\delta_{\mathrm{QCD}}))$ treatment of the EW correction in the combination of the higher-order EW and QCD effects. The uncertainty in the photon-induced correction is calculated based on the uncertainties in the quark masses and the photon PDF. Following the recommendations of the PDF4LHC forum [48], an additional uncertainty due to the choice of nominal

PDF set is derived by comparing the central values of CT14NNLO with those from other PDF sets, namely MMHT14 [49] and NNPDF3.0 [50]. The maximum absolute deviation from the envelope of these comparisons is used as the PDF choice uncertainty, where it is larger than the CT14NNLO PDF eigenvector variation envelope. Theoretical uncertainties are not applied to the signal prediction in the statistical interpretation.

Theoretical uncertainties on the estimation of the top quark and diboson backgrounds were also considered, both from the independent variation of the factorisation (μ_{F}) and renormalisation (μ_{R}) scales, and from the variations in the PDF and α_{S}, following the PDF4LHC prescription. Normalisation uncertainties in the top quark and diboson background are shown in the "Top Quarks Theoretical" and "Dibosons Theoretical" entry in table 2.

The following sources of experimental uncertainty are accounted for: lepton efficiencies due to triggering, identification, reconstruction, and isolation, lepton energy scale and resolution, pile-up effects, as well as the multi-jet and W+jets background estimate. The same sources of experimental uncertainty are considered for the DY background and signal treatment. Efficiencies are evaluated using events from the $Z \to \ell\ell$ peak and then extrapolated to high energies. The uncertainty in the muon reconstruction efficiency is the largest experimental uncertainty in the dimuon channel. It includes the uncertainty obtained from $Z \to \mu\mu$ data studies and a high-p_{T} extrapolation uncertainty corresponding to the decrease in the muon reconstruction and selection efficiency with increasing p_{T} which is predicted by the MC simulation. The effect on the muon reconstruction efficiency was found to be approximately 3% per TeV as a function of muon p_{T}. The uncertainty in the electron identification efficiency extrapolation is based on the differences in the electron shower shapes in the EM calorimeters between data and MC simulation in the $Z \to ee$ peak, which are propagated to the high-E_{T} electron sample. The effect on the electron identification efficiency was found to be 2.0% and is independent of E_{T} for electrons with E_{T} above 150 GeV. For the isolation efficiencies, uncertainties were estimated for $150 < p_{\mathrm{T}} < 500$ GeV and above 500 GeV separately, using DY candidates in data. The larger isolation uncertainty that is observed for electrons is due to the uncertainty inherent in calorimeter-based isolation for electrons (track-based isolation is also included), compared to the solely track-based only isolation for muons. Mismodelling of the muon momentum resolution due to residual misalignments in the MS can alter the steeply falling background shape at high dilepton mass and can significantly modify the width of the signals line shape. This uncertainty is obtained by studying the muon momentum resolution in dedicated data-taking periods with no magnetic field in the MS [44]. For the dielectron channel, the uncertainty includes a contribution from the multi-jet and W+jets data-driven estimate that is obtained by varying both the overall normalisation and the extrapolation methodology, which is explained in section 6. The systematic uncertainty from pile-up effects is assessed by inducing a variation in the pile-up reweighting of MC events and is included to cover the uncertainty on the ratio of the predicted and measured inelastic cross-section in the fiducial volume defined by $\mathrm{M}_X > 13$ GeV, where M_X is the mass of the non-diffractive hadronic system [51]. An uncertainty on the beam energy of 0.65% is estimated and included. The uncertainty on the combined 2015 and 2016 integrated lumi-

JHEP10(2017)182

Source	Dielectron channel [%]		Dimuon channel [%]	
	Signal	Background	Signal	Background
Luminosity	3.2 (3.2)	3.2 (3.2)	3.2 (3.2)	3.2 (3.2)
MC statistical	<1.0 (<1.0)	<1.0 (<1.0)	<1.0 (<1.0)	<1.0 (<1.0)
Beam energy	2.0 (4.1)	2.0 (4.1)	1.9 (3.1)	1.9 (3.1)
Pile-up effects	<1.0 (<1.0)	<1.0 (<1.0)	<1.0 (<1.0)	<1.0 (<1.0)
DY PDF choice	—	<1.0 (8.4)	—	<1.0 (1.9)
DY PDF variation	—	8.7 (19)	—	7.7 (13)
DY PDF scales	—	1.0 (2.0)	—	<1.0 (1.5)
DY α_S	—	1.6 (2.7)	—	1.4 (2.2)
DY EW corrections	—	2.4 (5.5)	—	2.1 (3.9)
DY γ-induced corrections	—	3.4 (7.6)	—	3.0 (5.4)
Top quarks theoretical	—	<1.0 (<1.0)	—	<1.0 (<1.0)
Dibosons theoretical	—	<1.0 (<1.0)	—	<1.0 (<1.0)
Reconstruction efficiency	<1.0 (<1.0)	<1.0 (<1.0)	10 (17)	10 (17)
Isolation efficiency	9.1 (9.7)	9.1 (9.7)	1.8 (2.0)	1.8 (2.0)
Trigger efficiency	<1.0 (<1.0)	<1.0 (<1.0)	<1.0 (<1.0)	<1.0 (<1.0)
Identification efficiency	2.6 (2.4)	2.6 (2.4)	—	—
Lepton energy scale	<1.0 (<1.0)	4.1 (6.1)	<1.0 (<1.0)	<1.0 (<1.0)
Lepton energy resolution	<1.0 (<1.0)	<1.0 (<1.0)	2.7 (2.7)	<1.0 (6.7)
Multi-jet & W+jets	—	10 (129)	—	—
Total	10 (11)	18 (132)	11 (18)	14 (24)

Table 2. Summary of the pre-marginalised relative systematic uncertainties in the expected number of events at dilepton masses of 2 TeV and 4 TeV. The values reported in parenthesis correspond to the 4 TeV mass. The values quoted for the background represent the relative change in the total expected number of events in the corresponding $m_{\ell\ell}$ histogram bin containing the reconstructed $m_{\ell\ell}$ mass of 2 TeV (4 TeV). For the signal uncertainties the values were computed using a Z'_χ signal model with a pole mass of 2 TeV (4 TeV) by comparing yields in the core of the mass peak (within the full width at half maximum) between the distribution varied due to a given uncertainty and the nominal distribution. "—" represents cases where the uncertainty is not applicable.

nosity is 3.2%. It is derived, following a methodology similar to that detailed in ref. [52], from a calibration of the luminosity scale using x–y beam-separation scans performed in August 2015 and May 2016. Systematic uncertainties used in the statistical analysis of the results are summarised in table 2 at dilepton mass values of 2 TeV and 4 TeV. The systematic uncertainties are constrained in the likelihood during the statistical interpretation through a marginalisation procedure, as described in section 9.

m_{ee} [GeV]	80–120	120–250	250–400	400–500	500–700
Drell-Yan	11 800 000 ± 700 000	216 000 ± 11 000	17 230 ± 1000	2640 ± 180	1620 ± 120
Top quarks	28 600 ± 1800	44 600 ± 2900	8300 ± 600	1130 ± 80	560 ± 40
Dibosons	31 400 ± 3300	7000 ± 700	1300 ± 140	228 ± 25	146 ± 16
Multi-jet & W+jets	11 000 ± 9000	5600 ± 2000	780 ± 80	151 ± 21	113 ± 17
Total SM	11 900 000 ± 700 000	273 000 ± 12 000	27 600 ± 1100	4150 ± 200	2440 ± 130
Data	12 415 434	275 711	27 538	4140	2390
Z'_χ (4 TeV)	0.00635 ± 0.00021	0.0390 ± 0.0015	0.0564 ± 0.0025	0.0334 ± 0.0027	0.064 ± 0.004
Z'_χ (5 TeV)	0.00305 ± 0.00012	0.0165 ± 0.0006	0.0225 ± 0.0010	0.0139 ± 0.0007	0.0275 ± 0.0015
m_{ee} [GeV]	700–900	900–1200	1200–1800	1800–3000	3000–6000
Drell-Yan	421 ± 34	176 ± 17	62 ± 7	8.7 ± 1.3	0.34 ± 0.07
Top quarks	94 ± 8	27.9 ± 2.8	5.1 ± 0.7	< 0.001	< 0.001
Dibosons	39 ± 4	16.9 ± 2.1	5.8 ± 0.8	0.74 ± 0.11	0.028 ± 0.004
Multi-jet & W+jets	39 ± 6	16.1 ± 2.0	7.9 ± 2.3	1.6 ± 1.2	0.08 ± 0.27
Total SM	590 ± 40	237 ± 17	81 ± 7	11.0 ± 1.8	0.45 ± 0.28
Data	589	209	61	10	0
Z'_χ (4 TeV)	0.0585 ± 0.0035	0.074 ± 0.005	0.121 ± 0.011	0.172 ± 0.017	2.57 ± 0.27
Z'_χ (5 TeV)	0.0218 ± 0.0013	0.0295 ± 0.0021	0.040 ± 0.004	0.040 ± 0.004	0.280 ± 0.030

Table 3. Expected and observed event yields in the dielectron channel in different dilepton mass intervals. The quoted errors correspond to the combined statistical, theoretical, and experimental systematic uncertainties. Expected event yields are reported for the Z'_χ model, for two values of the pole mass. All numbers shown are obtained before the marginalisation procedure.

8 Event yields

Expected and observed event yields, in bins of invariant mass, are shown in table 3 for the dielectron channel, and in table 4 for the dimuon channel. Expected event yields are split into the different background sources and the yields for two signal scenarios are also provided. In general, the observed data are in good agreement with the SM prediction, taking into account the uncertainties as described in section 7.

Distributions of $m_{\ell\ell}$ in the dielectron and dimuon channels are shown in figure 1. No clear excess is observed, but significances are quantified and discussed in section 9. The highest dilepton invariant mass event is 2.90 TeV in the dielectron channel, and 1.99 TeV in the dimuon channel. Both of these events are well-measured with little other detector activity.

9 Statistical analysis

The $m_{\ell\ell}$ distributions are scrutinised for a resonant or non-resonant new physics excess using two methods and are used to set limits on resonant and non-resonant new physics models, as well as on generic resonances. Tabulated values of all the observed results, along with their uncertainties, are also provided in the Durham HEP database.[2] The signal search and limit setting rely on a likelihood function, dependent on the parameter of interest, such

[2]A complete set of tables with the full results are available at the Durham HepData repository, https://hepdata.net.

JHEP10(2017)182

$m_{\mu\mu}$ [GeV]	80–120	120–250	250–400	400–500	500–700
Drell-Yan	10 700 000 ± 600 000	177 900 ± 10 000	12 200 ± 700	1770 ± 120	1060 ± 80
Top quarks	24 700 ± 1700	34 200 ± 2400	6100 ± 500	830 ± 70	401 ± 33
Dibosons	26 000 ± 2800	5400 ± 600	910 ± 100	155 ± 17	93 ± 11
Total SM	10 800 000 ± 600 000	218 000 ± 10 000	19 200 ± 900	2760 ± 140	1550 ± 90
Data	11 321 561	224 703	19 239	2766	1532
Z'_χ (4 TeV)	0.00873 ± 0.00032	0.0334 ± 0.0015	0.0441 ± 0.0021	0.0246 ± 0.0014	0.052 ± 0.004
Z'_χ (5 TeV)	0.00347 ± 0.00014	0.0137 ± 0.0006	0.0151 ± 0.0007	0.0105 ± 0.0006	0.0176 ± 0.0012
$m_{\mu\mu}$ [GeV]	700–900	900–1200	1200–1800	1800–3000	3000–6000
Drell-Yan	263 ± 23	110 ± 11	37 ± 4	5.4 ± 0.8	0.30 ± 0.07
Top quarks	68 ± 6	24.5 ± 3.0	5.3 ± 0.9	0.11 ± 0.08	< 0.001
Dibosons	24.3 ± 2.9	9.8 ± 1.2	3.2 ± 0.4	0.45 ± 0.07	0.0184 ± 0.0035
Total SM	355 ± 24	144 ± 11	45 ± 4	6.0 ± 0.8	0.32 ± 0.07
Data	322	141	48	4	0
Z'_χ (4 TeV)	0.0362 ± 0.0026	0.048 ± 0.004	0.067 ± 0.006	0.186 ± 0.022	1.24 ± 0.19
Z'_χ (5 TeV)	0.0153 ± 0.0011	0.0185 ± 0.0015	0.0233 ± 0.0021	0.0258 ± 0.0029	0.118 ± 0.020

Table 4. Expected and observed event yields in the dimuon channel in different dilepton mass intervals. The quoted errors correspond to the combined statistical, theoretical, and experimental systematic uncertainties. Expected event yields are reported for the Z'_χ model, for two values of the pole mass. All numbers shown are obtained before the marginalisation procedure.

as the signal cross-section, signal strength, coupling constant or the contact interaction scale. The likelihood function also depends on nuisance parameters which describe the systematic uncertainties. In this analysis the data are assumed to be Poisson-distributed in each bin of the $m_{\ell\ell}$ distribution and the likelihood is constructed as a product of individual bin likelihoods. In case of the individual channel results, the product is taken over the bins of the $m_{\ell\ell}$ histogram in the given channel, while for combined results the product is taken over bins of histograms in dielectron and dimuon channels. The logarithmic $m_{\ell\ell}$ histogram binning shown in figure 1 uses 66 mass bins and is chosen for setting limits on resonant signals. This binning is optimal for resonances with a width of 3%, therefore the chosen bin width for the $m_{\ell\ell}$ histogram in the search phase corresponds to the resolution in the dielectron (dimuon) channel, which varies from 10 (60) GeV at $m_{\ell\ell} = 1$ TeV to 15 (200) GeV at $m_{\ell\ell} = 2$ TeV, and 20 (420) GeV at $m_{\ell\ell} = 3$ TeV. For setting limits on the contact interaction scale, the $m_{\ell\ell}$ distribution has eight bins above 400 GeV with bin widths varying from 100 to 1500 GeV. The $m_{\ell\ell}$ region from 80 to 120 GeV is included in the likelihood as a single bin in the limit setting on resonant signals to help constrain mass-independent components of systematic uncertainties, but that region is not searched for a new-physics signal.

The parameter μ is defined as the ratio of the signal production cross-section times branching ratio into the dilepton final state (σB) to its theoretically predicted value. Upper limits on σB for specific Z' boson models and generic Z' bosons, γ' of the Minimal Z' boson, and lower limit on the CI scale Λ are set in a Bayesian approach. The calculations are performed with the Bayesian Analysis Toolkit (BAT) [53], which uses a Markov Chain MC

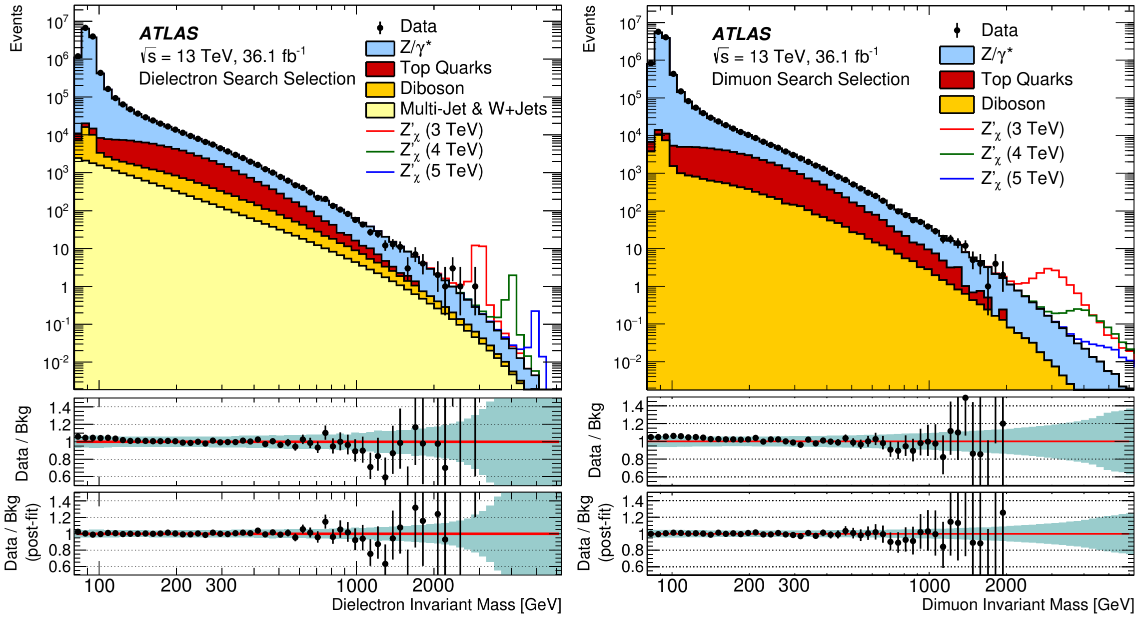

(a) **(b)**

Figure 1. Distributions of (a) dielectron and (b) dimuon reconstructed invariant mass ($m_{\ell\ell}$) after selection, for data and the SM background estimates as well as their ratio before and after marginalisation. Selected Z'_χ signals with a pole mass of 3, 4 and 5 TeV are overlaid. The bin width of the distributions is constant in $\log(m_{\ell\ell})$ and the shaded band in the lower panels illustrates the total systematic uncertainty, as explained in section 7. The data points are shown together with their statistical uncertainty. Exact bin edges and contents are provided in table 8 and table 9 in the appendix.

(MCMC) technique to compute the marginal posterior probability density of the parameter of interest (so-called "marginalisation"). Limit values obtained using the experimental data are quoted as observed limits, while median values of the limits obtained from a large number of simulated experiments, where only SM background is present, are quoted as the expected limits. The upper limits on σB are interpreted as lower limits on the Z' pole mass using the relationship between the pole mass and the theoretical Z' cross-section. In the context of the Minimal Z' model or CI scenarios, limits are set on the parameter of interest. In the case of the Minimal Z' model the parameter of interest is γ'^4. For a CI the parameter of interest is set either to $1/\Lambda^2$ or to $1/\Lambda^4$ as this corresponds to the scaling of the CI-SM interference contribution or the pure CI contribution respectively. In both the Minimal Z' and the CI cases, the nominal Poisson expectation in each $m_{\ell\ell}$ bin is expressed as a function of the parameter of interest. As in the context of the Z' limit setting, the Poisson mean is modified by shifts due to systematic uncertainties, but in both the Minimal Z' and the CI cases, these shifts are non-linear functions of the parameter of interest. A prior uniform in the parameter of interest is used for all limits.

Two complementary approaches are used in the search for a new-physics signal. The first approach, which does not rely on a specific signal model and therefore is sensitive to a wide range of new physics, uses the BumpHunter (BH) [54] utility. In this approach, all

JHEP10(2017)182

consecutive intervals in the $m_{\ell\ell}$ histogram ranging from two bins to half of the bins in the histogram are searched for an excess. In each such interval a Poisson probability (p-value) is computed for an event count greater or equal to the number observed found in data, given the SM prediction. The modes of marginalised posteriors of the nuisance parameters from the MCMC method are used to construct the SM prediction. The negative logarithm of the smallest p-value is the BH statistic. The BH statistic is then interpreted as a global p-value utilising simulated experiments where, in each simulated experiment, simulated data is generated from SM background model. The dielectron and dimuon channels are tested separately.

A search for Z'_χ signals as well as generic Z' signals with widths from 1% to 12% is performed utilising the log-likelihood ratio (LLR) test described in ref. [55]. This second approach is specifically sensitive to narrow Z'-like signals, and is thus complementary to the more general BH approach. To perform the LLR search, the Histfactory [56] package is used together with the RooStats [57] and RooFit [58] packages. The p-value for finding a Z'_χ signal excess (at a given pole mass), or a variable width generic Z' excess (at a given central mass and with a given width), more significant than that observed in the data, is computed analytically, using a test statistic q_0. The test statistic q_0 is based on the logarithm of the profile likelihood ratio $\lambda(\mu)$. The test statistic is modified for signal masses below 1.5 TeV to also quantify the significance of potential deficits in the data. As in the BH search the SM background model is constructed using the modes of marginalised posteriors of the nuisance parameters from the MCMC method, and these nuisance parameters are not included in the likelihood at this stage. Therefore, in the search-phase the background estimate and signal shapes are fixed to their post-marginalisation estimates, and systematic uncertainties are not included in the computation of the p-value. Starting with $M_{Z'} = 150$ GeV, multiple mass hypotheses are tested in pole-mass steps corresponding to the histogram bin width to compute the local p-values — i.e. p-values corresponding to specific signal mass hypotheses. Simulated experiments (for $M_{Z'} > 1.5$ TeV) and asymptotic relations (for $M_{Z'} < 1.5$ TeV) in ref. [55] are used to estimate the global p-value, which is the probability to find anywhere in the $m_{\ell\ell}$ distribution a Z'-like excess more significant than that observed in the data.

10 Results

The data, scrutinised using the statistical tests described in the previous section, show no significant excesses. The LLR tests for a Z'_χ resonance find global p-values of 58%, 91% and 83% in the dielectron, dimuon, and combined channels, respectively. The local and global p-values as a function of the Z' pole mass are shown in figure 2. The un-capped p-value, is used below a pole mass of 1.5 TeV, which quantifies both excesses and deficits, while above 1.5 TeV the signal strength parameter is constrained to be positive, yielding a capped p-value. This constraint is used in the high mass region where the expected background is very low, to avoid ill-defined configurations of the probability density function in the likelihood fit, with negative probabilities.

The largest deviation from the background-only hypothesis using the LLR tests for a Z'_χ is observed at 2.37 TeV in the dielectron mass spectrum with a local significance of

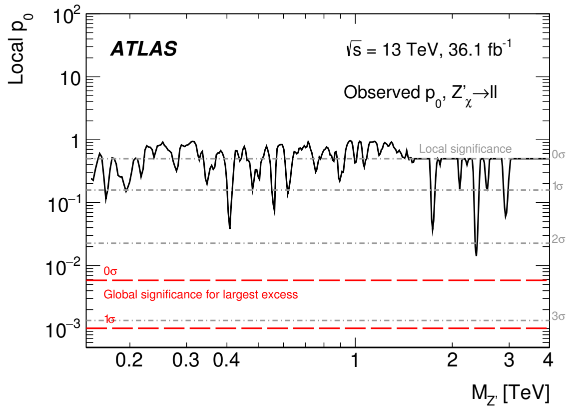

Figure 2. The local p-value derived assuming Z'_χ signal shapes with pole masses between 0.15 and 4.0 TeV for the combined dilepton channel. Accompanying local and global significance levels are shown as dashed lines. The *uncapped* p_0 value is used for pole masses below 1.5 TeV, while the *capped* p_0 value is used for higher pole masses.

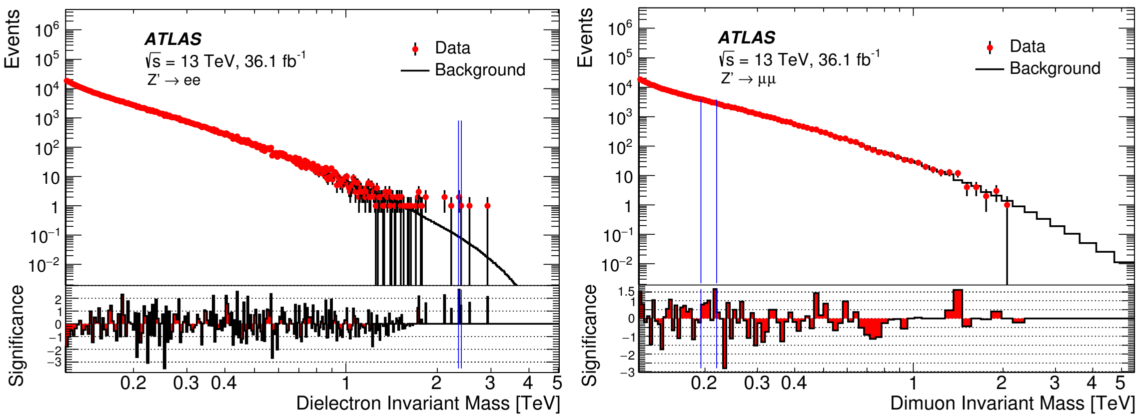

(a) (b)

Figure 3. Dilepton mass distribution in the (a) dielectron and (b) dimuon channel, showing the observed data together with their statistical uncertainty, combined background prediction, and corresponding bin-by-bin significance. The most significant interval is indicated by the vertical blue lines. Exact bin edges and contents are provided in table 10 and table 11 in the appendix.

2.5 σ, but globally the excess is not significant. The BumpHunter [54] test, which scans the mass spectrum with varying intervals to find the most significant excess in data, finds p-values of 71% and 94% in the dielectron and dimuon channels, respectively. Figure 3 shows the dilepton mass distribution in the dielectron and dimuon channels with the observed data overlaid on the combined background prediction, and also the local significance. The interval with the largest upward deviation is indicated by a pair of blue lines.

10.1 Z' cross-section and mass limits

Upper limits on the cross-section times branching ratio (σB) for Z' bosons are presented in figure 4. The observed and expected lower limits on the pole mass for various Z' scenarios,

JHEP10(2017)182

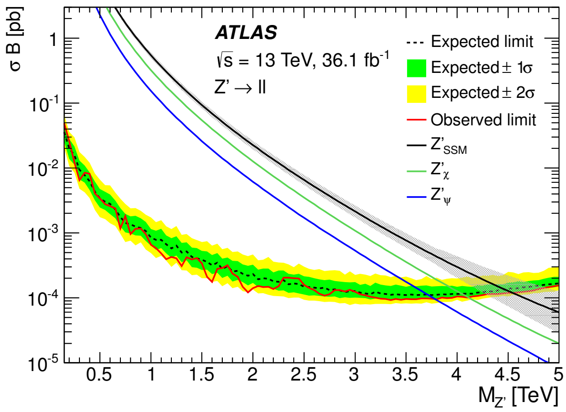

Figure 4. Upper 95% CL limits on the Z' production cross-section times branching ratio to two leptons of a single flavour as a function of Z' pole mass ($\mathrm{M}_{Z'}$). Results are shown for the combined dilepton channel. The signal theoretical σB are calculated with PYTHIA 8 using the NNPDF23LO PDF set [36], and corrected to next-to-next-to-leading order in QCD using VRAP [28] and the CT14NNLO PDF set [29]. The signals theoretical uncertainties are shown as a band on the Z'_{SSM} theory line for illustration purposes, but are not included in the σB limit calculation.

as described in section 2.1, are summarised in table 5. The Z'_χ signal is used to extract the limits, which is over-conservative for the other E_6 models presented, but slightly under-conservative for the Z'_{SSM}, although only by 100 GeV in the mass limit at most. The upper limits on σB for Z' bosons start to weaken above a pole mass of ~ 3.5 TeV. The effect is more pronounced in the dimuon channel due to worse mass resolution than in the dielectron channel. The weakening is mainly due to the combined effect of a rapidly falling signal cross-section as the kinematic limit is approached, with an increasing proportion of the signal being produced off-shell in the low-mass tail, and the natural width of the resonance. The selection efficiency also starts to slowly decrease at very high pole masses, but this is a subdominant effect.

10.2 Limits on Minimal Z' models

Limits are set on the relative coupling strength of the Z' boson relative to that of the SM Z boson (γ') as a function of the Z'_{Min} boson mass, and as a function of the mixing angle θ_{Min}, as shown in figure 5, and described in section 2.2. The two θ_{Min} values yielding the minimum and maximum cross-sections are used to define a band of limits in the (γ', $M_{Z_{\mathrm{Min}}}$) plane. It is possible to put lower mass limits on specific models which are covered by the (γ', θ_{Min}) parameterisation as in table 6. The structure observed in the limits as a function of θ_{Min}, such as the maximum around $\theta_{\mathrm{Min}} = 2.2$, is due to the changing shape of the resonance at a given pole mass, from narrow to wide.

10.3 Generic Z' limits

In order to derive more general limits, an approach which compares the data to signals that are more model-independent was developed. This was achieved by applying fiducial cuts to the signal (lepton $p_{\mathrm{T}} > 30$ GeV, and lepton $|\eta| < 2.5$) and a mass window of

JHEP10(2017)182

Model	Width [%]	θ_{E_6} [rad]	Lower limits on $\mathrm{M}_{Z'}$ [TeV]					
			ee		$\mu\mu$		$\ell\ell$	
			Obs	Exp	Obs	Exp	Obs	Exp
Z'_{SSM}	3.0	—	4.3	4.3	4.0	3.9	4.5	4.5
Z'_{χ}	1.2	$0.50\ \pi$	3.9	3.9	3.6	3.6	4.1	4.0
Z'_{S}	1.2	$0.63\ \pi$	3.9	3.8	3.6	3.5	4.0	4.0
Z'_{I}	1.1	$0.71\ \pi$	3.8	3.8	3.5	3.4	4.0	3.9
Z'_{η}	0.6	$0.21\ \pi$	3.7	3.7	3.4	3.3	3.9	3.8
Z'_{N}	0.6	$-0.08\ \pi$	3.6	3.6	3.4	3.3	3.8	3.8
Z'_{ψ}	0.5	$0\ \pi$	3.6	3.6	3.3	3.2	3.8	3.7

Table 5. Observed and expected 95% CL lower mass limits for various Z' gauge boson models. The widths are quoted as a percentage of the resonance mass.

Model	γ'	$\tan\theta_{\mathrm{Min}}$	Lower limits on $M_{Z'_{\mathrm{Min}}}$ [TeV]					
			ee		$\mu\mu$		$\ell\ell$	
			Obs	Exp	Obs	Exp	Obs	Exp
Z'_{χ}	$\sqrt{\frac{41}{24}}\sin\theta_{\mathrm{Min}}$	$-\frac{4}{5}$	3.7	3.7	3.4	3.3	3.9	3.8
Z'_{3R}	$\sqrt{\frac{5}{8}}\sin\theta_{\mathrm{Min}}$	-2	4.0	3.9	3.6	3.6	4.1	4.1
Z'_{B-L}	$\sqrt{\frac{25}{12}}\sin\theta_{\mathrm{Min}}$	0	4.0	4.0	3.6	3.6	4.2	4.1

Table 6. Observed and expected 95% CL lower mass limits for various Z'_{Min} models.

two times the true signal width (width of the Breit-Wigner) around the pole mass of the signal. This is expected to give limits that are more model independent since any effect on the sensitivity due to the tails of the resonance, foremost the parton luminosity tail and interference effects, are removed. The resulting limits can be seen in figure 6. For other models to be interpreted with these cross-section limits, the acceptance for a given model in the same fiducial region should be calculated, multiplied by the total cross-section, and the resulting acceptance-corrected cross-section theory curve overlaid, to extract the mass limit for that model. The dilepton invariant mass shape, and angular distributions for the chosen model, should be sufficiently close to a generic Z' resonance, such as those presented in this article, so as not to induce additional efficiency differences.

10.4 Limits on the energy scale of contact interactions

Lower limits are set at 95% CL on the energy scale Λ, for the LL, LR, RL, and RR Contact Interaction model, as described in section 2.3. Both the constructive and destructive

JHEP10(2017)182

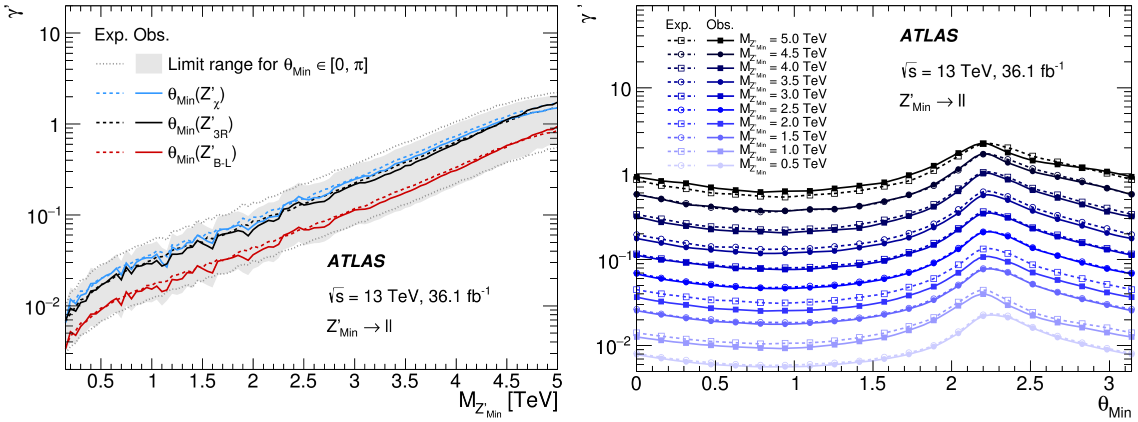

(a) **(b)**

Figure 5. (a) Expected (dotted and dashed lines) and observed (filled area and lines) limits are set at 95% CL on the relative coupling strength γ' for the dilepton channel as a function of the $Z'_{\rm Min}$ mass in the Minimal Z' model. Limit curves are shown for three representative values of the mixing angle, $\theta_{\rm Min}$, between the generators of the $({\rm B}-{\rm L})$ and the weak hypercharge Y gauge groups. These are: $\tan\theta_{\rm Min}=0$, $\tan\theta_{\rm Min}=-2$ and $\tan\theta_{\rm Min}=-0.8$, which correspond respectively to the $Z'_{\rm B-L}$, Z'_{3R} and Z'_{χ} models at specific values of γ'. The region above each line is excluded. The grey band envelops all observed limit curves, which depend on the choice of $\theta_{\rm Min}\in[0,\pi]$. The corresponding expected limit curves are within the area delimited by the two dotted lines. (b) Expected (empty markers and dashed lines) and observed (filled markers and lines) limits at 95% CL on γ' for the dilepton channel as a function of $\theta_{\rm Min}$. The limits are set for several representative values of the mass of the Z' boson, $M_{Z'_{\rm Min}}$. The region above each line is excluded.

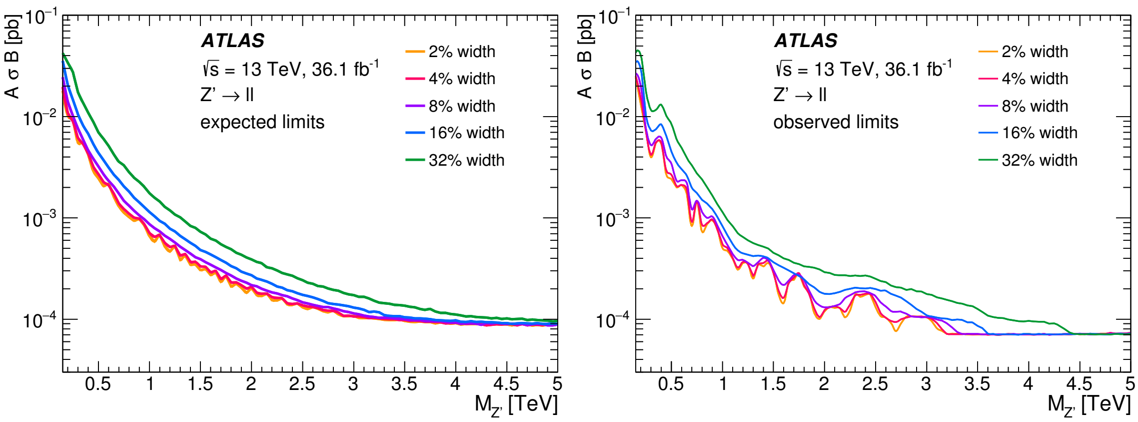

(a) **(b)**

Figure 6. Upper 95% CL limits on the acceptance times Z' production cross-section times branching ratio to two leptons of a single flavour as a function of Z' pole mass ($M_{Z'}$). (a) Expected and (b) observed limits in the combined dilepton channel for different widths with an applied mass window of two times the true width of the signal around the pole mass.

JHEP10(2017)182

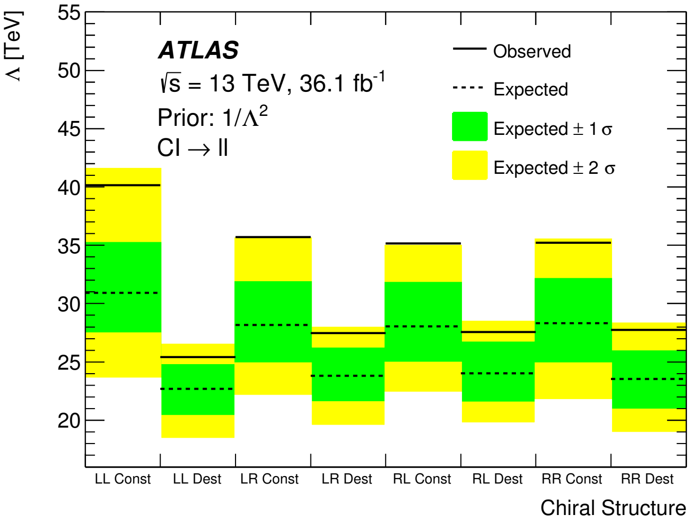

Figure 7. Lower limits on the energy scale Λ at 95% CL, for the Contact Interaction model with constructive (const) and destructive (dest) interference, and all considered chiral structures with left-handed (L) and right-handed (R) couplings. Results are shown for the combined dilepton channel.

interference scenarios are explored, as well as priors of $1/\Lambda^2$ and $1/\Lambda^4$. Limits are presented for the combined dilepton channel in figure 7 using a $1/\Lambda^2$ prior. All of the CI exclusion limits are summarised in table 7.

11 Conclusion

The ATLAS detector at the LHC has been used to search for both resonant and non-resonant new phenomena in the dilepton invariant mass spectrum above the Z boson's pole. The search is conducted with 36.1 fb^{-1} of pp collision data at $\sqrt{s} = 13$ TeV, recorded during 2015 and 2016. The highest invariant mass event is found at 2.90 TeV in the dielectron channel, and 1.99 TeV in the dimuon channel. The observed dilepton invariant mass spectrum is consistent with the Standard Model prediction, within systematic and statistical uncertainties. Among a choice of different models, the data are interpreted in terms of resonant spin-1 Z' gauge boson production and non-resonant $qq\ell\ell$ contact interactions. For the resonant interpretation, upper limits are set on the cross-section times branching ratio for a spin-1 Z' gauge boson. The resulting 95% CL lower mass limits are 4.5 TeV for the Z'_{SSM}, 4.1 TeV for the Z'_χ, and 3.8 TeV for the Z'_ψ. Other E_6 Z' models are also constrained in the range between those quoted for the Z'_χ and Z'_ψ. This result is more stringent than the previous ATLAS result at $\sqrt{s} = 13$ TeV obtained with 2015 data, by up to 700 GeV. Lower mass limits are also set on the Minimal Z' model, up to 4.1 TeV for the Z'_{3R}, and 4.2 TeV for the $Z'_{\mathrm{B-L}}$. Generic Z' cross-section limits are also provided for a range of true signal widths. The lower limits on the energy scale Λ for various $qq\ell\ell$ contact interaction models range between 24 TeV and 40 TeV, which are more stringent than the previous ATLAS result obtained at $\sqrt{s} = 13$ TeV, by up to 4 TeV.

Channel	Prior	Lower limits on Λ [TeV]							
		Left-Left		Left-Right		Right-Left		Right-Right	
		Const	Dest	Const	Dest	Const	Dest	Const	Dest
Obs: ee	$1/\Lambda^2$	37	24	33	26	33	26	33	26
Exp: ee		28	22	26	23	26	23	25	23
Obs: ee	$1/\Lambda^4$	32	22	29	24	29	24	29	24
Exp: ee		26	20	24	21	24	21	24	21
Obs: $\mu\mu$	$1/\Lambda^2$	30	20	28	22	28	22	28	20
Exp: $\mu\mu$		26	20	24	21	24	21	24	20
Obs: $\mu\mu$	$1/\Lambda^4$	27	19	25	21	25	21	25	19
Exp: $\mu\mu$		24	18	23	20	22	20	22	18
Obs: $\ell\ell$	$1/\Lambda^2$	40	25	36	28	35	28	35	28
Exp: $\ell\ell$		31	23	28	24	28	24	28	24
Obs: $\ell\ell$	$1/\Lambda^4$	35	24	32	25	32	25	31	25
Exp: $\ell\ell$		28	21	26	22	26	23	26	22

Table 7. Observed and expected 95% CL lower limits on Λ for the LL, LR, RL, and RR chiral coupling scenarios, for both the constructive (const) and destructive (dest) interference cases using a uniform positive prior in $1/\Lambda^2$ or $1/\Lambda^4$. The dielectron, dimuon, and combined dilepton channel limits are shown, rounded to two significant figures.

A Dilepton invariant mass tables

This appendix provides the exact bin edges and contents of the dilepton invariant mass plots presented in figures 1a, 1b, 3a, and 3b. These correspond to tables 8, 9, 10, and 11, respectively. Even more detailed information can be found in the Durham HEP database.[2]

JHEP10(2017)182

Lower edge [GeV]	Upper edge [GeV]	Data [N]	Total Background [N]
80	85.549	1176847	1112000
85.549	91.482	6608874	6322000
91.482	97.828	3928394	3756000
97.828	104.61	432217	414400
104.61	111.87	162962	156100
111.87	119.63	93773	90620
119.63	127.93	63446	62270
127.93	136.8	47190	46740
136.8	146.29	36539	36090
146.29	156.43	29267	28990
156.43	167.28	23874	23740
167.28	178.89	19689	19550
178.89	191.29	16548	16400
191.29	204.56	13671	13590
204.56	218.75	11337	11460
218.75	233.92	9358	9499
233.92	250.15	7877	7868
250.15	267.5	6434	6570
267.5	286.05	5500	5427
286.05	305.89	4445	4477
305.89	327.11	3648	3667
327.11	349.79	2981	2995
349.79	374.06	2431	2403
374.06	400	1964	1957
400	427.74	1606	1565
427.74	457.41	1231	1265
457.41	489.14	1013	1008
489.14	523.06	776	805.6
523.06	559.34	622	628.7
559.34	598.14	464	492.3
598.14	639.63	403	392.6
639.63	683.99	300	304.4
683.99	731.43	219	234.3
731.43	782.16	202	183.2
782.16	836.41	133	140.2
836.41	894.43	107	107.1
894.43	956.46	82	85.13
956.46	1022.8	57	63.86
1022.8	1093.7	43	47.9

JHEP10(2017)182

1093.7	1169.6	27	38.09
1169.6	1250.7	24	28.7
1250.7	1337.5	12	20.28
1337.5	1430.2	13	14.96
1430.2	1529.4	11	11.16
1529.4	1635.5	3	8.262
1635.5	1749	7	6.003
1749	1870.3	4	4.085
1870.3	2000	0	2.875
2000	2138.7	2	2.05
2138.7	2287.1	1	1.431
2287.1	2445.7	3	0.977
2445.7	2615.3	1	0.655
2615.3	2796.7	0	0.443
2796.7	2990.7	1	0.284
2990.7	3198.1	0	0.183
3198.1	3420	0	0.114
3420	3657.2	0	0.068
3657.2	3910.8	0	0.041
3910.8	4182.1	0	0.023
4182.1	4472.1	0	0.013
4472.1	4782.3	0	0.007
4782.3	5114	0	0.004
5114	5468.7	0	0.002
5468.7	5848	0	0.001
5848	6253.7	0	0

Table 8. Expected and observed event yields in the dielectron channel, directly corresponding to the non-linear binning presented in figure 1a. The expected yield is given up to at most 4 digit precision.

Lower edge [GeV]	Upper edge [GeV]	Data [N]	Total Background [N]
80	85.549	826504	786600
85.549	91.482	5730639	5465000
91.482	97.828	4062661	3848000
97.828	104.61	430822	405500
104.61	111.87	149927	141800
111.87	119.63	82971	79230
119.63	127.93	54641	52110
127.93	136.8	39501	37890
136.8	146.29	29742	28940

146.29	156.43	23871	23220
156.43	167.28	18942	18490
167.28	178.89	15482	15140
178.89	191.29	12495	12250
191.29	204.56	10462	10230
204.56	218.75	8583	8261
218.75	233.92	6868	6885
233.92	250.15	5649	5517
250.15	267.5	4723	4607
267.5	286.05	3762	3753
286.05	305.89	3064	3106
305.89	327.11	2471	2566
327.11	349.79	2031	1992
349.79	374.06	1595	1628
374.06	400	1333	1321
400	427.74	1018	1022
427.74	457.41	819	828.1
457.41	489.14	675	651.9
489.14	523.06	508	513.6
523.06	559.34	397	410.7
559.34	598.14	306	306
598.14	639.63	252	245.7
639.63	683.99	188	191.2
683.99	731.43	129	142.2
731.43	782.16	97	108.5
782.16	836.41	78	82.36
836.41	894.43	57	63.72
894.43	956.46	51	51.88
956.46	1022.8	39	39.04
1022.8	1093.7	29	29.74
1093.7	1169.6	18	21.83
1169.6	1250.7	18	16.12
1250.7	1337.5	14	12.7
1337.5	1430.2	12	8.053
1430.2	1529.4	5	5.803
1529.4	1635.5	4	4.667
1635.5	1749	1	3.241
1749	1870.3	4	2.135
1870.3	2000	2	1.663
2000	2138.7	0	1.102

JHEP10(2017)182

2138.7	2287.1	0	0.763
2287.1	2445.7	0	0.538
2445.7	2615.3	0	0.375
2615.3	2796.7	0	0.250
2796.7	2990.7	0	0.165
2990.7	3198.1	0	0.112
3198.1	3420	0	0.078
3420	3657.2	0	0.049
3657.2	3910.8	0	0.031
3910.8	4182.1	0	0.022
4182.1	4472.1	0	0.013
4472.1	4782.3	0	0.010
4782.3	5114	0	0.006
5114	5468.7	0	0.005
5468.7	5848	0	0.002
5848	6253.7	0	0.002

Table 9. Expected and observed event yields in the dimuon channel, directly corresponding to the non-linear binning presented in figure 1b. The expected yield is given up to at most 4 digit precision.

Lower edge [TeV]	Upper edge [TeV]	Data [N]	Total Background [N]
0.11962	0.12171	18432	18660
0.12171	0.12381	16720	16840
0.12381	0.12592	15291	15340
0.12592	0.12806	13924	14020
0.12806	0.13022	12931	12960
0.13022	0.13239	11976	11970
0.13239	0.13459	11154	11120
0.13459	0.1368	10273	10350
0.1368	0.13903	9637	9677
0.13903	0.14128	9017	9029
0.14128	0.14355	8392	8460
0.14355	0.14584	8043	7949
0.14584	0.14815	7387	7507
0.14815	0.15048	7122	7073
0.15048	0.15283	6695	6680
0.15283	0.1552	6382	6278
0.1552	0.15758	5933	6018
0.15758	0.15999	5737	5697
0.15999	0.16242	5352	5380

JHEP10(2017)182

0.16242	0.16487	5097	5158
0.16487	0.16733	4972	4893
0.16733	0.16982	4726	4622
0.16982	0.17233	4455	4437
0.17233	0.17486	4165	4198
0.17486	0.17741	3979	4058
0.17741	0.17998	3920	3868
0.17998	0.18257	3629	3687
0.18257	0.18518	3671	3531
0.18518	0.18782	3392	3349
0.18782	0.19047	3154	3207
0.19047	0.19315	3182	3081
0.19315	0.19584	2964	2957
0.19584	0.19856	2826	2825
0.19856	0.2013	2687	2712
0.2013	0.20406	2637	2593
0.20406	0.20685	2380	2510
0.20685	0.20965	2436	2396
0.20965	0.21248	2223	2295
0.21248	0.21533	2166	2202
0.21533	0.2182	2152	2089
0.2182	0.2211	2030	2003
0.2211	0.22402	1803	1938
0.22402	0.22696	1869	1831
0.22696	0.22992	1736	1774
0.22992	0.23291	1788	1726
0.23291	0.23591	1605	1646
0.23591	0.23895	1651	1576
0.23895	0.242	1530	1515
0.242	0.24508	1386	1453
0.24508	0.24818	1398	1398
0.24818	0.25131	1354	1328
0.25131	0.25446	1171	1297
0.25446	0.25763	1293	1246
0.25763	0.26083	1139	1191
0.26083	0.26405	1187	1155
0.26405	0.2673	1075	1117
0.2673	0.27057	1051	1073
0.27057	0.27387	1045	1022
0.27387	0.27719	1011	988.8

0.27719	0.28053	953	943.4
0.28053	0.2839	966	908.3
0.2839	0.2873	834	878.5
0.2873	0.29072	820	840.8
0.29072	0.29416	813	809.1
0.29416	0.29764	799	782.9
0.29764	0.30113	723	742.1
0.30113	0.30466	746	722.8
0.30466	0.30821	692	696.2
0.30821	0.31178	655	668.4
0.31178	0.31539	639	656.2
0.31539	0.31901	607	615.3
0.31901	0.32267	594	597.5
0.32267	0.32635	586	568.5
0.32635	0.33006	560	550.5
0.33006	0.3338	524	520.3
0.3338	0.33756	475	512.2
0.33756	0.34135	500	499
0.34135	0.34517	490	466.4
0.34517	0.34902	465	443.6
0.34902	0.35289	443	436.7
0.35289	0.3568	417	420.2
0.3568	0.36073	413	393.5
0.36073	0.36468	377	380.7
0.36468	0.36867	410	366.5
0.36867	0.37269	338	365.1
0.37269	0.37673	373	358.6
0.37673	0.38081	330	338.5
0.38081	0.38491	304	311.7
0.38491	0.38905	312	306.7
0.38905	0.39321	299	308.5
0.39321	0.3974	290	281.3
0.3974	0.40162	268	272.1
0.40162	0.40588	298	261.1
0.40588	0.41016	281	255.1
0.41016	0.41447	253	240
0.41447	0.41882	235	237.1
0.41882	0.42319	242	228.2
0.42319	0.4276	192	216.4
0.4276	0.43203	215	210.4

JHEP10(2017)182

0.43203	0.4365	192	204.7
0.4365	0.441	231	194.4
0.441	0.44553	171	186
0.44553	0.4501	184	181
0.4501	0.45469	153	172.6
0.45469	0.45932	153	168.9
0.45932	0.46398	178	156.2
0.46398	0.46867	150	157.4
0.46867	0.4734	139	158.8
0.4734	0.47816	171	144.5
0.47816	0.48295	138	143.3
0.48295	0.48778	140	131.8
0.48778	0.49264	121	127.9
0.49264	0.49753	117	127.2
0.49753	0.50246	127	119.3
0.50246	0.50742	127	114.7
0.50742	0.51242	100	113.8
0.51242	0.51745	101	105.1
0.51745	0.52252	113	105.4
0.52252	0.52762	94	100.9
0.52762	0.53276	82	95.19
0.53276	0.53793	101	90.98
0.53793	0.54314	74	87.16
0.54314	0.54839	89	85.14
0.54839	0.55367	92	81.42
0.55367	0.55898	91	81.14
0.55898	0.56434	84	78.37
0.56434	0.56973	96	74.86
0.56973	0.57516	51	73.66
0.57516	0.58062	60	65.09
0.58062	0.58613	59	66.37
0.58613	0.59167	64	63.71
0.59167	0.59725	47	63.18
0.59725	0.60286	62	62.67
0.60286	0.60852	64	59.51
0.60852	0.61422	54	51.24
0.61422	0.61995	62	52.4
0.61995	0.62572	49	49.37
0.62572	0.63153	57	50.37
0.63153	0.63739	48	48.26

JHEP10(2017)182

0.63739	0.64328	43	48.46
0.64328	0.64921	41	45.4
0.64921	0.65518	45	42.38
0.65518	0.6612	42	40.13
0.6612	0.66725	40	40.51
0.66725	0.67335	36	36.82
0.67335	0.67949	33	38.69
0.67949	0.68567	44	34.63
0.68567	0.69189	27	34.25
0.69189	0.69815	36	35.36
0.69815	0.70446	40	31.61
0.70446	0.71081	24	30.31
0.71081	0.7172	21	28.97
0.7172	0.72363	29	28.06
0.72363	0.73011	29	26.9
0.73011	0.73663	35	26.39
0.73663	0.7432	20	25.87
0.7432	0.74981	31	24.46
0.74981	0.75647	27	24.33
0.75647	0.76317	26	23.24
0.76317	0.76991	25	22.35
0.76991	0.77671	19	21.38
0.77671	0.78354	27	20.01
0.78354	0.79043	21	21
0.79043	0.79736	15	18.29
0.79736	0.80433	17	18.3
0.80433	0.81136	22	17.46
0.81136	0.81843	13	17.52
0.81843	0.82555	17	19.08
0.82555	0.83271	17	16.08
0.83271	0.83993	18	15.5
0.83993	0.84719	12	14.39
0.84719	0.8545	14	14.37
0.8545	0.86186	20	12.71
0.86186	0.86927	9	13.61
0.86927	0.87673	8	12.34
0.87673	0.88424	17	12.77
0.88424	0.8918	10	12.03
0.8918	0.89941	19	11.72
0.89941	0.90708	8	11

0.90708	0.91479	12	10.91
0.91479	0.92255	14	10.52
0.92255	0.93037	13	10.63
0.93037	0.93824	5	9.507
0.93824	0.94616	10	9.246
0.94616	0.95413	8	9.899
0.95413	0.96216	6	9.358
0.96216	0.97024	7	9.246
0.97024	0.97838	5	8.622
0.97838	0.98657	7	7.47
0.98657	0.99481	9	8.008
0.99481	1.0031	8	6.946
1.0031	1.0115	10	6.434
1.0115	1.0199	5	6.917
1.0199	1.0283	4	6.297
1.0283	1.0369	3	6.431
1.0369	1.0454	4	5.779
1.0454	1.0541	5	6.033
1.0541	1.0628	9	5.665
1.0628	1.0715	7	5.245
1.0715	1.0803	3	5.998
1.0803	1.0892	6	4.778
1.0892	1.0981	6	4.841
1.0981	1.1071	2	4.69
1.1071	1.1162	3	4.427
1.1162	1.1253	4	4.615
1.1253	1.1344	3	4.067
1.1344	1.1437	3	4.272
1.1437	1.1529	3	4.283
1.1529	1.1623	2	4.086
1.1623	1.1717	4	4.619
1.1717	1.1812	3	3.411
1.1812	1.1907	6	3.524
1.1907	1.2003	2	3.687
1.2003	1.21	2	3.449
1.21	1.2197	5	3.116
1.2197	1.2295	0	3.312
1.2295	1.2393	3	3.577
1.2393	1.2493	2	2.714
1.2493	1.2593	1	2.86

1.2593	1.2693	4	2.6
1.2693	1.2794	1	2.416
1.2794	1.2896	2	2.339
1.2896	1.2999	0	2.305
1.2999	1.3102	2	2.494
1.3102	1.3206	2	2.128
1.3206	1.331	1	1.947
1.331	1.3416	1	1.946
1.3416	1.3522	3	1.999
1.3522	1.3628	0	1.673
1.3628	1.3736	2	1.917
1.3736	1.3844	0	1.753
1.3844	1.3953	3	1.592
1.3953	1.4062	1	1.503
1.4062	1.4172	1	1.43
1.4172	1.4283	2	1.445
1.4283	1.4395	0	1.361
1.4395	1.4507	1	1.415
1.4507	1.462	1	1.253
1.462	1.4734	2	1.2
1.4734	1.4849	2	1.389
1.4849	1.4964	0	1.177
1.4964	1.5081	2	1.17
1.5081	1.5198	1	1.142
1.5198	1.5315	2	0.959
1.5315	1.5434	0	1.074
1.5434	1.5553	1	0.878
1.5553	1.5673	0	1.037
1.5673	1.5794	0	0.843
1.5794	1.5915	0	0.787
1.5915	1.6038	1	0.922
1.6038	1.6161	1	0.767
1.6161	1.6285	0	0.873
1.6285	1.641	1	0.711
1.641	1.6536	0	0.683
1.6536	1.6662	0	0.808
1.6662	1.6789	0	0.682
1.6789	1.6918	0	0.627
1.6918	1.7047	1	0.702
1.7047	1.7176	0	0.562

JHEP10(2017)182

1.7176	1.7307	2	0.569
1.7307	1.7439	3	0.530
1.7439	1.7571	0	0.513
1.7571	1.7704	1	0.478
1.7704	1.7839	1	0.475
1.7839	1.7974	0	0.440
1.7974	1.811	0	0.434
1.811	1.8246	0	0.418
1.8246	1.8384	2	0.384
1.8384	1.8523	0	0.370
1.8523	1.8662	0	0.367
1.8662	1.8803	0	0.341
1.8803	1.8944	0	0.338
1.8944	1.9086	0	0.323
1.9086	1.923	0	0.294
1.923	1.9374	0	0.293
1.9374	1.9519	0	0.295
1.9519	1.9665	0	0.257
1.9665	1.9812	0	0.266
1.9812	1.996	0	0.243
1.996	2.0109	0	0.241
2.0109	2.0259	0	0.226
2.0259	2.041	0	0.223
2.041	2.0561	0	0.207
2.0561	2.0714	0	0.204
2.0714	2.0868	0	0.196
2.0868	2.1023	0	0.189
2.1023	2.1179	2	0.174
2.1179	2.1336	0	0.173
2.1336	2.1494	0	0.163
2.1494	2.1653	0	0.159
2.1653	2.1813	0	0.146
2.1813	2.1974	0	0.146
2.1974	2.2136	0	0.138
2.2136	2.2299	1	0.131
2.2299	2.2463	0	0.128
2.2463	2.2629	0	0.121
2.2629	2.2795	0	0.119
2.2795	2.2963	0	0.109
2.2963	2.3131	0	0.106

2.3131	2.3301	0	0.099
2.3301	2.3472	0	0.095
2.3472	2.3643	2	0.092
2.3643	2.3816	0	0.089
2.3816	2.3991	1	0.082
2.3991	2.4166	0	0.078
2.4166	2.4342	0	0.077
2.4342	2.452	0	0.071
2.452	2.4699	0	0.068
2.4699	2.4879	0	0.064
2.4879	2.506	0	0.061
2.506	2.5242	0	0.059
2.5242	2.5425	0	0.054
2.5425	2.561	1	0.053
2.561	2.5796	0	0.050
2.5796	2.5983	0	0.046
2.5983	2.6171	0	0.045
2.6171	2.6361	0	0.042
2.6361	2.6551	0	0.040
2.6551	2.6743	0	0.039
2.6743	2.6937	0	0.035
2.6937	2.7131	0	0.036
2.7131	2.7327	0	0.032
2.7327	2.7524	0	0.031
2.7524	2.7722	0	0.028
2.7722	2.7922	0	0.026
2.7922	2.8123	0	0.025
2.8123	2.8325	0	0.023
2.8325	2.8529	0	0.022
2.8529	2.8734	0	0.021
2.8734	2.894	0	0.019
2.894	2.9147	0	0.018
2.9147	2.9356	1	0.016
2.9356	2.9567	0	0.015
2.9567	2.9778	0	0.015
2.9778	2.9991	0	0.013
2.9991	3.0206	0	0.012
3.0206	3.0421	0	0.012
3.0421	3.0639	0	0.010
3.0639	3.0857	0	0.010

JHEP10(2017)182

3.0857	3.1077	0	0.010
3.1077	3.1299	0	0.008
3.1299	3.1522	0	0.007
3.1522	3.1746	0	0.006
3.1746	3.1972	0	0.006
3.1972	3.2199	0	0.005
3.2199	3.2428	0	0.005
3.2428	3.2659	0	0.004
3.2659	3.289	0	0.004
3.289	3.3124	0	0.003
3.3124	3.3358	0	0.003
3.3358	3.3595	0	0.002
3.3595	3.3833	0	0.002
3.3833	3.4072	0	0.001
3.4072	3.4313	0	0
3.4313	3.4556	0	0
3.4556	3.48	0	0
3.48	3.5046	0	0
3.5046	3.5293	0	0
3.5293	3.5542	0	0
3.5542	3.5792	0	0
3.5792	3.6045	0	0
3.6045	3.6298	0	0
3.6298	3.6554	0	0
3.6554	3.6811	0	0
3.6811	3.707	0	0
3.707	3.733	0	0
3.733	3.7593	0	0
3.7593	3.7857	0	0
3.7857	3.8122	0	0
3.8122	3.839	0	0
3.839	3.8659	0	0
3.8659	3.893	0	0
3.893	3.9202	0	0
3.9202	3.9477	0	0
3.9477	3.9753	0	0
3.9753	4.0031	0	0
4.0031	4.031	0	0
4.031	4.0592	0	0
4.0592	4.0875	0	0

4.0875	4.1161	0	0
4.1161	4.1448	0	0
4.1448	4.1737	0	0
4.1737	4.2028	0	0
4.2028	4.2321	0	0
4.2321	4.2615	0	0
4.2615	4.2912	0	0
4.2912	4.321	0	0
4.321	4.3511	0	0
4.3511	4.3813	0	0
4.3813	4.4118	0	0
4.4118	4.4424	0	0
4.4424	4.4732	0	0
4.4732	4.5043	0	0
4.5043	4.5355	0	0
4.5355	4.5669	0	0
4.5669	4.5986	0	0
4.5986	4.6304	0	0
4.6304	4.6625	0	0
4.6625	4.6948	0	0
4.6948	4.7272	0	0
4.7272	4.7599	0	0
4.7599	4.7928	0	0
4.7928	4.8259	0	0
4.8259	4.8593	0	0
4.8593	4.8928	0	0
4.8928	4.9266	0	0
4.9266	4.9606	0	0
4.9606	4.9948	0	0
4.9948	5.0292	0	0

Table 10. Expected and observed event yields in the dielectron channel, directly corresponding to the non-linear binning presented in figure 3a. The expected yield is given up to at most 4 digit precision.

Lower edge [TeV]	Upper edge [TeV]	Data [N]	Total Background [N]
0.12016	0.12264	18410	18200
0.12264	0.12518	16432	16330
0.12518	0.12779	14813	14840
0.12779	0.13047	13545	13540
0.13047	0.13322	12246	12410

JHEP10(2017)182

0.13322	0.13605	11539	11430
0.13605	0.13895	10520	10540
0.13895	0.14193	9737	9778
0.14193	0.145	8911	9085
0.145	0.14816	8435	8435
0.14816	0.1514	7944	7904
0.1514	0.15474	7448	7365
0.15474	0.15817	6843	6907
0.15817	0.16171	6542	6490
0.16171	0.16535	6012	6107
0.16535	0.1691	5748	5707
0.1691	0.17296	5411	5364
0.17296	0.17695	5045	5023
0.17695	0.18106	4772	4739
0.18106	0.18529	4354	4437
0.18529	0.18966	4200	4209
0.18966	0.19417	3950	3968
0.19417	0.19883	3786	3740
0.19883	0.20364	3580	3530
0.20364	0.20862	3346	3290
0.20862	0.21376	3061	3069
0.21376	0.21908	2990	2902
0.21908	0.22458	2732	2716
0.22458	0.23027	2543	2546
0.23027	0.23617	2250	2387
0.23617	0.24229	2279	2238
0.24229	0.24862	2056	2109
0.24862	0.2552	1995	1973
0.2552	0.26202	1833	1844
0.26202	0.2691	1752	1711
0.2691	0.27646	1592	1596
0.27646	0.28411	1435	1476
0.28411	0.29207	1390	1376
0.29207	0.30036	1242	1294
0.30036	0.30899	1192	1198
0.30899	0.31798	1072	1113
0.31798	0.32736	1018	1038
0.32736	0.33716	948	928.1
0.33716	0.34739	879	859.4
0.34739	0.35809	788	790.5

0.35809	0.36928	710	741.1
0.36928	0.381	670	670.8
0.381	0.39328	639	625.3
0.39328	0.40617	554	554.9
0.40617	0.41971	488	500.2
0.41971	0.43394	462	461.4
0.43394	0.44892	423	415.9
0.44892	0.4647	373	380.8
0.4647	0.48135	369	338.4
0.48135	0.49893	305	298.3
0.49893	0.51752	285	267.7
0.51752	0.53721	241	241.8
0.53721	0.55808	208	215.6
0.55808	0.58025	184	185.6
0.58025	0.60383	182	166.6
0.60383	0.62894	147	147.7
0.62894	0.65575	137	130.5
0.65575	0.68441	109	113.4
0.68441	0.71511	88	96.05
0.71511	0.74806	74	83.54
0.74806	0.78351	62	70.07
0.78351	0.82173	58	59.76
0.82173	0.86303	51	51.36
0.86303	0.90778	42	42.21
0.90778	0.95641	34	37.59
0.95641	1.0094	31	31.15
1.0094	1.0673	27	26
1.0673	1.1308	20	20.31
1.1308	1.2007	16	15.91
1.2007	1.2779	13	13.11
1.2779	1.3636	13	10.92
1.3636	1.459	12	6.931
1.459	1.5659	4	5.6
1.5659	1.6861	4	4.324
1.6861	1.8222	2	2.72
1.8222	1.9772	3	2.067
1.9772	2.1548	1	1.374
2.1548	2.3599	0	0.882
2.3599	2.5987	0	0.570
2.5987	2.8794	0	0.333

JHEP10(2017)182

2.8794	3.2131	0	0.188
3.2131	3.6149	0	0.104
3.6149	4.1068	0	0.049
4.1068	4.7222	0	0.025
4.7222	5.5164	0	0.010

Table 11. Expected and observed event yields in the dimuon channel, directly corresponding to the non-linear binning presented in figure 3b. The expected yield is given up to at most 4 digit precision.

Acknowledgments

We thank CERN for the very successful operation of the LHC, as well as the support staff from our institutions without whom ATLAS could not be operated efficiently.

We acknowledge the support of ANPCyT, Argentina; YerPhI, Armenia; ARC, Australia; BMWFW and FWF, Austria; ANAS, Azerbaijan; SSTC, Belarus; CNPq and FAPESP, Brazil; NSERC, NRC and CFI, Canada; CERN; CONICYT, Chile; CAS, MOST and NSFC, China; COLCIENCIAS, Colombia; MSMT CR, MPO CR and VSC CR, Czech Republic; DNRF and DNSRC, Denmark; IN2P3-CNRS, CEA-DSM/IRFU, France; SRNSF, Georgia; BMBF, HGF, and MPG, Germany; GSRT, Greece; RGC, Hong Kong SAR, China; ISF, I-CORE and Benoziyo Center, Israel; INFN, Italy; MEXT and JSPS, Japan; CNRST, Morocco; NWO, Netherlands; RCN, Norway; MNiSW and NCN, Poland; FCT, Portugal; MNE/IFA, Romania; MES of Russia and NRC KI, Russian Federation; JINR; MESTD, Serbia; MSSR, Slovakia; ARRS and MIZŠ, Slovenia; DST/NRF, South Africa; MINECO, Spain; SRC and Wallenberg Foundation, Sweden; SERI, SNSF and Cantons of Bern and Geneva, Switzerland; MOST, Taiwan; TAEK, Turkey; STFC, United Kingdom; DOE and NSF, United States of America. In addition, individual groups and members have received support from BCKDF, the Canada Council, CANARIE, CRC, Compute Canada, FQRNT, and the Ontario Innovation Trust, Canada; EPLANET, ERC, ERDF, FP7, Horizon 2020 and Marie Sklodowska-Curie Actions, European Union; Investissements d'Avenir Labex and Idex, ANR, Région Auvergne and Fondation Partager le Savoir, France; DFG and AvH Foundation, Germany; Herakleitos, Thales and Aristeia programmes co-financed by EU-ESF and the Greek NSRF; BSF, GIF and Minerva, Israel; BRF, Norway; CERCA Programme Generalitat de Catalunya, Generalitat Valenciana, Spain; the Royal Society and Leverhulme Trust, United Kingdom.

The crucial computing support from all WLCG partners is acknowledged gratefully, in particular from CERN, the ATLAS Tier-1 facilities at TRIUMF (Canada), NDGF (Denmark, Norway, Sweden), CC-IN2P3 (France), KIT/GridKA (Germany), INFN-CNAF (Italy), NL-T1 (Netherlands), PIC (Spain), ASGC (Taiwan), RAL (U.K.) and BNL (U.S.A.), the Tier-2 facilities worldwide and large non-WLCG resource providers. Major contributors of computing resources are listed in ref. [59].

References

[1] D. London and J.L. Rosner, *Extra Gauge Bosons in E_6*, Phys. Rev. **D 34** (1986) 1530 [INSPIRE].

[2] P. Langacker, *The Physics of Heavy Z' Gauge Bosons*, Rev. Mod. Phys. **81** (2009) 1199 [arXiv:0801.1345] [INSPIRE].

[3] E. Salvioni, G. Villadoro and F. Zwirner, *Minimal Z' models: Present bounds and early LHC reach*, JHEP **11** (2009) 068 [arXiv:0909.1320] [INSPIRE].

[4] ATLAS collaboration, *Search for high-mass new phenomena in the dilepton final state using proton-proton collisions at $\sqrt{s} = 13$ TeV with the ATLAS detector*, Phys. Lett. **B 761** (2016) 372 [arXiv:1607.03669] [INSPIRE].

[5] CMS collaboration, *Search for narrow resonances in dilepton mass spectra in proton-proton collisions at $\sqrt{s} = 13$ TeV and combination with 8 TeV data*, Phys. Lett. **B 768** (2017) 57 [arXiv:1609.05391] [INSPIRE].

[6] L. Randall and R. Sundrum, *A Large mass hierarchy from a small extra dimension*, Phys. Rev. Lett. **83** (1999) 3370 [hep-ph/9905221] [INSPIRE].

[7] P. Meade and L. Randall, *Black Holes and Quantum Gravity at the LHC*, JHEP **05** (2008) 003 [arXiv:0708.3017] [INSPIRE].

[8] M.V. Chizhov, V.A. Bednyakov and J.A. Budagov, *Proposal for chiral bosons search at LHC via their unique new signature*, Phys. Atom. Nucl. **71** (2008) 2096 [arXiv:0801.4235] [INSPIRE].

[9] F. Sannino and K. Tuominen, *Orientifold theory dynamics and symmetry breaking*, Phys. Rev. **D 71** (2005) 051901 [hep-ph/0405209] [INSPIRE].

[10] CMS collaboration, *Search for physics beyond the standard model in dilepton mass spectra in proton-proton collisions at $\sqrt{s} = 8$ TeV*, JHEP **04** (2015) 025 [arXiv:1412.6302] [INSPIRE].

[11] M. Dittmar, A.-S. Nicollerat and A. Djouadi, *Z' studies at the LHC: An Update*, Phys. Lett. **B 583** (2004) 111 [hep-ph/0307020] [INSPIRE].

[12] E. Accomando, A. Belyaev, L. Fedeli, S.F. King and C. Shepherd-Themistocleous, *Z' physics with early LHC data*, Phys. Rev. **D 83** (2011) 075012 [arXiv:1010.6058] [INSPIRE].

[13] G. Senjanović and R.N. Mohapatra, *Exact Left-Right Symmetry and Spontaneous Violation of Parity*, Phys. Rev. **D 12** (1975) 1502 [INSPIRE].

[14] R.N. Mohapatra and J.C. Pati, *Left-Right Gauge Symmetry and an Isoconjugate Model of CP-violation*, Phys. Rev. **D 11** (1975) 566 [INSPIRE].

[15] L. Basso, A. Belyaev, S. Moretti and C.H. Shepherd-Themistocleous, *Phenomenology of the minimal $B - L$ extension of the Standard model: Z' and neutrinos*, Phys. Rev. **D 80** (2009) 055030 [arXiv:0812.4313] [INSPIRE].

[16] ATLAS collaboration, *Search for high-mass dilepton resonances in pp collisions at $\sqrt{s} = 8$ TeV with the ATLAS detector*, Phys. Rev. **D 90** (2014) 052005 [arXiv:1405.4123] [INSPIRE].

JHEP10(2017)182

[17] E. Eichten, K.D. Lane and M.E. Peskin, *New Tests for Quark and Lepton Substructure*, *Phys. Rev. Lett.* **50** (1983) 811 [INSPIRE].

[18] E. Eichten, I. Hinchliffe, K.D. Lane and C. Quigg, *Super Collider Physics*, *Rev. Mod. Phys.* **56** (1984) 579 [INSPIRE].

[19] N. Arkani-Hamed, S. Dimopoulos and G.R. Dvali, *Phenomenology, astrophysics and cosmology of theories with submillimeter dimensions and TeV scale quantum gravity*, *Phys. Rev.* **D 59** (1999) 086004 [hep-ph/9807344] [INSPIRE].

[20] ATLAS collaboration, *The ATLAS Experiment at the CERN Large Hadron Collider*, 2008 *JINST* **3** S08003 [INSPIRE].

[21] ATLAS collaboration, *ATLAS Insertable B-Layer Technical Design Report*, CERN-LHCC-2010-013 (2010) [ATLAS-TDR-19] [*Addendum* ATLAS-TDR-19-ADD-1 (2012)] [INSPIRE].

[22] ATLAS collaboration, *Performance of the ATLAS Trigger System in 2015*, *Eur. Phys. J.* **C 77** (2017) 317 [arXiv:1611.09661] [INSPIRE].

[23] S. Alioli, P. Nason, C. Oleari and E. Re, *A general framework for implementing NLO calculations in shower Monte Carlo programs: the POWHEG BOX*, *JHEP* **06** (2010) 043 [arXiv:1002.2581] [INSPIRE].

[24] H.-L. Lai et al., *New parton distributions for collider physics*, *Phys. Rev.* **D 82** (2010) 074024 [arXiv:1007.2241] [INSPIRE].

[25] T. Sjöstrand, S. Mrenna and P.Z. Skands, *A Brief Introduction to PYTHIA 8.1*, *Comput. Phys. Commun.* **178** (2008) 852 [arXiv:0710.3820] [INSPIRE].

[26] ATLAS collaboration, *Measurement of the Z/γ^* boson transverse momentum distribution in pp collisions at $\sqrt{s} = 7$ TeV with the ATLAS detector*, *JHEP* **09** (2014) 145 [arXiv:1406.3660] [INSPIRE].

[27] ATLAS collaboration, *Monte Carlo Generators for the Production of a W or Z/γ^* Boson in Association with Jets at ATLAS in Run 2*, ATL-PHYS-PUB-2016-003 (2016).

[28] C. Anastasiou, L.J. Dixon, K. Melnikov and F. Petriello, *High precision QCD at hadron colliders: Electroweak gauge boson rapidity distributions at NNLO*, *Phys. Rev.* **D 69** (2004) 094008 [hep-ph/0312266] [INSPIRE].

[29] S. Dulat et al., *New parton distribution functions from a global analysis of quantum chromodynamics*, *Phys. Rev.* **D 93** (2016) 033006 [arXiv:1506.07443] [INSPIRE].

[30] S.G. Bondarenko and A.A. Sapronov, *NLO EW and QCD proton-proton cross section calculations with mcsanc-v1.01*, *Comput. Phys. Commun.* **184** (2013) 2343 [arXiv:1301.3687] [INSPIRE].

[31] A.D. Martin, R.G. Roberts, W.J. Stirling and R.S. Thorne, *Parton distributions incorporating QED contributions*, *Eur. Phys. J.* **C 39** (2005) 155 [hep-ph/0411040] [INSPIRE].

[32] ATLAS collaboration, *Studies on top-quark Monte Carlo modelling for Top2016*, ATL-PHYS-PUB-2016-020 (2016).

[33] ATLAS collaboration, *Multi-Boson Simulation for* 13 *TeV ATLAS Analyses*, ATL-PHYS-PUB-2016-002 (2016).

JHEP10(2017)182

[34] T. Gleisberg et al., *Event generation with SHERPA 1.1*, *JHEP* **02** (2009) 007 [arXiv:0811.4622] [INSPIRE].

[35] M. Czakon and A. Mitov, *Top++: A Program for the Calculation of the Top-Pair Cross-Section at Hadron Colliders*, *Comput. Phys. Commun.* **185** (2014) 2930 [arXiv:1112.5675] [INSPIRE].

[36] R.D. Ball et al., *Parton distributions with LHC data*, *Nucl. Phys.* **B 867** (2013) 244 [arXiv:1207.1303] [INSPIRE].

[37] ATLAS collaboration, *ATLAS Run 1 PYTHIA8 tunes*, ATL-PHYS-PUB-2014-021 (2014).

[38] GEANT4 collaboration, S. Agostinelli et al., *GEANT4: A Simulation toolkit*, *Nucl. Instrum. Meth.* **A 506** (2003) 250 [INSPIRE].

[39] ATLAS collaboration, *The ATLAS Simulation Infrastructure*, *Eur. Phys. J.* **C 70** (2010) 823 [arXiv:1005.4568] [INSPIRE].

[40] A.D. Martin, W.J. Stirling, R.S. Thorne and G. Watt, *Parton distributions for the LHC*, *Eur. Phys. J.* **C 63** (2009) 189 [arXiv:0901.0002] [INSPIRE].

[41] ATLAS collaboration, *Electron efficiency measurements with the ATLAS detector using 2012 LHC proton-proton collision data*, *Eur. Phys. J.* **C 77** (2017) 195 [arXiv:1612.01456] [INSPIRE].

[42] ATLAS collaboration, *Electron efficiency measurements with the ATLAS detector using the 2015 LHC proton-proton collision data*, ATLAS-CONF-2016-024 (2016) [INSPIRE].

[43] ATLAS collaboration, *Electron and photon energy calibration with the ATLAS detector using data collected in 2015 at $\sqrt{s} = 13$ TeV*, ATL-PHYS-PUB-2016-015 (2016).

[44] ATLAS collaboration, *Muon reconstruction performance of the ATLAS detector in proton-proton collision data at $\sqrt{s} = 13$ TeV*, *Eur. Phys. J.* **C 76** (2016) 292 [arXiv:1603.05598] [INSPIRE].

[45] ATLAS collaboration, *Electron and photon energy calibration with the ATLAS detector using LHC Run 1 data*, *Eur. Phys. J.* **C 74** (2014) 3071 [arXiv:1407.5063] [INSPIRE].

[46] Particle Data Group collaboration, C. Patrignani et al., *Review of Particle Physics*, *Chin. Phys.* **C 40** (2016) 100001 [INSPIRE].

[47] J. Gao and P. Nadolsky, *A meta-analysis of parton distribution functions*, *JHEP* **07** (2014) 035 [arXiv:1401.0013] [INSPIRE].

[48] J. Butterworth et al., *PDF4LHC recommendations for LHC Run II*, *J. Phys.* **G 43** (2016) 023001 [arXiv:1510.03865] [INSPIRE].

[49] P. Motylinski, L. Harland-Lang, A.D. Martin and R.S. Thorne, *Updates of PDFs for the 2nd LHC run*, *Nucl. Part. Phys. Proc.* **273–275** (2016) 2136 [arXiv:1411.2560] [INSPIRE].

[50] NNPDF collaboration, R.D. Ball et al., *Parton distributions for the LHC Run II*, *JHEP* **04** (2015) 040 [arXiv:1410.8849] [INSPIRE].

[51] ATLAS collaboration, *Measurement of the Inelastic Proton-Proton Cross section at $\sqrt{s} = 13$ TeV with the ATLAS Detector at the LHC*, *Phys. Rev. Lett.* **117** (2016) 182002 [arXiv:1606.02625] [INSPIRE].

[52] ATLAS collaboration, *Luminosity determination in pp collisions at $\sqrt{s} = 8$ TeV using the ATLAS detector at the LHC*, *Eur. Phys. J.* **C 76** (2016) 653 [arXiv:1608.03953] [INSPIRE].

[53] A. Caldwell, D. Kollar and K. Kroninger, *BAT: The Bayesian Analysis Toolkit*, *Comput. Phys. Commun.* **180** (2009) 2197 [arXiv:0808.2552] [INSPIRE].

[54] G. Choudalakis, *On hypothesis testing, trials factor, hypertests and the BumpHunter*, arXiv:1101.0390 [INSPIRE].

[55] G. Cowan, K. Cranmer, E. Gross and O. Vitells, *Asymptotic formulae for likelihood-based tests of new physics*, *Eur. Phys. J.* **C 71** (2011) 1554 [*Erratum ibid.* **C 73** (2013) 2501] [arXiv:1007.1727] [INSPIRE].

[56] ROOT collaboration, K. Cranmer, G. Lewis, L. Moneta, A. Shibata and W. Verkerke, *HistFactory: A tool for creating statistical models for use with RooFit and RooStats*, CERN-OPEN-2012-016 (2012) [INSPIRE].

[57] L. Moneta et al., *The RooStats Project*, PoS(ACAT2010)057 [arXiv:1009.1003] [INSPIRE].

[58] W. Verkerke and D.P. Kirkby, *The RooFit toolkit for data modeling*, *eConf* **C 0303241** (2003) MOLT007 [physics/0306116] [INSPIRE].

[59] ATLAS collaboration, *ATLAS Computing Acknowledgements 2016–2017*, ATL-GEN-PUB-2016-002 (2016).

The ATLAS collaboration

M. Aaboud[137d], G. Aad[88], B. Abbott[115], O. Abdinov[12,*], B. Abeloos[119], S.H. Abidi[161], O.S. AbouZeid[139], N.L. Abraham[151], H. Abramowicz[155], H. Abreu[154], R. Abreu[118], Y. Abulaiti[148a,148b], B.S. Acharya[167a,167b,a], S. Adachi[157], L. Adamczyk[41a], J. Adelman[110], M. Adersberger[102], T. Adye[133], A.A. Affolder[139], T. Agatonovic-Jovin[14], C. Agheorghiesei[28c], J.A. Aguilar-Saavedra[128a,128f], S.P. Ahlen[24], F. Ahmadov[68,b], G. Aielli[135a,135b], S. Akatsuka[71], H. Akerstedt[148a,148b], T.P.A. Åkesson[84], E. Akilli[52], A.V. Akimov[98], G.L. Alberghi[22a,22b], J. Albert[172], P. Albicocco[50], M.J. Alconada Verzini[74], S.C. Alderweireldt[108], M. Aleksa[32], I.N. Aleksandrov[68], C. Alexa[28b], G. Alexander[155], T. Alexopoulos[10], M. Alhroob[115], B. Ali[130], M. Aliev[76a,76b], G. Alimonti[94a], J. Alison[33], S.P. Alkire[38], B.M.M. Allbrooke[151], B.W. Allen[118], P.P. Allport[19], A. Aloisio[106a,106b], A. Alonso[39], F. Alonso[74], C. Alpigiani[140], A.A. Alshehri[56], M.I. Alstaty[88], B. Alvarez Gonzalez[32], D. Álvarez Piqueras[170], M.G. Alviggi[106a,106b], B.T. Amadio[16], Y. Amaral Coutinho[26a], C. Amelung[25], D. Amidei[92], S.P. Amor Dos Santos[128a,128c], A. Amorim[128a,128b], S. Amoroso[32], G. Amundsen[25], C. Anastopoulos[141], L.S. Ancu[52], N. Andari[19], T. Andeen[11], C.F. Anders[60b], J.K. Anders[77], K.J. Anderson[33], A. Andreazza[94a,94b], V. Andrei[60a], S. Angelidakis[9], I. Angelozzi[109], A. Angerami[38], A.V. Anisenkov[111,c], N. Anjos[13], A. Annovi[126a,126b], C. Antel[60a], M. Antonelli[50], A. Antonov[100,*], D.J. Antrim[166], F. Anulli[134a], M. Aoki[69], L. Aperio Bella[32], G. Arabidze[93], Y. Arai[69], J.P. Araque[128a], V. Araujo Ferraz[26a], A.T.H. Arce[48], R.E. Ardell[80], F.A. Arduh[74], J-F. Arguin[97], S. Argyropoulos[66], M. Arik[20a], A.J. Armbruster[32], L.J. Armitage[79], O. Arnaez[161], H. Arnold[51], M. Arratia[30], O. Arslan[23], A. Artamonov[99], G. Artoni[122], S. Artz[86], S. Asai[157], N. Asbah[45], A. Ashkenazi[155], L. Asquith[151], K. Assamagan[27], R. Astalos[146a], M. Atkinson[169], N.B. Atlay[143], K. Augsten[130], G. Avolio[32], B. Axen[16], M.K. Ayoub[119], G. Azuelos[97,d], A.E. Baas[60a], M.J. Baca[19], H. Bachacou[138], K. Bachas[76a,76b], M. Backes[122], M. Backhaus[32], P. Bagnaia[134a,134b], M. Bahmani[42], H. Bahrasemani[144], J.T. Baines[133], M. Bajic[39], O.K. Baker[179], E.M. Baldin[111,c], P. Balek[175], F. Balli[138], W.K. Balunas[124], E. Banas[42], A. Bandyopadhyay[23], Sw. Banerjee[176,e], A.A.E. Bannoura[178], L. Barak[32], E.L. Barberio[91], D. Barberis[53a,53b], M. Barbero[88], T. Barillari[103], M-S Barisits[32], J.T. Barkeloo[118], T. Barklow[145], N. Barlow[30], S.L. Barnes[36c], B.M. Barnett[133], R.M. Barnett[16], Z. Barnovska-Blenessy[36a], A. Baroncelli[136a], G. Barone[25], A.J. Barr[122], L. Barranco Navarro[170], F. Barreiro[85], J. Barreiro Guimarães da Costa[35a], R. Bartoldus[145], A.E. Barton[75], P. Bartos[146a], A. Basalaev[125], A. Bassalat[119,f], R.L. Bates[56], S.J. Batista[161], J.R. Batley[30], M. Battaglia[139], M. Bauce[134a,134b], F. Bauer[138], H.S. Bawa[145,g], J.B. Beacham[113], M.D. Beattie[75], T. Beau[83], P.H. Beauchemin[165], P. Bechtle[23], H.P. Beck[18,h], H.C. Beck[57], K. Becker[122], M. Becker[86], M. Beckingham[173], C. Becot[112], A.J. Beddall[20e], A. Beddall[20b], V.A. Bednyakov[68], M. Bedognetti[109], C.P. Bee[150], T.A. Beermann[32], M. Begalli[26a], M. Begel[27], J.K. Behr[45], A.S. Bell[81], G. Bella[155], L. Bellagamba[22a], A. Bellerive[31], M. Bellomo[154], K. Belotskiy[100], O. Beltramello[32], N.L. Belyaev[100], O. Benary[155,*], D. Benchekroun[137a], M. Bender[102], K. Bendtz[148a,148b], N. Benekos[10], Y. Benhammou[155], E. Benhar Noccioli[179], J. Benitez[66], D.P. Benjamin[48], M. Benoit[52], J.R. Bensinger[25], S. Bentvelsen[109], L. Beresford[122], M. Beretta[50], D. Berge[109], E. Bergeaas Kuutmann[168], N. Berger[5], J. Beringer[16], S. Berlendis[58], N.R. Bernard[89], G. Bernardi[83], C. Bernius[145], F.U. Bernlochner[23], T. Berry[80], P. Berta[131], C. Bertella[35a], G. Bertoli[148a,148b], F. Bertolucci[126a,126b], I.A. Bertram[75], C. Bertsche[45], D. Bertsche[115], G.J. Besjes[39], O. Bessidskaia Bylund[148a,148b], M. Bessner[45], N. Besson[138], C. Betancourt[51], A. Bethani[87], S. Bethke[103], A.J. Bevan[79], J. Beyer[103], R.M. Bianchi[127], O. Biebel[102], D. Biedermann[17], R. Bielski[87], K. Bierwagen[86], N.V. Biesuz[126a,126b], M. Biglietti[136a], T.R.V. Billoud[97], H. Bilokon[50], M. Bindi[57], A. Bingul[20b], C. Bini[134a,134b],

JHEP10(2017)182

S. Biondi[22a,22b], T. Bisanz[57], C. Bittrich[47], D.M. Bjergaard[48], C.W. Black[152], J.E. Black[145], K.M. Black[24], R.E. Blair[6], T. Blazek[146a], I. Bloch[45], C. Blocker[25], A. Blue[56], W. Blum[86,*], U. Blumenschein[79], S. Blunier[34a], G.J. Bobbink[109], V.S. Bobrovnikov[111,c], S.S. Bocchetta[84], A. Bocci[48], C. Bock[102], M. Boehler[51], D. Boerner[178], D. Bogavac[102], A.G. Bogdanchikov[111], C. Bohm[148a], V. Boisvert[80], P. Bokan[168,i], T. Bold[41a], A.S. Boldyrev[101], A.E. Bolz[60b], M. Bomben[83], M. Bona[79], M. Boonekamp[138], A. Borisov[132], G. Borissov[75], J. Bortfeldt[32], D. Bortoletto[122], V. Bortolotto[62a,62b,62c], D. Boscherini[22a], M. Bosman[13], J.D. Bossio Sola[29], J. Boudreau[127], J. Bouffard[2], E.V. Bouhova-Thacker[75], D. Boumediene[37], C. Bourdarios[119], S.K. Boutle[56], A. Boveia[113], J. Boyd[32], I.R. Boyko[68], J. Bracinik[19], A. Brandt[8], G. Brandt[57], O. Brandt[60a], U. Bratzler[158], B. Brau[89], J.E. Brau[118], W.D. Breaden Madden[56], K. Brendlinger[45], A.J. Brennan[91], L. Brenner[109], R. Brenner[168], S. Bressler[175], D.L. Briglin[19], T.M. Bristow[49], D. Britton[56], D. Britzger[45], F.M. Brochu[30], I. Brock[23], R. Brock[93], G. Brooijmans[38], T. Brooks[80], W.K. Brooks[34b], J. Brosamer[16], E. Brost[110], J.H Broughton[19], P.A. Bruckman de Renstrom[42], D. Bruncko[146b], A. Bruni[22a], G. Bruni[22a], L.S. Bruni[109], BH Brunt[30], M. Bruschi[22a], N. Bruscino[23], P. Bryant[33], L. Bryngemark[45], T. Buanes[15], Q. Buat[144], P. Buchholz[143], A.G. Buckley[56], I.A. Budagov[68], F. Buehrer[51], M.K. Bugge[121], O. Bulekov[100], D. Bullock[8], T.J. Burch[110], S. Burdin[77], C.D. Burgard[51], A.M. Burger[5], B. Burghgrave[110], K. Burka[42], S. Burke[133], I. Burmeister[46], J.T.P. Burr[122], E. Busato[37], D. Büscher[51], V. Büscher[86], P. Bussey[56], J.M. Butler[24], C.M. Buttar[56], J.M. Butterworth[81], P. Butti[32], W. Buttinger[27], A. Buzatu[35c], A.R. Buzykaev[111,c], S. Cabrera Urbán[170], D. Caforio[130], V.M. Cairo[40a,40b], O. Cakir[4a], N. Calace[52], P. Calafiura[16], A. Calandri[88], G. Calderini[83], P. Calfayan[64], G. Callea[40a,40b], L.P. Caloba[26a], S. Calvente Lopez[85], D. Calvet[37], S. Calvet[37], T.P. Calvet[88], R. Camacho Toro[33], S. Camarda[32], P. Camarri[135a,135b], D. Cameron[121], R. Caminal Armadans[169], C. Camincher[58], S. Campana[32], M. Campanelli[81], A. Camplani[94a,94b], A. Campoverde[143], V. Canale[106a,106b], M. Cano Bret[36c], J. Cantero[116], T. Cao[155], M.D.M. Capeans Garrido[32], I. Caprini[28b], M. Caprini[28b], M. Capua[40a,40b], R.M. Carbone[38], R. Cardarelli[135a], F. Cardillo[51], I. Carli[131], T. Carli[32], G. Carlino[106a], B.T. Carlson[127], L. Carminati[94a,94b], R.M.D. Carney[148a,148b], S. Caron[108], E. Carquin[34b], S. Carrá[94a,94b], G.D. Carrillo-Montoya[32], J. Carvalho[128a,128c], D. Casadei[19], M.P. Casado[13,j], M. Casolino[13], D.W. Casper[166], R. Castelijn[109], V. Castillo Gimenez[170], N.F. Castro[128a,k], A. Catinaccio[32], J.R. Catmore[121], A. Cattai[32], J. Caudron[23], V. Cavaliere[169], E. Cavallaro[13], D. Cavalli[94a], M. Cavalli-Sforza[13], V. Cavasinni[126a,126b], E. Celebi[20d], F. Ceradini[136a,136b], L. Cerda Alberich[170], A.S. Cerqueira[26b], A. Cerri[151], L. Cerrito[135a,135b], F. Cerutti[16], A. Cervelli[18], S.A. Cetin[20d], A. Chafaq[137a], D. Chakraborty[110], S.K. Chan[59], W.S. Chan[109], Y.L. Chan[62a], P. Chang[169], J.D. Chapman[30], D.G. Charlton[19], C.C. Chau[31], C.A. Chavez Barajas[151], S. Che[113], S. Cheatham[167a,167c], A. Chegwidden[93], S. Chekanov[6], S.V. Chekulaev[163a], G.A. Chelkov[68,l], M.A. Chelstowska[32], C. Chen[67], H. Chen[27], J. Chen[36a], S. Chen[35b], S. Chen[157], X. Chen[35c,m], Y. Chen[70], H.C. Cheng[92], H.J. Cheng[35a], A. Cheplakov[68], E. Cheremushkina[132], R. Cherkaoui El Moursli[137e], E. Cheu[7], K. Cheung[63], L. Chevalier[138], V. Chiarella[50], G. Chiarelli[126a,126b], G. Chiodini[76a], A.S. Chisholm[32], A. Chitan[28b], Y.H. Chiu[172], M.V. Chizhov[68], K. Choi[64], A.R. Chomont[37], S. Chouridou[156], Y.S. Chow[62a], V. Christodoulou[81], M.C. Chu[62a], J. Chudoba[129], A.J. Chuinard[90], J.J. Chwastowski[42], L. Chytka[117], A.K. Ciftci[4a], D. Cinca[46], V. Cindro[78], I.A. Cioara[23], C. Ciocca[22a,22b], A. Ciocio[16], F. Cirotto[106a,106b], Z.H. Citron[175], M. Citterio[94a], M. Ciubancan[28b], A. Clark[52], B.L. Clark[59], M.R. Clark[38], P.J. Clark[49], R.N. Clarke[16], C. Clement[148a,148b], Y. Coadou[88], M. Cobal[167a,167c], A. Coccaro[52], J. Cochran[67], L. Colasurdo[108], B. Cole[38], A.P. Colijn[109], J. Collot[58], T. Colombo[166], P. Conde Muiño[128a,128b], E. Coniavitis[51], S.H. Connell[147b], I.A. Connelly[87], S. Constantinescu[28b], G. Conti[32], F. Conventi[106a,n], M. Cooke[16], A.M. Cooper-Sarkar[122],

F. Cormier[171], K.J.R. Cormier[161], M. Corradi[134a,134b], F. Corriveau[90,o], A. Cortes-Gonzalez[32], G. Cortiana[103], G. Costa[94a], M.J. Costa[170], D. Costanzo[141], G. Cottin[30], G. Cowan[80], B.E. Cox[87], K. Cranmer[112], S.J. Crawley[56], R.A. Creager[124], G. Cree[31], S. Crépé-Renaudin[58], F. Crescioli[83], W.A. Cribbs[148a,148b], M. Cristinziani[23], V. Croft[108], G. Crosetti[40a,40b], A. Cueto[85], T. Cuhadar Donszelmann[141], A.R. Cukierman[145], J. Cummings[179], M. Curatolo[50], J. Cúth[86], S. Czekierda[42], P. Czodrowski[32], G. D'amen[22a,22b], S. D'Auria[56], L. D'eramo[83], M. D'Onofrio[77], M.J. Da Cunha Sargedas De Sousa[128a,128b], C. Da Via[87], W. Dabrowski[41a], T. Dado[146a], T. Dai[92], O. Dale[15], F. Dallaire[97], C. Dallapiccola[89], M. Dam[39], J.R. Dandoy[124], M.F. Daneri[29], N.P. Dang[176], A.C. Daniells[19], N.S. Dann[87], M. Danninger[171], M. Dano Hoffmann[138], V. Dao[150], G. Darbo[53a], S. Darmora[8], J. Dassoulas[3], A. Dattagupta[118], T. Daubney[45], W. Davey[23], C. David[45], T. Davidek[131], D.R. Davis[48], P. Davison[81], E. Dawe[91], I. Dawson[141], K. De[8], R. de Asmundis[106a], A. De Benedetti[115], S. De Castro[22a,22b], S. De Cecco[83], N. De Groot[108], P. de Jong[109], H. De la Torre[93], F. De Lorenzi[67], A. De Maria[57], D. De Pedis[134a], A. De Salvo[134a], U. De Sanctis[135a,135b], A. De Santo[151], K. De Vasconcelos Corga[88], J.B. De Vivie De Regie[119], W.J. Dearnaley[75], R. Debbe[27], C. Debenedetti[139], D.V. Dedovich[68], N. Dehghanian[3], I. Deigaard[109], M. Del Gaudio[40a,40b], J. Del Peso[85], D. Delgove[119], F. Deliot[138], C.M. Delitzsch[7], A. Dell'Acqua[32], L. Dell'Asta[24], M. Dell'Orso[126a,126b], M. Della Pietra[106a,106b], D. della Volpe[52], M. Delmastro[5], C. Delporte[119], P.A. Delsart[58], D.A. DeMarco[161], S. Demers[179], M. Demichev[68], A. Demilly[83], S.P. Denisov[132], D. Denysiuk[138], D. Derendarz[42], J.E. Derkaoui[137d], F. Derue[83], P. Dervan[77], K. Desch[23], C. Deterre[45], K. Dette[46], M.R. Devesa[29], P.O. Deviveiros[32], A. Dewhurst[133], S. Dhaliwal[25], F.A. Di Bello[52], A. Di Ciaccio[135a,135b], L. Di Ciaccio[5], W.K. Di Clemente[124], C. Di Donato[106a,106b], A. Di Girolamo[32], B. Di Girolamo[32], B. Di Micco[136a,136b], R. Di Nardo[32], K.F. Di Petrillo[59], A. Di Simone[51], R. Di Sipio[161], D. Di Valentino[31], C. Diaconu[88], M. Diamond[161], F.A. Dias[39], M.A. Diaz[34a], E.B. Diehl[92], J. Dietrich[17], S. Díez Cornell[45], A. Dimitrievska[14], J. Dingfelder[23], P. Dita[28b], S. Dita[28b], F. Dittus[32], F. Djama[88], T. Djobava[54b], J.I. Djuvsland[60a], M.A.B. do Vale[26c], D. Dobos[32], M. Dobre[28b], C. Doglioni[84], J. Dolejsi[131], Z. Dolezal[131], M. Donadelli[26d], S. Donati[126a,126b], P. Dondero[123a,123b], J. Donini[37], J. Dopke[133], A. Doria[106a], M.T. Dova[74], A.T. Doyle[56], E. Drechsler[57], E. Dreyer[144], M. Dris[10], Y. Du[36b], J. Duarte-Campderros[155], A. Dubreuil[52], E. Duchovni[175], G. Duckeck[102], A. Ducourthial[83], O.A. Ducu[97,p], D. Duda[109], A. Dudarev[32], A.Chr. Dudder[86], E.M. Duffield[16], L. Duflot[119], M. Dührssen[32], M. Dumancic[175], A.E. Dumitriu[28b], A.K. Duncan[56], M. Dunford[60a], H. Duran Yildiz[4a], M. Düren[55], A. Durglishvili[54b], D. Duschinger[47], B. Dutta[45], D. Duvnjak[1], M. Dyndal[45], B.S. Dziedzic[42], C. Eckardt[45], K.M. Ecker[103], R.C. Edgar[92], T. Eifert[32], G. Eigen[15], K. Einsweiler[16], T. Ekelof[168], M. El Kacimi[137c], R. El Kosseifi[88], V. Ellajosyula[88], M. Ellert[168], S. Elles[5], F. Ellinghaus[178], A.A. Elliot[172], N. Ellis[32], J. Elmsheuser[27], M. Elsing[32], D. Emeliyanov[133], Y. Enari[157], O.C. Endner[86], J.S. Ennis[173], J. Erdmann[46], A. Ereditato[18], M. Ernst[27], S. Errede[169], M. Escalier[119], C. Escobar[170], B. Esposito[50], O. Estrada Pastor[170], A.I. Etienvre[138], E. Etzion[155], H. Evans[64], A. Ezhilov[125], M. Ezzi[137e], F. Fabbri[22a,22b], L. Fabbri[22a,22b], V. Fabiani[108], G. Facini[81], R.M. Fakhrutdinov[132], S. Falciano[134a], P.J. Falke[5], R.J. Falla[81], J. Faltova[32], Y. Fang[35a], M. Fanti[94a,94b], A. Farbin[8], A. Farilla[136a], C. Farina[127], E.M. Farina[123a,123b], T. Farooque[93], S. Farrell[16], S.M. Farrington[173], P. Farthouat[32], F. Fassi[137e], P. Fassnacht[32], D. Fassouliotis[9], M. Faucci Giannelli[80], A. Favareto[53a,53b], W.J. Fawcett[122], L. Fayard[119], O.L. Fedin[125,q], W. Fedorko[171], S. Feigl[121], L. Feligioni[88], C. Feng[36b], E.J. Feng[32], H. Feng[92], M.J. Fenton[56], A.B. Fenyuk[132], L. Feremenga[8], P. Fernandez Martinez[170], S. Fernandez Perez[13], J. Ferrando[45], A. Ferrari[168], P. Ferrari[109], R. Ferrari[123a], D.E. Ferreira de Lima[60b], A. Ferrer[170], D. Ferrere[52], C. Ferretti[92], F. Fiedler[86], A. Filipčič[78], M. Filipuzzi[45], F. Filthaut[108], M. Fincke-Keeler[172], K.D. Finelli[152], M.C.N. Fiolhais[128a,128c,r], L. Fiorini[170], A. Fischer[2], C. Fischer[13], J. Fischer[178], W.C. Fisher[93], N. Flaschel[45], I. Fleck[143], P. Fleischmann[92], R.R.M. Fletcher[124], T. Flick[178], B.M. Flierl[102], L.R. Flores Castillo[62a], M.J. Flowerdew[103], G.T. Forcolin[87], A. Formica[138], F.A. Förster[13], A. Forti[87], A.G. Foster[19], D. Fournier[119], H. Fox[75], S. Fracchia[141], P. Francavilla[83], M. Franchini[22a,22b], S. Franchino[60a], D. Francis[32], L. Franconi[121], M. Franklin[59], M. Frate[166], M. Fraternali[123a,123b], D. Freeborn[81], S.M. Fressard-Batraneanu[32], B. Freund[97], D. Froidevaux[32], J.A. Frost[122], C. Fukunaga[158], T. Fusayasu[104], J. Fuster[170], C. Gabaldon[58], O. Gabizon[154], A. Gabrielli[22a,22b], A. Gabrielli[16], G.P. Gach[41a], S. Gadatsch[32], S. Gadomski[80], G. Gagliardi[53a,53b], L.G. Gagnon[97], C. Galea[108], B. Galhardo[128a,128c], E.J. Gallas[122], B.J. Gallop[133], P. Gallus[130], G. Galster[39], K.K. Gan[113], S. Ganguly[37], Y. Gao[77], Y.S. Gao[145,g], F.M. Garay Walls[49], C. García[170], J.E. García Navarro[170], J.A. García Pascual[35a], M. Garcia-Sciveres[16], R.W. Gardner[33], N. Garelli[145], V. Garonne[121], A. Gascon Bravo[45], K. Gasnikova[45], C. Gatti[50], A. Gaudiello[53a,53b], G. Gaudio[123a], I.L. Gavrilenko[98], C. Gay[171], G. Gaycken[23], E.N. Gazis[10], C.N.P. Gee[133], J. Geisen[57], M. Geisen[86], M.P. Geisler[60a], K. Gellerstedt[148a,148b], C. Gemme[53a], M.H. Genest[58], C. Geng[92], S. Gentile[134a,134b], C. Gentsos[156], S. George[80], D. Gerbaudo[13], A. Gershon[155], G. Geßner[46], S. Ghasemi[143], M. Ghneimat[23], B. Giacobbe[22a], S. Giagu[134a,134b], N. Giangiacomi[22a,22b], P. Giannetti[126a,126b], S.M. Gibson[80], M. Gignac[171], M. Gilchriese[16], D. Gillberg[31], G. Gilles[178], D.M. Gingrich[3,d], N. Giokaris[9,*], M.P. Giordani[167a,167c], F.M. Giorgi[22a], P.F. Giraud[138], P. Giromini[59], G. Giugliarelli[167a,167c], D. Giugni[94a], F. Giuli[122], C. Giuliani[103], M. Giulini[60b], B.K. Gjelsten[121], S. Gkaitatzis[156], I. Gkialas[9,s], E.L. Gkougkousis[139], P. Gkountoumis[10], L.K. Gladilin[101], C. Glasman[85], J. Glatzer[13], P.C.F. Glaysher[45], A. Glazov[45], M. Goblirsch-Kolb[25], J. Godlewski[42], S. Goldfarb[91], T. Golling[52], D. Golubkov[132], A. Gomes[128a,128b,128d], R. Gonçalo[128a], R. Goncalves Gama[26a], J. Goncalves Pinto Firmino Da Costa[138], G. Gonella[51], L. Gonella[19], A. Gongadze[68], S. González de la Hoz[170], S. Gonzalez-Sevilla[52], L. Goossens[32], P.A. Gorbounov[99], H.A. Gordon[27], I. Gorelov[107], B. Gorini[32], E. Gorini[76a,76b], A. Gorišek[78], A.T. Goshaw[48], C. Gössling[46], M.I. Gostkin[68], C.A. Gottardo[23], C.R. Goudet[119], D. Goujdami[137c], A.G. Goussiou[140], N. Govender[147b,t], E. Gozani[154], L. Graber[57], I. Grabowska-Bold[41a], P.O.J. Gradin[168], J. Gramling[166], E. Gramstad[121], S. Grancagnolo[17], V. Gratchev[125], P.M. Gravila[28f], C. Gray[56], H.M. Gray[16], Z.D. Greenwood[82,u], C. Grefe[23], K. Gregersen[81], I.M. Gregor[45], P. Grenier[145], K. Grevtsov[5], J. Griffiths[8], A.A. Grillo[139], K. Grimm[75], S. Grinstein[13,v], Ph. Gris[37], J.-F. Grivaz[119], S. Groh[86], E. Gross[175], J. Grosse-Knetter[57], G.C. Grossi[82], Z.J. Grout[81], A. Grummer[107], L. Guan[92], W. Guan[176], J. Guenther[65], F. Guescini[163a], D. Guest[166], O. Gueta[155], B. Gui[113], E. Guido[53a,53b], T. Guillemin[5], S. Guindon[2], U. Gul[56], C. Gumpert[32], J. Guo[36c], W. Guo[92], Y. Guo[36a], R. Gupta[43], S. Gupta[122], G. Gustavino[115], P. Gutierrez[115], N.G. Gutierrez Ortiz[81], C. Gutschow[81], C. Guyot[138], M.P. Guzik[41a], C. Gwenlan[122], C.B. Gwilliam[77], A. Haas[112], C. Haber[16], H.K. Hadavand[8], N. Haddad[137e], A. Hadef[88], S. Hageböck[23], M. Hagihara[164], H. Hakobyan[180,*], M. Haleem[45], J. Haley[116], G. Halladjian[93], G.D. Hallewell[88], K. Hamacher[178], P. Hamal[117], K. Hamano[172], A. Hamilton[147a], G.N. Hamity[141], P.G. Hamnett[45], L. Han[36a], S. Han[35a], K. Hanagaki[69,w], K. Hanawa[157], M. Hance[139], B. Haney[124], P. Hanke[60a], J.B. Hansen[39], J.D. Hansen[39], M.C. Hansen[23], P.H. Hansen[39], K. Hara[164], A.S. Hard[176], T. Harenberg[178], F. Hariri[119], S. Harkusha[95], R.D. Harrington[49], P.F. Harrison[173], N.M. Hartmann[102], M. Hasegawa[70], Y. Hasegawa[142], A. Hasib[49], S. Hassani[138], S. Haug[18], R. Hauser[93], L. Hauswald[47], L.B. Havener[38], M. Havranek[130], C.M. Hawkes[19], R.J. Hawkings[32], D. Hayakawa[159], D. Hayden[93], C.P. Hays[122], J.M. Hays[79], H.S. Hayward[77], S.J. Haywood[133], S.J. Head[19], T. Heck[86], V. Hedberg[84], L. Heelan[8], S. Heer[23], K.K. Heidegger[51], S. Heim[45], T. Heim[16], B. Heinemann[45,x], J.J. Heinrich[102], L. Heinrich[112], C. Heinz[55], J. Hejbal[129],

JHEP10(2017)182

L. Helary[32], A. Held[171], S. Hellman[148a,148b], C. Helsens[32], R.C.W. Henderson[75], Y. Heng[176], S. Henkelmann[171], A.M. Henriques Correia[32], S. Henrot-Versille[119], G.H. Herbert[17], H. Herde[25], V. Herget[177], Y. Hernández Jiménez[147c], H. Herr[86], G. Herten[51], R. Hertenberger[102], L. Hervas[32], T.C. Herwig[124], G.G. Hesketh[81], N.P. Hessey[163a], J.W. Hetherly[43], S. Higashino[69], E. Higón-Rodriguez[170], K. Hildebrand[33], E. Hill[172], J.C. Hill[30], K.H. Hiller[45], S.J. Hillier[19], M. Hils[47], I. Hinchliffe[16], M. Hirose[51], D. Hirschbuehl[178], B. Hiti[78], O. Hladik[129], X. Hoad[49], J. Hobbs[150], N. Hod[163a], M.C. Hodgkinson[141], P. Hodgson[141], A. Hoecker[32], M.R. Hoeferkamp[107], F. Hoenig[102], D. Hohn[23], T.R. Holmes[33], M. Homann[46], S. Honda[164], T. Honda[69], T.M. Hong[127], B.H. Hooberman[169], W.H. Hopkins[118], Y. Horii[105], A.J. Horton[144], J-Y. Hostachy[58], S. Hou[153], A. Hoummada[137a], J. Howarth[87], J. Hoya[74], M. Hrabovsky[117], J. Hrdinka[32], I. Hristova[17], J. Hrivnac[119], T. Hryn'ova[5], A. Hrynevich[96], P.J. Hsu[63], S.-C. Hsu[140], Q. Hu[36a], S. Hu[36c], Y. Huang[35a], Z. Hubacek[130], F. Hubaut[88], F. Huegging[23], T.B. Huffman[122], E.W. Hughes[38], G. Hughes[75], M. Huhtinen[32], P. Huo[150], N. Huseynov[68,b], J. Huston[93], J. Huth[59], G. Iacobucci[52], G. Iakovidis[27], I. Ibragimov[143], L. Iconomidou-Fayard[119], Z. Idrissi[137e], P. Iengo[32], O. Igonkina[109,y], T. Iizawa[174], Y. Ikegami[69], M. Ikeno[69], Y. Ilchenko[11,z], D. Iliadis[156], N. Ilic[145], G. Introzzi[123a,123b], P. Ioannou[9,*], M. Iodice[136a], K. Iordanidou[38], V. Ippolito[59], M.F. Isacson[168], N. Ishijima[120], M. Ishino[157], M. Ishitsuka[159], C. Issever[122], S. Istin[20a], F. Ito[164], J.M. Iturbe Ponce[62a], R. Iuppa[162a,162b], H. Iwasaki[69], J.M. Izen[44], V. Izzo[106a], S. Jabbar[3], P. Jackson[1], R.M. Jacobs[23], V. Jain[2], K.B. Jakobi[86], K. Jakobs[51], S. Jakobsen[65], T. Jakoubek[129], D.O. Jamin[116], D.K. Jana[82], R. Jansky[52], J. Janssen[23], M. Janus[57], P.A. Janus[41a], G. Jarlskog[84], N. Javadov[68,b], T. Javůrek[51], M. Javurkova[51], F. Jeanneau[138], L. Jeanty[16], J. Jejelava[54a,aa], A. Jelinskas[173], P. Jenni[51,ab], C. Jeske[173], S. Jézéquel[5], H. Ji[176], J. Jia[150], H. Jiang[67], Y. Jiang[36a], Z. Jiang[145], S. Jiggins[81], J. Jimenez Pena[170], S. Jin[35a], A. Jinaru[28b], O. Jinnouchi[159], H. Jivan[147c], P. Johansson[141], K.A. Johns[7], C.A. Johnson[64], W.J. Johnson[140], K. Jon-And[148a,148b], R.W.L. Jones[75], S.D. Jones[151], S. Jones[7], T.J. Jones[77], J. Jongmanns[60a], P.M. Jorge[128a,128b], J. Jovicevic[163a], X. Ju[176], A. Juste Rozas[13,v], M.K. Köhler[175], A. Kaczmarska[42], M. Kado[119], H. Kagan[113], M. Kagan[145], S.J. Kahn[88], T. Kaji[174], E. Kajomovitz[48], C.W. Kalderon[84], A. Kaluza[86], S. Kama[43], A. Kamenshchikov[132], N. Kanaya[157], L. Kanjir[78], V.A. Kantserov[100], J. Kanzaki[69], B. Kaplan[112], L.S. Kaplan[176], D. Kar[147c], K. Karakostas[10], N. Karastathis[10], M.J. Kareem[57], E. Karentzos[10], S.N. Karpov[68], Z.M. Karpova[68], K. Karthik[112], V. Kartvelishvili[75], A.N. Karyukhin[132], K. Kasahara[164], L. Kashif[176], R.D. Kass[113], A. Kastanas[149], Y. Kataoka[157], C. Kato[157], A. Katre[52], J. Katzy[45], K. Kawade[70], K. Kawagoe[73], T. Kawamoto[157], G. Kawamura[57], E.F. Kay[77], V.F. Kazanin[111,c], R. Keeler[172], R. Kehoe[43], J.S. Keller[31], E. Kellermann[84], J.J. Kempster[80], J Kendrick[19], H. Keoshkerian[161], O. Kepka[129], B.P. Kerševan[78], S. Kersten[178], R.A. Keyes[90], M. Khader[169], F. Khalil-zada[12], A. Khanov[116], A.G. Kharlamov[111,c], T. Kharlamova[111,c], E.E. Khoda[171], A. Khodinov[160], T.J. Khoo[52], V. Khovanskiy[99,*], E. Khramov[68], J. Khubua[54b,ac], S. Kido[70], C.R. Kilby[80], H.Y. Kim[8], S.H. Kim[164], Y.K. Kim[33], N. Kimura[156], O.M. Kind[17], B.T. King[77], D. Kirchmeier[47], J. Kirk[133], A.E. Kiryunin[103], T. Kishimoto[157], D. Kisielewska[41a], V. Kitali[45], K. Kiuchi[164], O. Kivernyk[5], E. Kladiva[146b], T. Klapdor-Kleingrothaus[51], M.H. Klein[38], M. Klein[77], U. Klein[77], K. Kleinknecht[86], P. Klimek[110], A. Klimentov[27], R. Klingenberg[46], T. Klingl[23], T. Klioutchnikova[32], E.-E. Kluge[60a], P. Kluit[109], S. Kluth[103], E. Kneringer[65], E.B.F.G. Knoops[88], A. Knue[103], A. Kobayashi[157], D. Kobayashi[159], T. Kobayashi[157], M. Kobel[47], M. Kocian[145], P. Kodys[131], T. Koffas[31], E. Koffeman[109], N.M. Köhler[103], T. Koi[145], M. Kolb[60b], I. Koletsou[5], A.A. Komar[98,*], Y. Komori[157], T. Kondo[69], N. Kondrashova[36c], K. Köneke[51], A.C. König[108], T. Kono[69,ad], R. Konoplich[112,ae], N. Konstantinidis[81], R. Kopeliansky[64], S. Koperny[41a], A.K. Kopp[51], K. Korcyl[42], K. Kordas[156], A. Korn[81], A.A. Korol[111,c], I. Korolkov[13], E.V. Korolkova[141], O. Kortner[103], S. Kortner[103], T. Kosek[131], V.V. Kostyukhin[23], A. Kotwal[48], A. Koulouris[10], A. Kourkoumeli-Charalampidi[123a,123b], C. Kourkoumelis[9], E. Kourlitis[141], V. Kouskoura[27], A.B. Kowalewska[42], R. Kowalewski[172], T.Z. Kowalski[41a], C. Kozakai[157], W. Kozanecki[138], A.S. Kozhin[132], V.A. Kramarenko[101], G. Kramberger[78], D. Krasnopevtsev[100], M.W. Krasny[83], A. Krasznahorkay[32], D. Krauss[103], J.A. Kremer[41a], J. Kretzschmar[77], K. Kreutzfeldt[55], P. Krieger[161], K. Krizka[33], K. Kroeninger[46], H. Kroha[103], J. Kroll[129], J. Kroll[124], J. Kroseberg[23], J. Krstic[14], U. Kruchonak[68], H. Krüger[23], N. Krumnack[67], M.C. Kruse[48], T. Kubota[91], H. Kucuk[81], S. Kuday[4b], J.T. Kuechler[178], S. Kuehn[32], A. Kugel[60a], F. Kuger[177], T. Kuhl[45], V. Kukhtin[68], R. Kukla[88], Y. Kulchitsky[95], S. Kuleshov[34b], Y.P. Kulinich[169], M. Kuna[134a,134b], T. Kunigo[71], A. Kupco[129], T. Kupfer[46], O. Kuprash[155], H. Kurashige[70], L.L. Kurchaninov[163a], Y.A. Kurochkin[95], M.G. Kurth[35a], V. Kus[129], E.S. Kuwertz[172], M. Kuze[159], J. Kvita[117], T. Kwan[172], D. Kyriazopoulos[141], A. La Rosa[103], J.L. La Rosa Navarro[26d], L. La Rotonda[40a,40b], F. La Ruffa[40a,40b], C. Lacasta[170], F. Lacava[134a,134b], J. Lacey[45], H. Lacker[17], D. Lacour[83], E. Ladygin[68], R. Lafaye[5], B. Laforge[83], T. Lagouri[179], S. Lai[57], S. Lammers[64], W. Lampl[7], E. Lançon[27], U. Landgraf[51], M.P.J. Landon[79], M.C. Lanfermann[52], V.S. Lang[60a], J.C. Lange[13], R.J. Langenberg[32], A.J. Lankford[166], F. Lanni[27], K. Lantzsch[23], A. Lanza[123a], A. Lapertosa[53a,53b], S. Laplace[83], J.F. Laporte[138], T. Lari[94a], F. Lasagni Manghi[22a,22b], M. Lassnig[32], P. Laurelli[50], W. Lavrijsen[16], A.T. Law[139], P. Laycock[77], T. Lazovich[59], M. Lazzaroni[94a,94b], B. Le[91], O. Le Dortz[83], E. Le Guirriec[88], E.P. Le Quilleuc[138], M. LeBlanc[172], T. LeCompte[6], F. Ledroit-Guillon[58], C.A. Lee[27], G.R. Lee[133,af], S.C. Lee[153], L. Lee[59], B. Lefebvre[90], G. Lefebvre[83], M. Lefebvre[172], F. Legger[102], C. Leggett[16], G. Lehmann Miotto[32], X. Lei[7], W.A. Leight[45], M.A.L. Leite[26d], R. Leitner[131], D. Lellouch[175], B. Lemmer[57], K.J.C. Leney[81], T. Lenz[23], B. Lenzi[32], R. Leone[7], S. Leone[126a,126b], C. Leonidopoulos[49], G. Lerner[151], C. Leroy[97], A.A.J. Lesage[138], C.G. Lester[30], M. Levchenko[125], J. Levêque[5], D. Levin[92], L.J. Levinson[175], M. Levy[19], D. Lewis[79], B. Li[36a,ag], Changqiao Li[36a], H. Li[150], L. Li[36c], Q. Li[35a], S. Li[48], X. Li[36c], Y. Li[143], Z. Liang[35a], B. Liberti[135a], A. Liblong[161], K. Lie[62c], J. Liebal[23], W. Liebig[15], A. Limosani[152], S.C. Lin[182], T.H. Lin[86], R.A. Linck[64], B.E. Lindquist[150], A.E. Lionti[52], E. Lipeles[124], A. Lipniacka[15], M. Lisovyi[60b], T.M. Liss[169,ah], A. Lister[171], A.M. Litke[139], B. Liu[153,ai], H. Liu[92], H. Liu[27], J.K.K. Liu[122], J. Liu[36b], J.B. Liu[36a], K. Liu[88], L. Liu[169], M. Liu[36a], Y.L. Liu[36a], Y. Liu[36a], M. Livan[123a,123b], A. Lleres[58], J. Llorente Merino[35a], S.L. Lloyd[79], C.Y. Lo[62b], F. Lo Sterzo[153], E.M. Lobodzinska[45], P. Loch[7], F.K. Loebinger[87], A. Loesle[51], K.M. Loew[25], A. Loginov[179,*], T. Lohse[17], K. Lohwasser[141], M. Lokajicek[129], B.A. Long[24], J.D. Long[169], R.E. Long[75], L. Longo[76a,76b], K.A. Looper[113], J.A. Lopez[34b], D. Lopez Mateos[59], I. Lopez Paz[13], A. Lopez Solis[83], J. Lorenz[102], N. Lorenzo Martinez[5], M. Losada[21], P.J. Lösel[102], X. Lou[35a], A. Lounis[119], J. Love[6], P.A. Love[75], H. Lu[62a], N. Lu[92], Y.J. Lu[63], H.J. Lubatti[140], C. Luci[134a,134b], A. Lucotte[58], C. Luedtke[51], F. Luehring[64], W. Lukas[65], L. Luminari[134a], O. Lundberg[148a,148b], B. Lund-Jensen[149], M.S. Lutz[89], P.M. Luzi[83], D. Lynn[27], R. Lysak[129], E. Lytken[84], F. Lyu[35a], V. Lyubushkin[68], H. Ma[27], L.L. Ma[36b], Y. Ma[36b], G. Maccarrone[50], A. Macchiolo[103], C.M. Macdonald[141], B. Maček[78], J. Machado Miguens[124,128b], D. Madaffari[170], R. Madar[37], W.F. Mader[47], A. Madsen[45], J. Maeda[70], S. Maeland[15], T. Maeno[27], A.S. Maevskiy[101], V. Magerl[51], J. Mahlstedt[109], C. Maiani[119], C. Maidantchik[26a], A.A. Maier[103], T. Maier[102], A. Maio[128a,128b,128d], O. Majersky[146a], S. Majewski[118], Y. Makida[69], N. Makovec[119], B. Malaescu[83], Pa. Malecki[42], V.P. Maleev[125], F. Malek[58], U. Mallik[66], D. Malon[6], C. Malone[30], S. Maltezos[10], S. Malyukov[32], J. Mamuzic[170], G. Mancini[50], I. Mandić[78], J. Maneira[128a,128b], L. Manhaes de Andrade Filho[26b], J. Manjarres Ramos[47], K.H. Mankinen[84], A. Mann[102], A. Manousos[32], B. Mansoulie[138], J.D. Mansour[35a], R. Mantifel[90], M. Mantoani[57], S. Manzoni[94a,94b], L. Mapelli[32], G. Marceca[29], L. March[52], L. Marchese[122],

JHEP10(2017)182

G. Marchiori[83], M. Marcisovsky[129], M. Marjanovic[37], D.E. Marley[92], F. Marroquim[26a], S.P. Marsden[87], Z. Marshall[16], M.U.F Martensson[168], S. Marti-Garcia[170], C.B. Martin[113], T.A. Martin[173], V.J. Martin[49], B. Martin dit Latour[15], M. Martinez[13,v], V.I. Martinez Outschoorn[169], S. Martin-Haugh[133], V.S. Martoiu[28b], A.C. Martyniuk[81], A. Marzin[32], L. Masetti[86], T. Mashimo[157], R. Mashinistov[98], J. Masik[87], A.L. Maslennikov[111,c], L. Massa[135a,135b], P. Mastrandrea[5], A. Mastroberardino[40a,40b], T. Masubuchi[157], P. Mättig[178], J. Maurer[28b], S.J. Maxfield[77], D.A. Maximov[111,c], R. Mazini[153], I. Maznas[156], S.M. Mazza[94a,94b], N.C. Mc Fadden[107], G. Mc Goldrick[161], S.P. Mc Kee[92], A. McCarn[92], R.L. McCarthy[150], T.G. McCarthy[103], L.I. McClymont[81], E.F. McDonald[91], J.A. Mcfayden[81], G. Mchedlidze[57], S.J. McMahon[133], P.C. McNamara[91], R.A. McPherson[172,o], S. Meehan[140], T.J. Megy[51], S. Mehlhase[102], A. Mehta[77], T. Meideck[58], K. Meier[60a], B. Meirose[44], D. Melini[170,aj], B.R. Mellado Garcia[147c], J.D. Mellenthin[57], M. Melo[146a], F. Meloni[18], A. Melzer[23], S.B. Menary[87], L. Meng[77], X.T. Meng[92], A. Mengarelli[22a,22b], S. Menke[103], E. Meoni[40a,40b], S. Mergelmeyer[17], P. Mermod[52], L. Merola[106a,106b], C. Meroni[94a], F.S. Merritt[33], A. Messina[134a,134b], J. Metcalfe[6], A.S. Mete[166], C. Meyer[124], J-P. Meyer[138], J. Meyer[109], H. Meyer Zu Theenhausen[60a], F. Miano[151], R.P. Middleton[133], S. Miglioranzi[53a,53b], L. Mijović[49], G. Mikenberg[175], M. Mikestikova[129], M. Mikuž[78], M. Milesi[91], A. Milic[161], D.W. Miller[33], C. Mills[49], A. Milov[175], D.A. Milstead[148a,148b], A.A. Minaenko[132], Y. Minami[157], I.A. Minashvili[68], A.I. Mincer[112], B. Mindur[41a], M. Mineev[68], Y. Minegishi[157], Y. Ming[176], L.M. Mir[13], K.P. Mistry[124], T. Mitani[174], J. Mitrevski[102], V.A. Mitsou[170], A. Miucci[18], P.S. Miyagawa[141], A. Mizukami[69], J.U. Mjörnmark[84], T. Mkrtchyan[180], M. Mlynarikova[131], T. Moa[148a,148b], K. Mochizuki[97], P. Mogg[51], S. Mohapatra[38], S. Molander[148a,148b], R. Moles-Valls[23], R. Monden[71], M.C. Mondragon[93], K. Mönig[45], J. Monk[39], E. Monnier[88], A. Montalbano[150], J. Montejo Berlingen[32], F. Monticelli[74], S. Monzani[94a,94b], R.W. Moore[3], N. Morange[119], D. Moreno[21], M. Moreno Llácer[32], P. Morettini[53a], S. Morgenstern[32], D. Mori[144], T. Mori[157], M. Morii[59], M. Morinaga[157], V. Morisbak[121], A.K. Morley[32], G. Mornacchi[32], J.D. Morris[79], L. Morvaj[150], P. Moschovakos[10], M. Mosidze[54b], H.J. Moss[141], J. Moss[145,ak], K. Motohashi[159], R. Mount[145], E. Mountricha[27], E.J.W. Moyse[89], S. Muanza[88], F. Mueller[103], J. Mueller[127], R.S.P. Mueller[102], D. Muenstermann[75], P. Mullen[56], G.A. Mullier[18], F.J. Munoz Sanchez[87], W.J. Murray[173,133], H. Musheghyan[32], M. Muškinja[78], A.G. Myagkov[132,al], M. Myska[130], B.P. Nachman[16], O. Nackenhorst[52], K. Nagai[122], R. Nagai[69,ad], K. Nagano[69], Y. Nagasaka[61], K. Nagata[164], M. Nagel[51], E. Nagy[88], A.M. Nairz[32], Y. Nakahama[105], K. Nakamura[69], T. Nakamura[157], I. Nakano[114], R.F. Naranjo Garcia[45], R. Narayan[11], D.I. Narrias Villar[60a], I. Naryshkin[125], T. Naumann[45], G. Navarro[21], R. Nayyar[7], H.A. Neal[92], P.Yu. Nechaeva[98], T.J. Neep[138], A. Negri[123a,123b], M. Negrini[22a], S. Nektarijevic[108], C. Nellist[119], A. Nelson[166], M.E. Nelson[122], S. Nemecek[129], P. Nemethy[112], M. Nessi[32,am], M.S. Neubauer[169], M. Neumann[178], P.R. Newman[19], T.Y. Ng[62c], T. Nguyen Manh[97], R.B. Nickerson[122], R. Nicolaidou[138], J. Nielsen[139], V. Nikolaenko[132,al], I. Nikolic-Audit[83], K. Nikolopoulos[19], J.K. Nilsen[121], P. Nilsson[27], Y. Ninomiya[157], A. Nisati[134a], N. Nishu[35c], R. Nisius[103], I. Nitsche[46], T. Nitta[174], T. Nobe[157], Y. Noguchi[71], M. Nomachi[120], I. Nomidis[31], M.A. Nomura[27], T. Nooney[79], M. Nordberg[32], N. Norjoharuddeen[122], O. Novgorodova[47], S. Nowak[103], M. Nozaki[69], L. Nozka[117], K. Ntekas[166], E. Nurse[81], F. Nuti[91], K. O'connor[25], D.C. O'Neil[144], A.A. O'Rourke[45], V. O'Shea[56], F.G. Oakham[31,d], H. Oberlack[103], T. Obermann[23], J. Ocariz[83], A. Ochi[70], I. Ochoa[38], J.P. Ochoa-Ricoux[34a], S. Oda[73], S. Odaka[69], A. Oh[87], S.H. Oh[48], C.C. Ohm[16], H. Ohman[168], H. Oide[53a,53b], H. Okawa[164], Y. Okumura[157], T. Okuyama[69], A. Olariu[28b], L.F. Oleiro Seabra[128a], S.A. Olivares Pino[34a], D. Oliveira Damazio[27], A. Olszewski[42], J. Olszowska[42], A. Onofre[128a,128e], K. Onogi[105], P.U.E. Onyisi[11,z], H. Oppen[121], M.J. Oreglia[33], Y. Oren[155], D. Orestano[136a,136b], N. Orlando[62b], R.S. Orr[161], B. Osculati[53a,53b,*], R. Ospanov[36a], G. Otero y Garzon[29], H. Otono[73], M. Ouchrif[137d], F. Ould-Saada[121], A. Ouraou[138], K.P. Oussoren[109], Q. Ouyang[35a], M. Owen[56], R.E. Owen[19], V.E. Ozcan[20a], N. Ozturk[8], K. Pachal[144], A. Pacheco Pages[13], L. Pacheco Rodriguez[138], C. Padilla Aranda[13], S. Pagan Griso[16], M. Paganini[179], F. Paige[27], G. Palacino[64], S. Palazzo[40a,40b], S. Palestini[32], M. Palka[41b], D. Pallin[37], E.St. Panagiotopoulou[10], I. Panagoulias[10], C.E. Pandini[126a,126b], J.G. Panduro Vazquez[80], P. Pani[32], S. Panitkin[27], D. Pantea[28b], L. Paolozzi[52], Th.D. Papadopoulou[10], K. Papageorgiou[9,s], A. Paramonov[6], D. Paredes Hernandez[179], A.J. Parker[75], M.A. Parker[30], K.A. Parker[45], F. Parodi[53a,53b], J.A. Parsons[38], U. Parzefall[51], V.R. Pascuzzi[161], J.M. Pasner[139], E. Pasqualucci[134a], S. Passaggio[53a], Fr. Pastore[80], S. Pataraia[86], J.R. Pater[87], T. Pauly[32], B. Pearson[103], S. Pedraza Lopez[170], R. Pedro[128a,128b], S.V. Peleganchuk[111,c], O. Penc[129], C. Peng[35a], H. Peng[36a], J. Penwell[64], B.S. Peralva[26b], M.M. Perego[138], D.V. Perepelitsa[27], F. Peri[17], L. Perini[94a,94b], H. Pernegger[32], S. Perrella[106a,106b], R. Peschke[45], V.D. Peshekhonov[68,*], K. Peters[45], R.F.Y. Peters[87], B.A. Petersen[32], T.C. Petersen[39], E. Petit[58], A. Petridis[1], C. Petridou[156], P. Petroff[119], E. Petrolo[134a], M. Petrov[122], F. Petrucci[136a,136b], N.E. Pettersson[89], A. Peyaud[138], R. Pezoa[34b], F.H. Phillips[93], P.W. Phillips[133], G. Piacquadio[150], E. Pianori[173], A. Picazio[89], E. Piccaro[79], M.A. Pickering[122], R. Piegaia[29], J.E. Pilcher[33], A.D. Pilkington[87], A.W.J. Pin[87], M. Pinamonti[135a,135b], J.L. Pinfold[3], H. Pirumov[45], M. Pitt[175], L. Plazak[146a], M.-A. Pleier[27], V. Pleskot[86], E. Plotnikova[68], D. Pluth[67], P. Podberezko[111], R. Poettgen[84], R. Poggi[123a,123b], L. Poggioli[119], D. Pohl[23], G. Polesello[123a], A. Poley[45], A. Policicchio[40a,40b], R. Polifka[32], A. Polini[22a], C.S. Pollard[56], V. Polychronakos[27], K. Pommès[32], D. Ponomarenko[100], L. Pontecorvo[134a], G.A. Popeneciu[28d], S. Pospisil[130], K. Potamianos[16], I.N. Potrap[68], C.J. Potter[30], T. Poulsen[84], J. Poveda[32], M.E. Pozo Astigarraga[32], P. Pralavorio[88], A. Pranko[16], S. Prell[67], D. Price[87], M. Primavera[76a], S. Prince[90], N. Proklova[100], K. Prokofiev[62c], F. Prokoshin[34b], S. Protopopescu[27], J. Proudfoot[6], M. Przybycien[41a], A. Puri[169], P. Puzo[119], J. Qian[92], G. Qin[56], Y. Qin[87], A. Quadt[57], M. Queitsch-Maitland[45], D. Quilty[56], S. Raddum[121], V. Radeka[27], V. Radescu[122], S.K. Radhakrishnan[150], P. Radloff[118], P. Rados[91], F. Ragusa[94a,94b], G. Rahal[181], J.A. Raine[87], S. Rajagopalan[27], C. Rangel-Smith[168], T. Rashid[119], S. Raspopov[5], M.G. Ratti[94a,94b], D.M. Rauch[45], F. Rauscher[102], S. Rave[86], I. Ravinovich[175], J.H. Rawling[87], M. Raymond[32], A.L. Read[121], N.P. Readioff[58], M. Reale[76a,76b], D.M. Rebuzzi[123a,123b], A. Redelbach[177], G. Redlinger[27], R. Reece[139], R.G. Reed[147c], K. Reeves[44], L. Rehnisch[17], J. Reichert[124], A. Reiss[86], C. Rembser[32], H. Ren[35a], M. Rescigno[134a], S. Resconi[94a], E.D. Resseguie[124], S. Rettie[171], E. Reynolds[19], O.L. Rezanova[111,c], P. Reznicek[131], R. Rezvani[97], R. Richter[103], S. Richter[81], E. Richter-Was[41b], O. Ricken[23], M. Ridel[83], P. Rieck[103], C.J. Riegel[178], J. Rieger[57], O. Rifki[115], M. Rijssenbeek[150], A. Rimoldi[123a,123b], M. Rimoldi[18], L. Rinaldi[22a], G. Ripellino[149], B. Ristić[32], E. Ritsch[32], I. Riu[13], F. Rizatdinova[116], E. Rizvi[79], C. Rizzi[13], R.T. Roberts[87], S.H. Robertson[90,o], A. Robichaud-Veronneau[90], D. Robinson[30], J.E.M. Robinson[45], A. Robson[56], E. Rocco[86], C. Roda[126a,126b], Y. Rodina[88,an], S. Rodriguez Bosca[170], A. Rodriguez Perez[13], D. Rodriguez Rodriguez[170], S. Roe[32], C.S. Rogan[59], O. Røhne[121], J. Roloff[59], A. Romaniouk[100], M. Romano[22a,22b], S.M. Romano Saez[37], E. Romero Adam[170], N. Rompotis[77], M. Ronzani[51], L. Roos[83], S. Rosati[134a], K. Rosbach[51], P. Rose[139], N.-A. Rosien[57], E. Rossi[106a,106b], L.P. Rossi[53a], J.H.N. Rosten[30], R. Rosten[140], M. Rotaru[28b], J. Rothberg[140], D. Rousseau[119], A. Rozanov[88], Y. Rozen[154], X. Ruan[147c], F. Rubbo[145], F. Rühr[51], A. Ruiz-Martinez[31], Z. Rurikova[51], N.A. Rusakovich[68], H.L. Russell[90], J.P. Rutherfoord[7], N. Ruthmann[32], Y.F. Ryabov[125], M. Rybar[169], G. Rybkin[119], S. Ryu[6], A. Ryzhov[132], G.F. Rzehorz[57], A.F. Saavedra[152], G. Sabato[109], S. Sacerdoti[29], H.F-W. Sadrozinski[139], R. Sadykov[68], F. Safai Tehrani[134a], P. Saha[110], M. Sahinsoy[60a], M. Saimpert[45], M. Saito[157], T. Saito[157],

JHEP10(2017)182

H. Sakamoto[157], Y. Sakurai[174], G. Salamanna[136a,136b], J.E. Salazar Loyola[34b], D. Salek[109], P.H. Sales De Bruin[168], D. Salihagic[103], A. Salnikov[145], J. Salt[170], D. Salvatore[40a,40b], F. Salvatore[151], A. Salvucci[62a,62b,62c], A. Salzburger[32], D. Sammel[51], D. Sampsonidis[156], D. Sampsonidou[156], J. Sánchez[170], V. Sanchez Martinez[170], A. Sanchez Pineda[167a,167c], H. Sandaker[121], R.L. Sandbach[79], C.O. Sander[45], M. Sandhoff[178], C. Sandoval[21], D.P.C. Sankey[133], M. Sannino[53a,53b], Y. Sano[105], A. Sansoni[50], C. Santoni[37], H. Santos[128a], I. Santoyo Castillo[151], A. Sapronov[68], J.G. Saraiva[128a,128d], B. Sarrazin[23], O. Sasaki[69], K. Sato[164], E. Sauvan[5], G. Savage[80], P. Savard[161,d], N. Savic[103], C. Sawyer[133], L. Sawyer[82,u], J. Saxon[33], C. Sbarra[22a], A. Sbrizzi[22a,22b], T. Scanlon[81], D.A. Scannicchio[166], M. Scarcella[152], J. Schaarschmidt[140], P. Schacht[103], B.M. Schachtner[102], D. Schaefer[32], L. Schaefer[124], R. Schaefer[45], J. Schaeffer[86], S. Schaepe[23], S. Schaetzel[60b], U. Schäfer[86], A.C. Schaffer[119], D. Schaile[102], R.D. Schamberger[150], V.A. Schegelsky[125], D. Scheirich[131], M. Schernau[166], C. Schiavi[53a,53b], S. Schier[139], L.K. Schildgen[23], C. Schillo[51], M. Schioppa[40a,40b], S. Schlenker[32], K.R. Schmidt-Sommerfeld[103], K. Schmieden[32], C. Schmitt[86], S. Schmitt[45], S. Schmitz[86], U. Schnoor[51], L. Schoeffel[138], A. Schoening[60b], B.D. Schoenrock[93], E. Schopf[23], M. Schott[86], J.F.P. Schouwenberg[108], J. Schovancova[32], S. Schramm[52], N. Schuh[86], A. Schulte[86], M.J. Schultens[23], H.-C. Schultz-Coulon[60a], H. Schulz[17], M. Schumacher[51], B.A. Schumm[139], Ph. Schune[138], A. Schwartzman[145], T.A. Schwarz[92], H. Schweiger[87], Ph. Schwemling[138], R. Schwienhorst[93], J. Schwindling[138], A. Sciandra[23], G. Sciolla[25], M. Scornajenghi[40a,40b], F. Scuri[126a,126b], F. Scutti[91], J. Searcy[92], P. Seema[23], S.C. Seidel[107], A. Seiden[139], J.M. Seixas[26a], G. Sekhniaidze[106a], K. Sekhon[92], S.J. Sekula[43], N. Semprini-Cesari[22a,22b], S. Senkin[37], C. Serfon[121], L. Serin[119], L. Serkin[167a,167b], M. Sessa[136a,136b], R. Seuster[172], H. Severini[115], T. Sfiligoj[78], F. Sforza[32], A. Sfyrla[52], E. Shabalina[57], N.W. Shaikh[148a,148b], L.Y. Shan[35a], R. Shang[169], J.T. Shank[24], M. Shapiro[16], P.B. Shatalov[99], K. Shaw[167a,167b], S.M. Shaw[87], A. Shcherbakova[148a,148b], C.Y. Shehu[151], Y. Shen[115], N. Sherafati[31], P. Sherwood[81], L. Shi[153,ao], S. Shimizu[70], C.O. Shimmin[179], M. Shimojima[104], I.P.J. Shipsey[122], S. Shirabe[73], M. Shiyakova[68,ap], J. Shlomi[175], A. Shmeleva[98], D. Shoaleh Saadi[97], M.J. Shochet[33], S. Shojaii[94a], D.R. Shope[115], S. Shrestha[113], E. Shulga[100], M.A. Shupe[7], P. Sicho[129], A.M. Sickles[169], P.E. Sidebo[149], E. Sideras Haddad[147c], O. Sidiropoulou[177], A. Sidoti[22a,22b], F. Siegert[47], Dj. Sijacki[14], J. Silva[128a,128d], S.B. Silverstein[148a], V. Simak[130], Lj. Simic[14], S. Simion[119], E. Simioni[86], B. Simmons[81], M. Simon[86], P. Sinervo[161], N.B. Sinev[118], M. Sioli[22a,22b], G. Siragusa[177], I. Siral[92], S.Yu. Sivoklokov[101], J. Sjölin[148a,148b], M.B. Skinner[75], P. Skubic[115], M. Slater[19], T. Slavicek[130], M. Slawinska[42], K. Sliwa[165], R. Slovak[131], V. Smakhtin[175], B.H. Smart[5], J. Smiesko[146a], N. Smirnov[100], S.Yu. Smirnov[100], Y. Smirnov[100], L.N. Smirnova[101,aq], O. Smirnova[84], J.W. Smith[57], M.N.K. Smith[38], R.W. Smith[38], M. Smizanska[75], K. Smolek[130], A.A. Snesarev[98], I.M. Snyder[118], S. Snyder[27], R. Sobie[172,o], F. Socher[47], A. Soffer[155], A. Søgaard[49], D.A. Soh[153], G. Sokhrannyi[78], C.A. Solans Sanchez[32], M. Solar[130], E.Yu. Soldatov[100], U. Soldevila[170], A.A. Solodkov[132], A. Soloshenko[68], O.V. Solovyanov[132], V. Solovyev[125], P. Sommer[51], H. Son[165], A. Sopczak[130], D. Sosa[60b], C.L. Sotiropoulou[126a,126b], R. Soualah[167a,167c], A.M. Soukharev[111,c], D. South[45], B.C. Sowden[80], S. Spagnolo[76a,76b], M. Spalla[126a,126b], M. Spangenberg[173], F. Spanò[80], D. Sperlich[17], F. Spettel[103], T.M. Spieker[60a], R. Spighi[22a], G. Spigo[32], L.A. Spiller[91], M. Spousta[131], R.D. St. Denis[56,*], A. Stabile[94a], R. Stamen[60a], S. Stamm[17], E. Stanecka[42], R.W. Stanek[6], C. Stanescu[136a], M.M. Stanitzki[45], B.S. Stapf[109], S. Stapnes[121], E.A. Starchenko[132], G.H. Stark[33], J. Stark[58], S.H Stark[39], P. Staroba[129], P. Starovoitov[60a], S. Stärz[32], R. Staszewski[42], P. Steinberg[27], B. Stelzer[144], H.J. Stelzer[32], O. Stelzer-Chilton[163a], H. Stenzel[55], G.A. Stewart[56], M.C. Stockton[118], M. Stoebe[90], G. Stoicea[28b], P. Stolte[57], S. Stonjek[103], A.R. Stradling[8], A. Straessner[47], M.E. Stramaglia[18], J. Strandberg[149], S. Strandberg[148a,148b],

M. Strauss[115], P. Strizenec[146b], R. Ströhmer[177], D.M. Strom[118], R. Stroynowski[43], A. Strubig[49], S.A. Stucci[27], B. Stugu[15], N.A. Styles[45], D. Su[145], J. Su[127], S. Suchek[60a], Y. Sugaya[120], M. Suk[130], V.V. Sulin[98], DMS Sultan[162a,162b], S. Sultansoy[4c], T. Sumida[71], S. Sun[59], X. Sun[3], K. Suruliz[151], C.J.E. Suster[152], M.R. Sutton[151], S. Suzuki[69], M. Svatos[129], M. Swiatlowski[33], S.P. Swift[2], I. Sykora[146a], T. Sykora[131], D. Ta[51], K. Tackmann[45], J. Taenzer[155], A. Taffard[166], R. Tafirout[163a], E. Tahirovic[79], N. Taiblum[155], H. Takai[27], R. Takashima[72], E.H. Takasugi[103], T. Takeshita[142], Y. Takubo[69], M. Talby[88], A.A. Talyshev[111,c], J. Tanaka[157], M. Tanaka[159], R. Tanaka[119], S. Tanaka[69], R. Tanioka[70], B.B. Tannenwald[113], S. Tapia Araya[34b], S. Tapprogge[86], S. Tarem[154], G.F. Tartarelli[94a], P. Tas[131], M. Tasevsky[129], T. Tashiro[71], E. Tassi[40a,40b], A. Tavares Delgado[128a,128b], Y. Tayalati[137e], A.C. Taylor[107], G.N. Taylor[91], P.T.E. Taylor[91], W. Taylor[163b], P. Teixeira-Dias[80], D. Temple[144], H. Ten Kate[32], P.K. Teng[153], J.J. Teoh[120], F. Tepel[178], S. Terada[69], K. Terashi[157], J. Terron[85], S. Terzo[13], M. Testa[50], R.J. Teuscher[161,o], T. Theveneaux-Pelzer[88], F. Thiele[39], J.P. Thomas[19], J. Thomas-Wilsker[80], P.D. Thompson[19], A.S. Thompson[56], L.A. Thomsen[179], E. Thomson[124], M.J. Tibbetts[16], R.E. Ticse Torres[88], V.O. Tikhomirov[98,ar], Yu.A. Tikhonov[111,c], S. Timoshenko[100], P. Tipton[179], S. Tisserant[88], K. Todome[159], S. Todorova-Nova[5], S. Todt[47], J. Tojo[73], S. Tokár[146a], K. Tokushuku[69], E. Tolley[59], L. Tomlinson[87], M. Tomoto[105], L. Tompkins[145,as], K. Toms[107], B. Tong[59], P. Tornambe[51], E. Torrence[118], H. Torres[144], E. Torró Pastor[140], J. Toth[88,at], F. Touchard[88], D.R. Tovey[141], C.J. Treado[112], T. Trefzger[177], F. Tresoldi[151], A. Tricoli[27], I.M. Trigger[163a], S. Trincaz-Duvoid[83], M.F. Tripiana[13], W. Trischuk[161], B. Trocmé[58], A. Trofymov[45], C. Troncon[94a], M. Trottier-McDonald[16], M. Trovatelli[172], L. Truong[147b], M. Trzebinski[42], A. Trzupek[42], K.W. Tsang[62a], J.C-L. Tseng[122], P.V. Tsiareshka[95], G. Tsipolitis[10], N. Tsirintanis[9], S. Tsiskaridze[13], V. Tsiskaridze[51], E.G. Tskhadadze[54a], K.M. Tsui[62a], I.I. Tsukerman[99], V. Tsulaia[16], S. Tsuno[69], D. Tsybychev[150], Y. Tu[62b], A. Tudorache[28b], V. Tudorache[28b], T.T. Tulbure[28a], A.N. Tuna[59], S.A. Tupputi[22a,22b], S. Turchikhin[68], D. Turgeman[175], I. Turk Cakir[4b,au], R. Turra[94a], P.M. Tuts[38], G. Ucchielli[22a,22b], I. Ueda[69], M. Ughetto[148a,148b], F. Ukegawa[164], G. Unal[32], A. Undrus[27], G. Unel[166], F.C. Ungaro[91], Y. Unno[69], C. Unverdorben[102], J. Urban[146b], P. Urquijo[91], P. Urrejola[86], G. Usai[8], J. Usui[69], L. Vacavant[88], V. Vacek[130], B. Vachon[90], K.O.H. Vadla[121], A. Vaidya[81], C. Valderanis[102], E. Valdes Santurio[148a,148b], M. Valente[52], S. Valentinetti[22a,22b], A. Valero[170], L. Valéry[13], S. Valkar[131], A. Vallier[5], J.A. Valls Ferrer[170], W. Van Den Wollenberg[109], H. van der Graaf[109], P. van Gemmeren[6], J. Van Nieuwkoop[144], I. van Vulpen[109], M.C. van Woerden[109], M. Vanadia[135a,135b], W. Vandelli[32], A. Vaniachine[160], P. Vankov[109], G. Vardanyan[180], R. Vari[134a], E.W. Varnes[7], C. Varni[53a,53b], T. Varol[43], D. Varouchas[119], A. Vartapetian[8], K.E. Varvell[152], J.G. Vasquez[179], G.A. Vasquez[34b], F. Vazeille[37], T. Vazquez Schroeder[90], J. Veatch[57], V. Veeraraghavan[7], L.M. Veloce[161], F. Veloso[128a,128c], S. Veneziano[134a], A. Ventura[76a,76b], M. Venturi[172], N. Venturi[32], A. Venturini[25], V. Vercesi[123a], M. Verducci[136a,136b], W. Verkerke[109], A.T. Vermeulen[109], J.C. Vermeulen[109], M.C. Vetterli[144,d], N. Viaux Maira[34b], O. Viazlo[84], I. Vichou[169,*], T. Vickey[141], O.E. Vickey Boeriu[141], G.H.A. Viehhauser[122], S. Viel[16], L. Vigani[122], M. Villa[22a,22b], M. Villaplana Perez[94a,94b], E. Vilucchi[50], M.G. Vincter[31], V.B. Vinogradov[68], A. Vishwakarma[45], C. Vittori[22a,22b], I. Vivarelli[151], S. Vlachos[10], M. Vogel[178], P. Vokac[130], G. Volpi[126a,126b], H. von der Schmitt[103], E. von Toerne[23], V. Vorobel[131], K. Vorobev[100], M. Vos[170], R. Voss[32], J.H. Vossebeld[77], N. Vranjes[14], M. Vranjes Milosavljevic[14], V. Vrba[130], M. Vreeswijk[109], R. Vuillermet[32], I. Vukotic[33], P. Wagner[23], W. Wagner[178], J. Wagner-Kuhr[102], H. Wahlberg[74], S. Wahrmund[47], J. Wakabayashi[105], J. Walder[75], R. Walker[102], W. Walkowiak[143], V. Wallangen[148a,148b], C. Wang[35b], C. Wang[36b,av], F. Wang[176], H. Wang[16], H. Wang[3], J. Wang[45], J. Wang[152], Q. Wang[115], R. Wang[6], S.M. Wang[153], T. Wang[38],

W. Wang[153,aw], W. Wang[36a], Z. Wang[36c], C. Wanotayaroj[118], A. Warburton[90], C.P. Ward[30], D.R. Wardrope[81], A. Washbrook[49], P.M. Watkins[19], A.T. Watson[19], M.F. Watson[19], G. Watts[140], S. Watts[87], B.M. Waugh[81], A.F. Webb[11], S. Webb[86], M.S. Weber[18], S.W. Weber[177], S.A. Weber[31], J.S. Webster[6], A.R. Weidberg[122], B. Weinert[64], J. Weingarten[57], M. Weirich[86], C. Weiser[51], H. Weits[109], P.S. Wells[32], T. Wenaus[27], T. Wengler[32], S. Wenig[32], N. Wermes[23], M.D. Werner[67], P. Werner[32], M. Wessels[60a], T.D. Weston[18], K. Whalen[118], N.L. Whallon[140], A.M. Wharton[75], A.S. White[92], A. White[8], M.J. White[1], R. White[34b], D. Whiteson[166], B.W. Whitmore[75], F.J. Wickens[133], W. Wiedenmann[176], M. Wielers[133], C. Wiglesworth[39], L.A.M. Wiik-Fuchs[51], A. Wildauer[103], F. Wilk[87], H.G. Wilkens[32], H.H. Williams[124], S. Williams[109], C. Willis[93], S. Willocq[89], J.A. Wilson[19], I. Wingerter-Seez[5], E. Winkels[151], F. Winklmeier[118], O.J. Winston[151], B.T. Winter[23], M. Wittgen[145], M. Wobisch[82,u], T.M.H. Wolf[109], R. Wolff[88], M.W. Wolter[42], H. Wolters[128a,128c], V.W.S. Wong[171], S.D. Worm[19], B.K. Wosiek[42], J. Wotschack[32], K.W. Wozniak[42], M. Wu[33], S.L. Wu[176], X. Wu[52], Y. Wu[92], T.R. Wyatt[87], B.M. Wynne[49], S. Xella[39], Z. Xi[92], L. Xia[35c], D. Xu[35a], L. Xu[27], T. Xu[138], B. Yabsley[152], S. Yacoob[147a], D. Yamaguchi[159], Y. Yamaguchi[120], A. Yamamoto[69], S. Yamamoto[157], T. Yamanaka[157], M. Yamatani[157], K. Yamauchi[105], Y. Yamazaki[70], Z. Yan[24], H. Yang[36c], H. Yang[16], Y. Yang[153], Z. Yang[15], W-M. Yao[16], Y.C. Yap[83], Y. Yasu[69], E. Yatsenko[5], K.H. Yau Wong[23], J. Ye[43], S. Ye[27], I. Yeletskikh[68], E. Yigitbasi[24], E. Yildirim[86], K. Yorita[174], K. Yoshihara[124], C. Young[145], C.J.S. Young[32], J. Yu[8], J. Yu[67], S.P.Y. Yuen[23], I. Yusuff[30,ax], B. Zabinski[42], G. Zacharis[10], R. Zaidan[13], A.M. Zaitsev[132,al], N. Zakharchuk[45], J. Zalieckas[15], A. Zaman[150], S. Zambito[59], D. Zanzi[91], C. Zeitnitz[178], G. Zemaityte[122], A. Zemla[41a], J.C. Zeng[169], Q. Zeng[145], O. Zenin[132], T. Ženiš[146a], D. Zerwas[119], D. Zhang[92], F. Zhang[176], G. Zhang[36a,ay], H. Zhang[35b], J. Zhang[6], L. Zhang[51], L. Zhang[36a], M. Zhang[169], P. Zhang[35b], R. Zhang[23], R. Zhang[36a,av], X. Zhang[36b], Y. Zhang[35a], Z. Zhang[119], X. Zhao[43], Y. Zhao[36b,az], Z. Zhao[36a], A. Zhemchugov[68], B. Zhou[92], C. Zhou[176], L. Zhou[43], M. Zhou[35a], M. Zhou[150], N. Zhou[35c], C.G. Zhu[36b], H. Zhu[35a], J. Zhu[92], Y. Zhu[36a], X. Zhuang[35a], K. Zhukov[98], A. Zibell[177], D. Zieminska[64], N.I. Zimine[68], C. Zimmermann[86], S. Zimmermann[51], Z. Zinonos[103], M. Zinser[86], M. Ziolkowski[143], L. Živković[14], G. Zobernig[176], A. Zoccoli[22a,22b], R. Zou[33], M. zur Nedden[17], L. Zwalinski[32].

[1] *Department of Physics, University of Adelaide, Adelaide, Australia*
[2] *Physics Department, SUNY Albany, Albany NY, United States of America*
[3] *Department of Physics, University of Alberta, Edmonton AB, Canada*
[4] [(a)] *Department of Physics, Ankara University, Ankara;* [(b)] *Istanbul Aydin University, Istanbul;* [(c)] *Division of Physics, TOBB University of Economics and Technology, Ankara, Turkey*
[5] *LAPP, CNRS/IN2P3 and Université Savoie Mont Blanc, Annecy-le-Vieux, France*
[6] *High Energy Physics Division, Argonne National Laboratory, Argonne IL, United States of America*
[7] *Department of Physics, University of Arizona, Tucson AZ, United States of America*
[8] *Department of Physics, The University of Texas at Arlington, Arlington TX, United States of America*
[9] *Physics Department, National and Kapodistrian University of Athens, Athens, Greece*
[10] *Physics Department, National Technical University of Athens, Zografou, Greece*
[11] *Department of Physics, The University of Texas at Austin, Austin TX, United States of America*
[12] *Institute of Physics, Azerbaijan Academy of Sciences, Baku, Azerbaijan*
[13] *Institut de Física d'Altes Energies (IFAE), The Barcelona Institute of Science and Technology, Barcelona, Spain*
[14] *Institute of Physics, University of Belgrade, Belgrade, Serbia*
[15] *Department for Physics and Technology, University of Bergen, Bergen, Norway*
[16] *Physics Division, Lawrence Berkeley National Laboratory and University of California, Berkeley CA, United States of America*

[17] *Department of Physics, Humboldt University, Berlin, Germany*
[18] *Albert Einstein Center for Fundamental Physics and Laboratory for High Energy Physics, University of Bern, Bern, Switzerland*
[19] *School of Physics and Astronomy, University of Birmingham, Birmingham, United Kingdom*
[20] [(a)] *Department of Physics, Bogazici University, Istanbul;* [(b)] *Department of Physics Engineering, Gaziantep University, Gaziantep;* [(d)] *Istanbul Bilgi University, Faculty of Engineering and Natural Sciences, Istanbul;* [(e)] *Bahcesehir University, Faculty of Engineering and Natural Sciences, Istanbul, Turkey*
[21] *Centro de Investigaciones, Universidad Antonio Narino, Bogota, Colombia*
[22] [(a)] *INFN Sezione di Bologna;* [(b)] *Dipartimento di Fisica e Astronomia, Università di Bologna, Bologna, Italy*
[23] *Physikalisches Institut, University of Bonn, Bonn, Germany*
[24] *Department of Physics, Boston University, Boston MA, United States of America*
[25] *Department of Physics, Brandeis University, Waltham MA, United States of America*
[26] [(a)] *Universidade Federal do Rio De Janeiro COPPE/EE/IF, Rio de Janeiro;* [(b)] *Electrical Circuits Department, Federal University of Juiz de Fora (UFJF), Juiz de Fora;* [(c)] *Federal University of Sao Joao del Rei (UFSJ), Sao Joao del Rei;* [(d)] *Instituto de Fisica, Universidade de Sao Paulo, Sao Paulo, Brazil*
[27] *Physics Department, Brookhaven National Laboratory, Upton NY, United States of America*
[28] [(a)] *Transilvania University of Brasov, Brasov;* [(b)] *Horia Hulubei National Institute of Physics and Nuclear Engineering, Bucharest;* [(c)] *Department of Physics, Alexandru Ioan Cuza University of Iasi, Iasi;* [(d)] *National Institute for Research and Development of Isotopic and Molecular Technologies, Physics Department, Cluj Napoca;* [(e)] *University Politehnica Bucharest, Bucharest;* [(f)] *West University in Timisoara, Timisoara, Romania*
[29] *Departamento de Física, Universidad de Buenos Aires, Buenos Aires, Argentina*
[30] *Cavendish Laboratory, University of Cambridge, Cambridge, United Kingdom*
[31] *Department of Physics, Carleton University, Ottawa ON, Canada*
[32] *CERN, Geneva, Switzerland*
[33] *Enrico Fermi Institute, University of Chicago, Chicago IL, United States of America*
[34] [(a)] *Departamento de Física, Pontificia Universidad Católica de Chile, Santiago;* [(b)] *Departamento de Física, Universidad Técnica Federico Santa María, Valparaíso, Chile*
[35] [(a)] *Institute of High Energy Physics, Chinese Academy of Sciences, Beijing;* [(b)] *Department of Physics, Nanjing University, Jiangsu;* [(c)] *Physics Department, Tsinghua University, Beijing 100084, China*
[36] [(a)] *Department of Modern Physics and State Key Laboratory of Particle Detection and Electronics, University of Science and Technology of China, Anhui;* [(b)] *School of Physics, Shandong University, Shandong;* [(c)] *Department of Physics and Astronomy, Key Laboratory for Particle Physics, Astrophysics and Cosmology, Ministry of Education; Shanghai Key Laboratory for Particle Physics and Cosmology, Shanghai Jiao Tong University, Shanghai(also at PKU-CHEP), China*
[37] *Université Clermont Auvergne, CNRS/IN2P3, LPC, Clermont-Ferrand, France*
[38] *Nevis Laboratory, Columbia University, Irvington NY, United States of America*
[39] *Niels Bohr Institute, University of Copenhagen, Kobenhavn, Denmark*
[40] [(a)] *INFN Gruppo Collegato di Cosenza, Laboratori Nazionali di Frascati;* [(b)] *Dipartimento di Fisica, Università della Calabria, Rende, Italy*
[41] [(a)] *AGH University of Science and Technology, Faculty of Physics and Applied Computer Science, Krakow;* [(b)] *Marian Smoluchowski Institute of Physics, Jagiellonian University, Krakow, Poland*
[42] *Institute of Nuclear Physics Polish Academy of Sciences, Krakow, Poland*
[43] *Physics Department, Southern Methodist University, Dallas TX, United States of America*
[44] *Physics Department, University of Texas at Dallas, Richardson TX, United States of America*
[45] *DESY, Hamburg and Zeuthen, Germany*
[46] *Lehrstuhl für Experimentelle Physik IV, Technische Universität Dortmund, Dortmund, Germany*
[47] *Institut für Kern- und Teilchenphysik, Technische Universität Dresden, Dresden, Germany*

[48] Department of Physics, Duke University, Durham NC, United States of America
[49] SUPA - School of Physics and Astronomy, University of Edinburgh, Edinburgh, United Kingdom
[50] INFN e Laboratori Nazionali di Frascati, Frascati, Italy
[51] Fakultät für Mathematik und Physik, Albert-Ludwigs-Universität, Freiburg, Germany
[52] Departement de Physique Nucleaire et Corpusculaire, Université de Genève, Geneva, Switzerland
[53] [(a)] INFN Sezione di Genova; [(b)] Dipartimento di Fisica, Università di Genova, Genova, Italy
[54] [(a)] E. Andronikashvili Institute of Physics, Iv. Javakhishvili Tbilisi State University, Tbilisi; [(b)] High Energy Physics Institute, Tbilisi State University, Tbilisi, Georgia
[55] II Physikalisches Institut, Justus-Liebig-Universität Giessen, Giessen, Germany
[56] SUPA - School of Physics and Astronomy, University of Glasgow, Glasgow, United Kingdom
[57] II Physikalisches Institut, Georg-August-Universität, Göttingen, Germany
[58] Laboratoire de Physique Subatomique et de Cosmologie, Université Grenoble-Alpes, CNRS/IN2P3, Grenoble, France
[59] Laboratory for Particle Physics and Cosmology, Harvard University, Cambridge MA, United States of America
[60] [(a)] Kirchhoff-Institut für Physik, Ruprecht-Karls-Universität Heidelberg, Heidelberg; [(b)] Physikalisches Institut, Ruprecht-Karls-Universität Heidelberg, Heidelberg, Germany
[61] Faculty of Applied Information Science, Hiroshima Institute of Technology, Hiroshima, Japan
[62] [(a)] Department of Physics, The Chinese University of Hong Kong, Shatin, N.T., Hong Kong; [(b)] Department of Physics, The University of Hong Kong, Hong Kong; [(c)] Department of Physics and Institute for Advanced Study, The Hong Kong University of Science and Technology, Clear Water Bay, Kowloon, Hong Kong, China
[63] Department of Physics, National Tsing Hua University, Taiwan
[64] Department of Physics, Indiana University, Bloomington IN, United States of America
[65] Institut für Astro- und Teilchenphysik, Leopold-Franzens-Universität, Innsbruck, Austria
[66] University of Iowa, Iowa City IA, United States of America
[67] Department of Physics and Astronomy, Iowa State University, Ames IA, United States of America
[68] Joint Institute for Nuclear Research, JINR Dubna, Dubna, Russia
[69] KEK, High Energy Accelerator Research Organization, Tsukuba, Japan
[70] Graduate School of Science, Kobe University, Kobe, Japan
[71] Faculty of Science, Kyoto University, Kyoto, Japan
[72] Kyoto University of Education, Kyoto, Japan
[73] Research Center for Advanced Particle Physics and Department of Physics, Kyushu University, Fukuoka, Japan
[74] Instituto de Física La Plata, Universidad Nacional de La Plata and CONICET, La Plata, Argentina
[75] Physics Department, Lancaster University, Lancaster, United Kingdom
[76] [(a)] INFN Sezione di Lecce; [(b)] Dipartimento di Matematica e Fisica, Università del Salento, Lecce, Italy
[77] Oliver Lodge Laboratory, University of Liverpool, Liverpool, United Kingdom
[78] Department of Experimental Particle Physics, Jožef Stefan Institute and Department of Physics, University of Ljubljana, Ljubljana, Slovenia
[79] School of Physics and Astronomy, Queen Mary University of London, London, United Kingdom
[80] Department of Physics, Royal Holloway University of London, Surrey, United Kingdom
[81] Department of Physics and Astronomy, University College London, London, United Kingdom
[82] Louisiana Tech University, Ruston LA, United States of America
[83] Laboratoire de Physique Nucléaire et de Hautes Energies, UPMC and Université Paris-Diderot and CNRS/IN2P3, Paris, France
[84] Fysiska institutionen, Lunds universitet, Lund, Sweden
[85] Departamento de Fisica Teorica C-15, Universidad Autonoma de Madrid, Madrid, Spain
[86] Institut für Physik, Universität Mainz, Mainz, Germany
[87] School of Physics and Astronomy, University of Manchester, Manchester, United Kingdom
[88] CPPM, Aix-Marseille Université and CNRS/IN2P3, Marseille, France

[89] *Department of Physics, University of Massachusetts, Amherst MA, United States of America*
[90] *Department of Physics, McGill University, Montreal QC, Canada*
[91] *School of Physics, University of Melbourne, Victoria, Australia*
[92] *Department of Physics, The University of Michigan, Ann Arbor MI, United States of America*
[93] *Department of Physics and Astronomy, Michigan State University, East Lansing MI, United States of America*
[94] [(a)] *INFN Sezione di Milano;* [(b)] *Dipartimento di Fisica, Università di Milano, Milano, Italy*
[95] *B.I. Stepanov Institute of Physics, National Academy of Sciences of Belarus, Minsk, Republic of Belarus*
[96] *Research Institute for Nuclear Problems of Byelorussian State University, Minsk, Republic of Belarus*
[97] *Group of Particle Physics, University of Montreal, Montreal QC, Canada*
[98] *P.N. Lebedev Physical Institute of the Russian Academy of Sciences, Moscow, Russia*
[99] *Institute for Theoretical and Experimental Physics (ITEP), Moscow, Russia*
[100] *National Research Nuclear University MEPhI, Moscow, Russia*
[101] *D.V. Skobeltsyn Institute of Nuclear Physics, M.V. Lomonosov Moscow State University, Moscow, Russia*
[102] *Fakultät für Physik, Ludwig-Maximilians-Universität München, München, Germany*
[103] *Max-Planck-Institut für Physik (Werner-Heisenberg-Institut), München, Germany*
[104] *Nagasaki Institute of Applied Science, Nagasaki, Japan*
[105] *Graduate School of Science and Kobayashi-Maskawa Institute, Nagoya University, Nagoya, Japan*
[106] [(a)] *INFN Sezione di Napoli;* [(b)] *Dipartimento di Fisica, Università di Napoli, Napoli, Italy*
[107] *Department of Physics and Astronomy, University of New Mexico, Albuquerque NM, United States of America*
[108] *Institute for Mathematics, Astrophysics and Particle Physics, Radboud University Nijmegen/Nikhef, Nijmegen, Netherlands*
[109] *Nikhef National Institute for Subatomic Physics and University of Amsterdam, Amsterdam, Netherlands*
[110] *Department of Physics, Northern Illinois University, DeKalb IL, United States of America*
[111] *Budker Institute of Nuclear Physics, SB RAS, Novosibirsk, Russia*
[112] *Department of Physics, New York University, New York NY, United States of America*
[113] *Ohio State University, Columbus OH, United States of America*
[114] *Faculty of Science, Okayama University, Okayama, Japan*
[115] *Homer L. Dodge Department of Physics and Astronomy, University of Oklahoma, Norman OK, United States of America*
[116] *Department of Physics, Oklahoma State University, Stillwater OK, United States of America*
[117] *Palacký University, RCPTM, Olomouc, Czech Republic*
[118] *Center for High Energy Physics, University of Oregon, Eugene OR, United States of America*
[119] *LAL, Univ. Paris-Sud, CNRS/IN2P3, Université Paris-Saclay, Orsay, France*
[120] *Graduate School of Science, Osaka University, Osaka, Japan*
[121] *Department of Physics, University of Oslo, Oslo, Norway*
[122] *Department of Physics, Oxford University, Oxford, United Kingdom*
[123] [(a)] *INFN Sezione di Pavia;* [(b)] *Dipartimento di Fisica, Università di Pavia, Pavia, Italy*
[124] *Department of Physics, University of Pennsylvania, Philadelphia PA, United States of America*
[125] *National Research Centre "Kurchatov Institute" B.P. Konstantinov Petersburg Nuclear Physics Institute, St. Petersburg, Russia*
[126] [(a)] *INFN Sezione di Pisa;* [(b)] *Dipartimento di Fisica E. Fermi, Università di Pisa, Pisa, Italy*
[127] *Department of Physics and Astronomy, University of Pittsburgh, Pittsburgh PA, United States of America*
[128] [(a)] *Laboratório de Instrumentação e Física Experimental de Partículas - LIP, Lisboa;* [(b)] *Faculdade de Ciências, Universidade de Lisboa, Lisboa;* [(c)] *Department of Physics, University of Coimbra, Coimbra;* [(d)] *Centro de Física Nuclear da Universidade de Lisboa, Lisboa;* [(e)] *Departamento de*

JHEP10(2017)182

Fisica, Universidade do Minho, Braga; [f] *Departamento de Fisica Teorica y del Cosmos and CAFPE, Universidad de Granada, Granada;* [g] *Dep Fisica and CEFITEC of Faculdade de Ciencias e Tecnologia, Universidade Nova de Lisboa, Caparica, Portugal*

[129] *Institute of Physics, Academy of Sciences of the Czech Republic, Praha, Czech Republic*

[130] *Czech Technical University in Prague, Praha, Czech Republic*

[131] *Charles University, Faculty of Mathematics and Physics, Prague, Czech Republic*

[132] *State Research Center Institute for High Energy Physics (Protvino), NRC KI, Russia*

[133] *Particle Physics Department, Rutherford Appleton Laboratory, Didcot, United Kingdom*

[134] [a] *INFN Sezione di Roma;* [b] *Dipartimento di Fisica, Sapienza Università di Roma, Roma, Italy*

[135] [a] *INFN Sezione di Roma Tor Vergata;* [b] *Dipartimento di Fisica, Università di Roma Tor Vergata, Roma, Italy*

[136] [a] *INFN Sezione di Roma Tre;* [b] *Dipartimento di Matematica e Fisica, Università Roma Tre, Roma, Italy*

[137] [a] *Faculté des Sciences Ain Chock, Réseau Universitaire de Physique des Hautes Energies - Université Hassan II, Casablanca;* [b] *Centre National de l'Energie des Sciences Techniques Nucleaires, Rabat;* [c] *Faculté des Sciences Semlalia, Université Cadi Ayyad, LPHEA-Marrakech;* [d] *Faculté des Sciences, Université Mohamed Premier and LPTPM, Oujda;* [e] *Faculté des sciences, Université Mohammed V, Rabat, Morocco*

[138] *DSM/IRFU (Institut de Recherches sur les Lois Fondamentales de l'Univers), CEA Saclay (Commissariat à l'Energie Atomique et aux Energies Alternatives), Gif-sur-Yvette, France*

[139] *Santa Cruz Institute for Particle Physics, University of California Santa Cruz, Santa Cruz CA, United States of America*

[140] *Department of Physics, University of Washington, Seattle WA, United States of America*

[141] *Department of Physics and Astronomy, University of Sheffield, Sheffield, United Kingdom*

[142] *Department of Physics, Shinshu University, Nagano, Japan*

[143] *Department Physik, Universität Siegen, Siegen, Germany*

[144] *Department of Physics, Simon Fraser University, Burnaby BC, Canada*

[145] *SLAC National Accelerator Laboratory, Stanford CA, United States of America*

[146] [a] *Faculty of Mathematics, Physics & Informatics, Comenius University, Bratislava;* [b] *Department of Subnuclear Physics, Institute of Experimental Physics of the Slovak Academy of Sciences, Kosice, Slovak Republic*

[147] [a] *Department of Physics, University of Cape Town, Cape Town;* [b] *Department of Physics, University of Johannesburg, Johannesburg;* [c] *School of Physics, University of the Witwatersrand, Johannesburg, South Africa*

[148] [a] *Department of Physics, Stockholm University;* [b] *The Oskar Klein Centre, Stockholm, Sweden*

[149] *Physics Department, Royal Institute of Technology, Stockholm, Sweden*

[150] *Departments of Physics & Astronomy and Chemistry, Stony Brook University, Stony Brook NY, United States of America*

[151] *Department of Physics and Astronomy, University of Sussex, Brighton, United Kingdom*

[152] *School of Physics, University of Sydney, Sydney, Australia*

[153] *Institute of Physics, Academia Sinica, Taipei, Taiwan*

[154] *Department of Physics, Technion: Israel Institute of Technology, Haifa, Israel*

[155] *Raymond and Beverly Sackler School of Physics and Astronomy, Tel Aviv University, Tel Aviv, Israel*

[156] *Department of Physics, Aristotle University of Thessaloniki, Thessaloniki, Greece*

[157] *International Center for Elementary Particle Physics and Department of Physics, The University of Tokyo, Tokyo, Japan*

[158] *Graduate School of Science and Technology, Tokyo Metropolitan University, Tokyo, Japan*

[159] *Department of Physics, Tokyo Institute of Technology, Tokyo, Japan*

[160] *Tomsk State University, Tomsk, Russia*

[161] *Department of Physics, University of Toronto, Toronto ON, Canada*

[162] [a] *INFN-TIFPA;* [b] *University of Trento, Trento, Italy*

JHEP10(2017)182

[163] [(a)] TRIUMF, Vancouver BC; [(b)] Department of Physics and Astronomy, York University, Toronto ON, Canada
[164] Faculty of Pure and Applied Sciences, and Center for Integrated Research in Fundamental Science and Engineering, University of Tsukuba, Tsukuba, Japan
[165] Department of Physics and Astronomy, Tufts University, Medford MA, United States of America
[166] Department of Physics and Astronomy, University of California Irvine, Irvine CA, United States of America
[167] [(a)] INFN Gruppo Collegato di Udine, Sezione di Trieste, Udine; [(b)] ICTP, Trieste; [(c)] Dipartimento di Chimica, Fisica e Ambiente, Università di Udine, Udine, Italy
[168] Department of Physics and Astronomy, University of Uppsala, Uppsala, Sweden
[169] Department of Physics, University of Illinois, Urbana IL, United States of America
[170] Instituto de Fisica Corpuscular (IFIC), Centro Mixto Universidad de Valencia - CSIC, Spain
[171] Department of Physics, University of British Columbia, Vancouver BC, Canada
[172] Department of Physics and Astronomy, University of Victoria, Victoria BC, Canada
[173] Department of Physics, University of Warwick, Coventry, United Kingdom
[174] Waseda University, Tokyo, Japan
[175] Department of Particle Physics, The Weizmann Institute of Science, Rehovot, Israel
[176] Department of Physics, University of Wisconsin, Madison WI, United States of America
[177] Fakultät für Physik und Astronomie, Julius-Maximilians-Universität, Würzburg, Germany
[178] Fakultät für Mathematik und Naturwissenschaften, Fachgruppe Physik, Bergische Universität Wuppertal, Wuppertal, Germany
[179] Department of Physics, Yale University, New Haven CT, United States of America
[180] Yerevan Physics Institute, Yerevan, Armenia
[181] Centre de Calcul de l'Institut National de Physique Nucléaire et de Physique des Particules (IN2P3), Villeurbanne, France
[182] Academia Sinica Grid Computing, Institute of Physics, Academia Sinica, Taipei, Taiwan
[a] Also at Department of Physics, King's College London, London, United Kingdom
[b] Also at Institute of Physics, Azerbaijan Academy of Sciences, Baku, Azerbaijan
[c] Also at Novosibirsk State University, Novosibirsk, Russia
[d] Also at TRIUMF, Vancouver BC, Canada
[e] Also at Department of Physics & Astronomy, University of Louisville, Louisville, KY, United States of America
[f] Also at Physics Department, An-Najah National University, Nablus, Palestine
[g] Also at Department of Physics, California State University, Fresno CA, United States of America
[h] Also at Department of Physics, University of Fribourg, Fribourg, Switzerland
[i] Also at II Physikalisches Institut, Georg-August-Universität, Göttingen, Germany
[j] Also at Departament de Fisica de la Universitat Autonoma de Barcelona, Barcelona, Spain
[k] Also at Departamento de Fisica e Astronomia, Faculdade de Ciencias, Universidade do Porto, Portugal
[l] Also at Tomsk State University, Tomsk, Russia
[m] Also at The Collaborative Innovation Center of Quantum Matter (CICQM), Beijing, China
[n] Also at Universita di Napoli Parthenope, Napoli, Italy
[o] Also at Institute of Particle Physics (IPP), Canada
[p] Also at Horia Hulubei National Institute of Physics and Nuclear Engineering, Bucharest, Romania
[q] Also at Department of Physics, St. Petersburg State Polytechnical University, St. Petersburg, Russia
[r] Also at Borough of Manhattan Community College, City University of New York, New York City, United States of America
[s] Also at Department of Financial and Management Engineering, University of the Aegean, Chios, Greece
[t] Also at Centre for High Performance Computing, CSIR Campus, Rosebank, Cape Town, South Africa
[u] Also at Louisiana Tech University, Ruston LA, United States of America

[v] Also at Institucio Catalana de Recerca i Estudis Avancats, ICREA, Barcelona, Spain
[w] Also at Graduate School of Science, Osaka University, Osaka, Japan
[x] Also at Fakultät für Mathematik und Physik, Albert-Ludwigs-Universität, Freiburg, Germany
[y] Also at Institute for Mathematics, Astrophysics and Particle Physics, Radboud University Nijmegen/Nikhef, Nijmegen, Netherlands
[z] Also at Department of Physics, The University of Texas at Austin, Austin TX, United States of America
[aa] Also at Institute of Theoretical Physics, Ilia State University, Tbilisi, Georgia
[ab] Also at CERN, Geneva, Switzerland
[ac] Also at Georgian Technical University (GTU),Tbilisi, Georgia
[ad] Also at Ochadai Academic Production, Ochanomizu University, Tokyo, Japan
[ae] Also at Manhattan College, New York NY, United States of America
[af] Also at Departamento de Física, Pontificia Universidad Católica de Chile, Santiago, Chile
[ag] Also at Department of Physics, The University of Michigan, Ann Arbor MI, United States of America
[ah] Also at The City College of New York, New York NY, United States of America
[ai] Also at School of Physics, Shandong University, Shandong, China
[aj] Also at Departamento de Fisica Teorica y del Cosmos and CAFPE, Universidad de Granada, Granada, Portugal
[ak] Also at Department of Physics, California State University, Sacramento CA, United States of America
[al] Also at Moscow Institute of Physics and Technology State University, Dolgoprudny, Russia
[am] Also at Departement de Physique Nucleaire et Corpusculaire, Université de Genève, Geneva, Switzerland
[an] Also at Institut de Física d'Altes Energies (IFAE), The Barcelona Institute of Science and Technology, Barcelona, Spain
[ao] Also at School of Physics, Sun Yat-sen University, Guangzhou, China
[ap] Also at Institute for Nuclear Research and Nuclear Energy (INRNE) of the Bulgarian Academy of Sciences, Sofia, Bulgaria
[aq] Also at Faculty of Physics, M.V. Lomonosov Moscow State University, Moscow, Russia
[ar] Also at National Research Nuclear University MEPhI, Moscow, Russia
[as] Also at Department of Physics, Stanford University, Stanford CA, United States of America
[at] Also at Institute for Particle and Nuclear Physics, Wigner Research Centre for Physics, Budapest, Hungary
[au] Also at Giresun University, Faculty of Engineering, Turkey
[av] Also at CPPM, Aix-Marseille Université and CNRS/IN2P3, Marseille, France
[aw] Also at Department of Physics, Nanjing University, Jiangsu, China
[ax] Also at University of Malaya, Department of Physics, Kuala Lumpur, Malaysia
[ay] Also at Institute of Physics, Academia Sinica, Taipei, Taiwan
[az] Also at LAL, Univ. Paris-Sud, CNRS/IN2P3, Université Paris-Saclay, Orsay, France
[*] Deceased

JHEP10(2017)182